PITTING CORROSION OF NICKEL

PITTING CORROSION OF NICKEL

By

MOHAMMED ZAMIN, B. TECH. (HONS.), D.I.I.T.

A Thesis
Submitted to the School of Graduate Studies
in Partial Fulfilment of the Requirements
for the Degree
Master of Engineering

McMaster University

March, 1972

MASTER OF ENGINEERING (1972)
(Metallurgy and Materials Science)

McMASTER UNIVERSITY
Hamilton, Ontario

TITLE: Pitting Corrosion of Nickel

AUTHOR: Mohammed Zamin, B. Tech. (Hons.) (Indian Institute of Technology, Kharagpur, India)

D.I.I.T. (Indian Institute of Technology, Kharagpur, India)

SUPERVISOR: Professor M. B. Ives

NUMBER OF PAGES: v, 131

SCOPE AND CONTENTS:

The pitting corrosion of nickel has been investigated using potentiostatic techniques, optical and scanning electron microscopy. The effect of grain size, cold work, annealing procedure and chlorine ion concentration has been investigated and analyzed from the point of view of the pitting susceptibility and passivity of nickel. It has been shown that electrochemical data must be supplemented by metallographic observations for a complete appreciation of the pitting phenomenon.

ACKNOWLEDGEMENTS

My thanks and gratitude to Dr. M. B. Ives for his interest, guidance and help throughout the entire duration of this work.

I wish to thank the faculty, graduate students and technical staff of the Department of Metallurgy and Materials Science for their assistance in so many different ways.

My thanks are due to Miss V. Komczynski for her co-operation and skill in typing the manuscript.

Finally, I gratefully acknowledge the financial support from McMaster University in the form of a graduate assistantship.

TABLE OF CONTENTS

CHAPTER I

INTRODUCTION

The advent of modern technology has necessitated the search for materials with a higher resistance to corrosion. Corrosion is the destruction or deterioration of a material by chemical or electrochemical reaction with its environment.

Though the E.M.F. series (based on the thermodynamic reactivity of metals) places nickel mid-way between the two corrosion extremes, its position in the galvanic series (which is based on the practical nobility of metals and alloys) is considerably higher - closer to the nobler or cathodic side.[1] Nickel possesses a high degree of resistance to corrosion in many atmospheres.[2] Many of its alloys with copper, chromium, molybdenum and iron exhibit remarkable corrosion resistance. Nickel forms an important constituent of many of the stainless steels.

The various forms of corrosion which a material may be subjected to, can be classified under one or more of the following:[1]

i) General corrosion
ii) Galvanic corrosion
iii) Crevice corrosion
iv) Pitting corrosion
v) Intergranular corrosion
vi) Selective leaching
vii) Erosion corrosion
viii) Stress corrosion

1.1 Definition of Pitting Corrosion

i) Pitting is a form of extremely localized attack that results in holes in the metal.[1]

ii) Pitting is a localized type of attack, the rate of corrosion being greater at some areas than at others.[3]

iii) Pitting is corrosion confined to small points, so that definite holes are produced in an otherwise almost unattacked surface.[4]

1.2 Cause of Pitting Corrosion

Pitting may be considered as the intermediate stage between general overall corrosion and complete corrosion resistance (Figure 1). Thus, if a metal is in the corrosion resistant or 'passive' state, the entire surface of the metal is inert and no corrosion occurs. However, if this resistance breaks down at some places, these exposed areas become anodic to the rest of the surface which is cathodic. Owing to the unfavourable area ratio, corrosion at the exposed points is extremely high. This results in pitting of the surface.

1.3 Nature of Pitting Corrosion

A corrosion pit is a unique type of anodic reaction. It is an autocatalytic process. That is, the corrosion processes within a pit produce conditions which are both stimulating and necessary for the continuing activity of the pit. In Figure 2 a metal M is being pitted by an acid sodium chloride solution. Rapid dissolution occurs within the pit, while hydrogen reduction takes place on adjacent surfaces. This process is self-stimulating and self-propagating. The rapid dissolution of metal within the pit tends to produce an excess of positive charge in this area,

Figure 1. Diagramatic representation of pitting as an intermediate stage

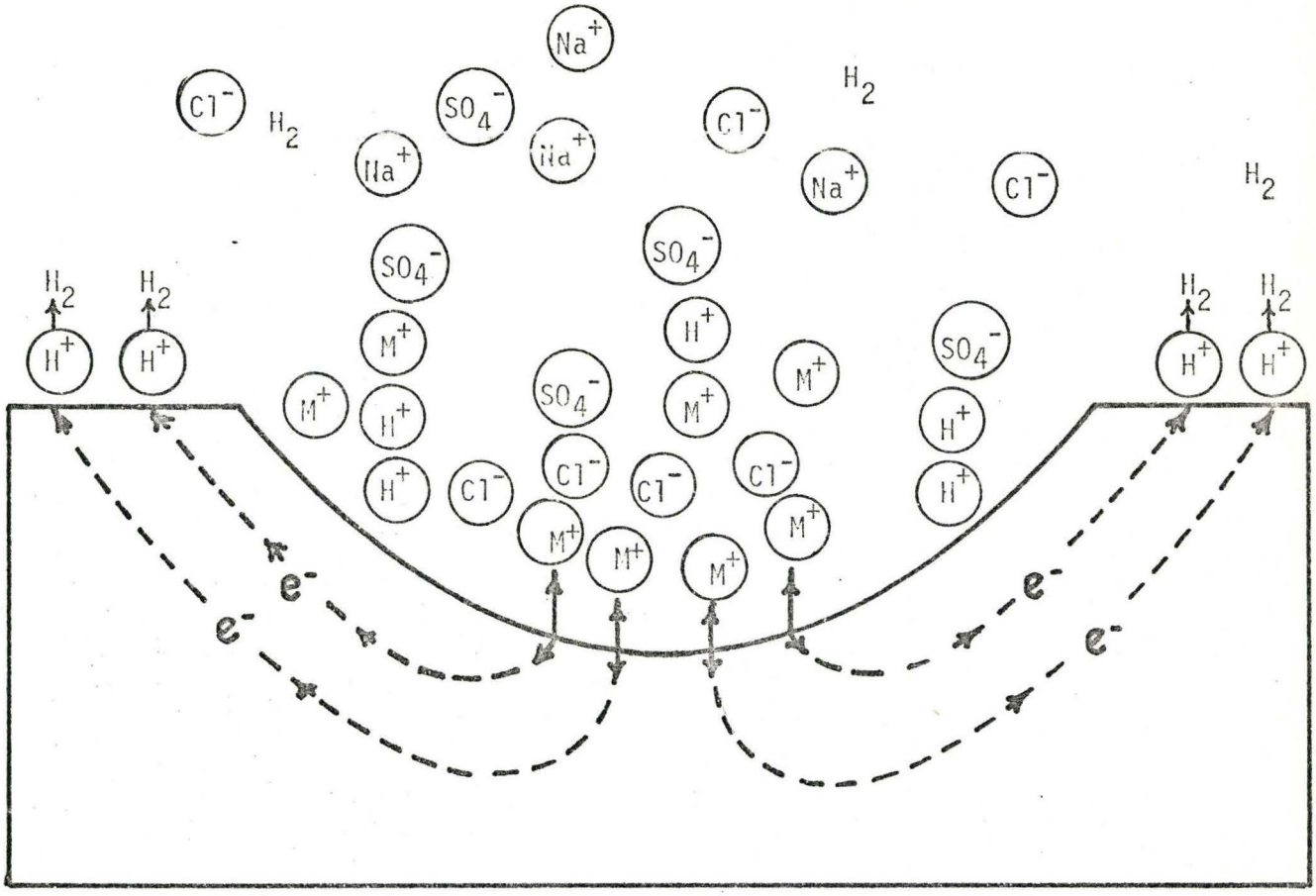

Figure 2. The autocatalytic processes occurring in a corrosion pit

resulting in the migration of chloride ions to maintain electroneutrality. Thus, in the pit there is a high concentration of MCl and, as a result of hydrolysis, a high concentration of hydrogen ions. Both hydrogen and chloride ions stimulate the dissolution of most metals and alloys, and the entire process accelerates with time. Owing to the active dissolution of the metal, no hydrogen reduction occurs within a pit. The cathodic hydrogen reduction on the surfaces adjacent to the pits tends to suppress corrosion. In a sense, pits cathodically protect the rest of the metal surface.

1.4 Importance of Pitting Corrosion

Pitting stands as an extremely destructive and one of the most insidious forms of aqueous corrosion. Various metals, including nickel, iron, chromium, aluminum, magnesium, zirconium, copper, tin, zinc and many of their alloys are subject to this attack.

1.5 Nature and Scope of the Present Investigation

With a qualitative idea of the nature and significance of pitting corrosion, it is apparent that a clearer and more thorough understanding of the pitting mechanism is of prime importance. It is extremely important to be able to predict the conditions and sites of nucleation and the possible mechanism of growth because this will determine the preventive treatment to be used.

In the present investigation, two aspects of pitting corrosion have been studied:

i) Kinetic and,

ii) Morphological

The kinetic aspect deals with the sites for pit initiation and the effect of various factors such as chlorine ion concentration, grain size and cold work on the passivity and pitting susceptibility of nickel.

The morphological aspect concerns itself with the size, shape and distribution of pits in cold worked and annealed materials.

CHAPTER II

LITERATURE SURVEY

2.1 The Phenomenon of Passivity

The phenomenon of metallic passivity has fascinated scientists and engineers since the days of Faraday. The phenomenon itself is rather difficult to define because of its complex nature and the specific conditions under which it occurs.

2.1.1 Definition of Passivity

Not withstanding the comparatively frequent and readily observed manifestations of passivity, no all-inclusive definition of this phenomenon has been advanced. Many investigators do not provide concrete definitions of passivity but substitute a description of the phenomenon. However, passivity has been defined in the following ways:[5]

i) An active metal becomes passive when its electrode potential approaches that of a less active, noble metal.

ii) A metal is considered passive when, along with its high corrosion resistance, its corrosion reaction has a high thermodynamic probability.

iii) Passivity is a state of high chemical stability of a metal under certain conditions if under somewhat similar conditions the metal behaves as a normal active metal.

iv) Passivity is the acquisition by a metal, after treatment, of chemical stability to reagents or conditions in which it would be rapidly corroded without such treatment.

For various reasons, such as not taking into account corrosion resistance and limiting itself only to the measurement of potential [definition (i)], being based on the characteristic corrosion properties of the metal, including all types of corrosion inhibition and being too broad [definitions (ii) and (iii)], relating passivity only to creation of an inert condition on the metal with lack of any kind of indication of its nature [definition (iv)], the above definitions of passivity have been criticized as being inadequate.

However, on the basis of the theory of electrochemical corrosion, the phenomenon of passivity of metals is most rationally defined in the following manner:[5]

> "Passivity is a state of high corrosion resistance of metals or alloys (under conditions when their reactions are thermodynamically possible) caused by inhibition of the anodic process, that is, a passive state is a state of corrosion resistance caused by an increased anodic control."

This definition includes the ennoblement of potential observed in most cases of passivity and is not confined only to a particular positive shift of potential.

2.1.2 Anodic Passivation

When a material is anodically polarized, i.e. its electrode potential is made more positive, the dissolution rate increases exponentially. In materials which are capable of exhibiting an active-passive transition, a certain stage is reached when the dissolution rate falls markedly, and the material is said to be passivated. The passivation occurs owing to

the formation of a thin film. The potential at which this passivation occurs is known as the "primary passive potential", E_{pp}, and the critical anodic current maximum at this potential is designated by I_c. If the polarization of the material is continued further, there is no appreciable increase in the corrosion current. The current required to maintain passivity is known as the "passive current" and is designated by I_p. On still further polarization, a potential is reached after which the anodic current again begins to increase. At this potential the initially formed passive film breaks down and metal dissolution commences again. This potential is termed as the "critical potential for the breakdown of passivity", E_c. Thus, based upon the manner in which the material behaves, the anodic polarization curve (Figure 3) exhibits three regions, called "active", "passive" and "transpassive".

2.1.3 Theories of Passivity

Many theories of passivity have been put forward and numerous modifications of the basic theories have been proposed. The most fundamental and generally accepted theories at present are those explaining the passive state on the basis of a film or adsorption mechanism accounting for inhibition of anodic dissolution.

2.1.3 (a) Film Theory

While considering the behaviour of iron in concentrated nitric acid, the mechanism of passivity was proposed by Faraday[6] more than 100 years ago in the following terms: "The surface of iron is oxidized... or is in such relation to the oxygen of the electrolyte as to be equivalent to oxidation..." The film theory of passivity, as it is known

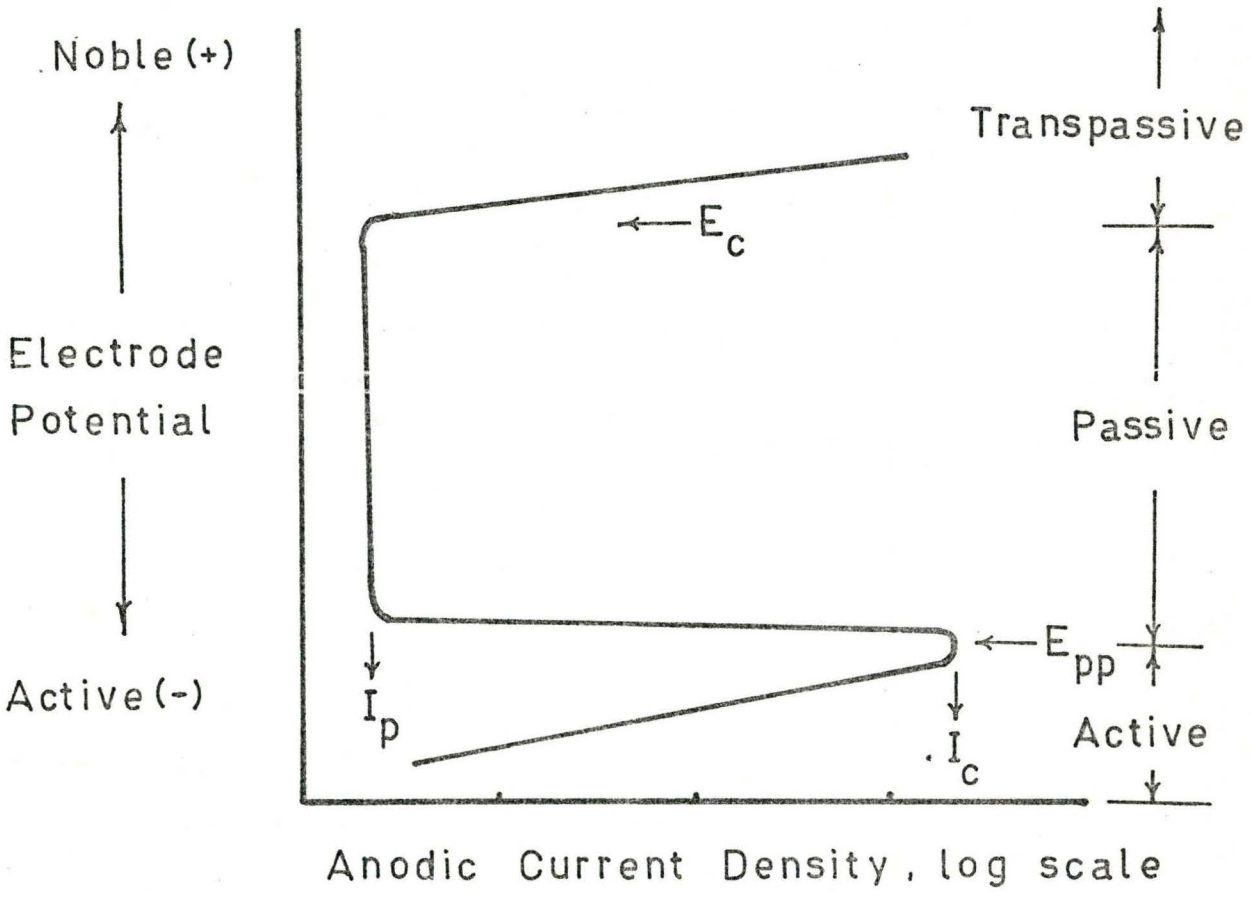

Figure 3. Typical anodic dissolution behaviour of an active-passive metal

today, is due to Evans.[4] This theory considers the passive state as the appearance of a very thin, often invisible protective film of products formed by reaction of the environment with the metal. Very often this thin film represents some form of metallic oxide.

The generalized film theory embraces the special cases where a film of oxygen rather than oxide causes passivity. It was Tammann[7] who later suggested that a film of adsorbed oxygen, rather than the oxide, is responsible for the passivity of iron, nickel, cobalt and chromium.

2.1.3 (b) Adsorption Theory

In a number of cases, besides films that inhibit the anodic process and that have thickness of hundreds or even tens of atomic layers, thinner monomolecular protective adsorption layers of oxygen, oxidant, or other substances can exist and produce passivity - that is, cause a so-called adsorption passivity.

The adsorption theory of passivity has been developed mainly by Uhlig.[2] This theory describes anodic inhibition as an electrochemical mechanism. It is assumed that adsorption of oxygen atoms (and sometimes other species) leads to a reorganization or shift of the electrode potential in the double layer which strongly inhibits metal dissolution.

Some workers[8] believe that the establishment of passivity requires at least a continuous coverage of the surface with an adsorbed monomolecular layer of oxygen atoms. Others,[9] on the other hand, think that it is only necessary to have oxygen adsorption on the more actively dissolving surface area.

In recent years, the advocates of the adsorption theory have come to believe that, in addition to the purely electrochemical adsorption

mechanism, consideration must be also given to the formation on the surface of adsorbed (chemisorbed) compounds, and the formation of electric dipoles as a result of partial ionization of the oxygen atom by an electron from the metal which change the chemical and electrochemical reactivity of the metal.

2.1.3 (c) Electron Configuration Theory

The first qualitative suggestion of a relation between electron configuration of atoms and passivity was made by Russell[10] in 1925. A theory accounting quantitatively for critical passivity concentrations in alloys was outlined by Uhlig.[11] According to this theory, the ease in forming a passive state is associated with noncomplexity of the internal shells of a metal, as, for instance, the easily passivated transition metals of the periodic table (chromium, nickel, cobalt, iron, molybdenum and tungsten), which have incomplete d levels in the metallic state.

Adsorption of oxygen or oxidant is accompanied by the phenomenon of passivity, because the adsorption of the oxidant leads to the incorporation of electrons from the metal and consequently to unfilled electron levels in the metal. Adsorption of hydrogen or reducing agents in general, on the contrary, provides electrons to the metal, filling the d level and converting the metal into the active state.

The corrosion behaviour of Ni-Cu alloys has extended considerable support to this theory. When nickel with 0.6 electron holes per atom in the d band, is alloyed with a non-transition metal, e.g., copper (with no d-electron holes), electrons from copper contribute to the unfilled d-electron levels of nickel. The alloy retains the transition metal characteristics of nickel so long as the d-electron holes are not completely

filled. Specific heat and magnetic measurements of the Ni-Cu alloys show that the d band of energy levels is filled at about 60 atom % or 58 wt % Cu and is unfilled at lower copper compositions. The alloys therefore are expected to be passive and to behave like nickel below 60 atom % Cu(> 40% Ni), but to be active and to behave more like copper at higher copper compositions. Corrosion rate and anodic polarization data[12,13] confirm that lowest corrosion occurs in alloys containing a minimum of about 40-50% Ni at which composition and above, d-electron holes exist.

Several other alloy systems exhibit critical compositions for passivity.[14] Examples are the Ni-Mo, Co-Cr, and Ni-Cr alloys for which the critical alloy compositions as determined from the value of $I_{critical}$ come at values specific to each alloy. Critical alloy compositions for passivity have also been observed in three- or four-component alloy systems, e.g. Fe-Cr-Ni-Mo, Fe-Ni-Mo and Cr-Ni-Fe.

The condition that determines whether a substance capable of reaction will react or adsorb is related to the work function of the metal (a measure of the heat of evaporation of electrons from a metal) and the heat of sublimation of the metal. When oxygen, for example, approaches a metal surface it will either extract an electron from the metal surface and become adsorbed, or a metal atom will be dislodged from its position in the lattice to form an oxide. Thermodynamically, the preferred process is that accompanying a greater decrease of free energy. Thus, since the state of adsorption corresponds to passivity we have,

$$\frac{\text{Work Function}}{\text{Heat of Sublimation}} < 1, \text{ for passivity}$$

$$> 1, \text{ for reactivity}$$

Alloying, which affects both the work function and the sublimation energy, changes the above ratio depending on the particular alloy composition. This explains why an alloy exhibits passivity above a critical composition and behaves actively below it.

Properties of metals depend on the internal structure of the atoms and consequently on the electron configuration in the metal. But passivity is determined not only by the metal but to a large extent also by the environmental conditions. Therefore to assume that the passive state is explained by the electron configuration only, is apparently fallacious. Actually the electron configuration theory does not explain all the aspects of the passive state that are not covered by the film or adsorption theory. The major objection to this theory is that capability of transition into a passive state is a property not only of the transition metals but also of aluminum, magnesium, berylium and many others. Under suitable conditions almost all metals can be rendered passive, including those metals that do not have any free electron levels.

It must be pointed out that the film and adsorption theories of passivity do not contradict, but rather supplement one another. As the adsorbed film in the process of thickening gradually transforms into an oxide film, the retardation of the anodic process promoted by change in the double layer structure will also be supplemented by the greater difficulty encountered by ions passing through the protective film. Evidently, a combination of the film and adsorption theories can more fully explain all the experimentally observed manifestations of passivity.

2.2 Theories of Pitting Corrosion

The phenomenon of pitting corrosion may be divided into two distinct stages:-

i) nucleation of pits

ii) development of pits

Among the different conceptions of the pitting corrosion mechanism, there are theories that explain both the above stages, and those which are concerned only with the second stage. It is not possible to categorize the several divergent views that have been put forward. Nevertheless, two broad divisions may be made.

2.2 (a) Adsorption Theory

This theory owes its origin to Hoar, and, over the years has been modified by many workers including Hoar himself.

Hoar et al.[15] proposed that the initiation of pits might be due to the adsorption of aggressive anions on the surface of the oxide film followed by the penetration of ions through the film. Anion entry, without exchange, into the film is postulated as producing a greatly induced ionic conduction in the contaminated oxide film, which thus becomes able (at certain points) to sustain high current density and to produce brightening by random removal of cations. When the field across the film-solution interface reaches a critical value, pitting occurs.

Later, Hoar[16] suggested the so-called mechanical breakdown process of pit initiation. He proposed that during anion adsorption, water molecules are replaced and this causes the lowering of the interfacial tension on the oxide-solution interface by the mutually repulsive forces

between charged particles. The adsorbed anions push one another and the oxide to which they are strongly adsorbed causing slip and forming cracks which are the nuclei of pits.

The last modification[17] of this theory stands as follows: "Three or four halide ions jointly 'adsorb' on the oxide film surface around a lattice cation - one next to a surface anion vacancy for preference. The transitional complex thus formed has high energy and the probability of its formation at any instant is very small. But, once formed the complex can readily and immediately separate from the oxide ions in the lattice, the cation dissolving in the solution, very much more readily than the non- or aquo-complexed cations present in the film surface in the absence of halide ions. Under the anodic field, another cation comes up through the film to replace the dissolved cation - the field at constant anode potential increases at the 'thinned' point of the film; but arriving at the film-solution interface, it finds, not stabilizing oxide ion formed from water (nor, in de-aerated solution, oxygen molecules), but several halide ions, so that the 'catalytic' process, once begun, has a strong probability of repeating itself, and of accelerating because of the increasing electrostatic field. Thus, once localized breakdown starts with the initial transitional complex, it accelerates 'explosively'".

2.2 (b) Displacement Theory

On the basis of the adsorption theory of passivation, the formation of pits is described as a result of a competitive adsorption of Cl^- ions and oxygen. Pits develop on the spots where oxygen adsorbed on the metal surface is displaced by Cl^- ions. Kolotyrkin[18] presumes that even during the dissolution of a passivated metal, irregular distribution of the current

does exist on the metal surface, since the latter is never quite homogeneous. On some spots occur a stronger adsorption of Cl^- ions and a more rapid dissolution of the metal. According to this theory, the breakdown potential represents that minimum electrode potential value, at which the aggressive anions become capable of producing a reversible displacement of the passivating oxygen from the metal surface.

Rosenfeld and Danilov[19] adapted the displacement theory to the case when the surface of the metal is covered by a passive film in the form of a separate phase. They presumed that the exchange of oxygen by chlorine ions occurs at sites where the metal-oxygen bonding is the weakest. Aggressive anions which displace oxygen from the surface penetrate into the passive film and collect inside of pits. Since the pits are closed crevices covered by a porous surface layer, they suggested that pitting corrosion is a specific case of crevice corrosion, and similarly as in nucleation of crevice corrosion, geometrical factors, such as presence of microcrevices, microcracks, etc. influence pitting corrosion. If pitting corrosion is to be regarded as a special case of crevice corrosion where the electrochemical behaviour of the metal is known to be caused only by the difference in the access of the corrosive medium and in the removal of the corrosion products, pitting corrosion should stop if the pit and the rest of the surface are equally accessible to the electrolyte. Rosenfeld and Danilov's observations confirm this belief. Destruction of the shielding layer over the pit in 18-8 stainless steel with resultant free access of the solution from the bulk led to the immediate passivation of the pit.

On the basis of the data on the composition of the solution in the pits (increased acidity), it can be concluded that the reaction of

displacement of the passivating oxygen takes place only on those sections of the metal surface near which the concentration of the aggressive anion reaches a certain critical value, greater than its bulk concentration. This increase in concentration of aggressive anions near separate areas of the metal surface, leading to depassivation of these sections, can be affected by means of anion transport by the current. This hypothesis is supported by the results of Engell and Stolica[20] who showed that the activating influence of chlorine ions is not observed immediately after their addition into the solution but only after a certain period of time which is longer the lower the concentration of the chlorine ions in solution.

Regarding the influence of the halide ions on the dissolution kinetics of metals in the active state, available data shows[18] that the direct participation of the solution components in the elementary act of ionization of metallic atoms appears to be an inevitable stage in these processes. Apparently, the first step of the process is the chemico-adsorptional interaction between the surface atoms of the metal and one of the components of the solution, with the formation of a surface complex which, when a certain potential is reached, passes into solution. Because of the difference in the polarizability of anions, their influence (relative and absolute) on the kinetics of metal dissolution changes substantially with a change in the electrode potential. Therefore, when a certain potential is reached, conditions are created for displacement of one component by another, and consequently for a change in mechanism of the process. Thus, it is reasonable to assume that the initial dissolution products in pits are compounds of the metal with the aggressive anion. This compound

is hydrolysed with the formation of an oxygen compound of the metal (or hydrated ions), hydrogen ions and free aggressive anions which can again affect the process, now as catalyst. Thus, the increased acidity of solution in the pits is a result of the growth of the pits, but not the cause of their formation.

Surprising as it may appear, none of the existing theories is able to clarify all the known phenomenon of pitting.

2.3 Factors Affecting Pitting Corrosion

2.3.1 Effect of Physical State of Metal

The susceptibility of metals to pitting corrosion depends largely on their own nature, structure and surface state. The defects of the metal surface could be carried over to the passive film and provide sites for pit nucleation.

Tokuda and Ives[21] found that the reactivity for active dissolution, and consequently the susceptibility to pitting corrosion, is greater for a mechanically polished {111} face of a Ni-single crystal than for an electrolytically polished one.

In general, disturbed metal layer, local cold work and rough surfaces exhibit a greater tendency to pitting corrosion.

2.3.2 Effect of Alloying Elements

Pitting susceptibility may be taken to be the tendency of metals to undergo pitting corrosion. Tendency towards pitting corrosion - pitting susceptibility - is distinctly higher in ferritic steels than in austenitic stainless steels. Consequently, susceptibility to pitting corrosion decreases as the content in silicon , nickel, and especially chromium and

molybdenum increases. Usually, the influence of alloying additions on the value of the breakdown potential is taken as an indication of its effect. Constituents which decrease pitting susceptibility shift E_c to more positive values, while components which increase pitting susceptibility shift E_c to more negative values. It has been found that[22] while Cr, Mo, Ni, V, Re, Mn and Si shift E_c to more positive values, elements such as C, Ti, Ce, Nb shift E_c to more negative values. Zr, Ta and W have been found to be without any effect on E_c.

2.3.3 Effect of Electrolyte Composition

Pitting corrosion depends not only on the concentration of Cl^- ions, but also on the concentration of unaggressive anions, and more precisely on the ratio of aggressive to unaggressive anions.

It has been found[23] that both nitrates and chromates added in appropriate concentrations to a solution containing Cl^- ions act as pitting corrosion inhibitors. A similar effect is produced by SO_4^{2-}, OH^-, ClO_3^-, and CO_3^{2-} ions. All these anions cause the shift of E_c values to more positive potentials. However, though NO_3^- anions cause the increase of E_c, at a particular NO_3^-/Cl^- ratio further anodic polarization initiates pitting.

In general, the presence of unaggressive anions produces three different effects.

a) increase in E_c

b) prolongation of the induction period, and

c) reduction in pit density.

It is difficult to classify the effect of unaggressive anions in any series because it depends not only on their concentration and the

potential, but also on the material they are protecting. Leckie and Uhlig[24] studied the effect of various unaggressive anions in solutions of different Cl^- activities for 18 Cr - 8 Ni stainless steel under potentiostatic conditions. They found that the inhibition efficiency decreases in the order $OH^- > NO_3^- > Ac^- > SO_4^{2-} > ClO_4^{2-}$. For aluminium,[25] the inhibition efficiency decreases in the order $NO_3^- > CrO_4^{2-} > Ac^-$ > benzoate > SO_4^{2-}.

The action of unaggressive ions in the presence of Cl^- ions has been explained by a competitive adsorption of anions on the surface of the metal or oxide at anodic potentials which lead either to pitting or to inhibition of pitting corrosion. However, the results of Forchhammer and Engell[26] contradict this belief. In their study of pitting corrosion of 18 Cr - 8 Ni stainless steel using a potentiostatic method, they claim no indication of a preferential Cl^- adsorption. Cl^- ions caused an increase of the corrosion current in the passive range while SO_4^{2-} and NO_3^- ions decreased this current.

In the absence of imposed polarization, pitting corrosion in solutions containing aggressive anions is observed only in the presence of oxidizing agents such as Fe^{3+}, Hg^{2+}, Cu^{2+}, H_2O_2 and dissolved oxygen. Oxidizing agents, in all cases, play the part of passivators. Their effect can be explained by their simple depolarizing action which on reduction on the metal surface shifts its potential in the positive direction with respect to E_c.

The nature of a solution can be borne out by its redox potential. Uhlig[27] has proposed that a metal is subject to pitting corrosion only

if the redox potential of the solution containing aggressive anions lies at values more positive than E_c.

2.3.4 Effect of pH of Solution

Though there is some controversy, in general, it has been found that the value of the breakdown potential is constant within a large range of pH. The reason for this, however, is not quite clear.

Leckie and Uhlig[24] found that for 18 Cr - 8 Ni stainless steel, the critical potential is not greatly affected in acid 0.1 N NaCl ranging in pH from 1 to 7. However, it moves markedly in the noble direction in alkaline solutions of pH 7 to 10. This is accompanied by an increased resistance to pitting corrosion. Beyond pH 10, E_c decreases. However, the increase of current observed at corresponding values of potential does not correspond to pitting but to the attainment of the transpassive state with the formation of CrO_4^{2-}.

2.3.5 Effect of Temperature

Leckie and Uhlig[24] observed that the breakdown potential for an 18 Cr - 8 Ni stainless steel in 0.1 N NaCl at 0^0C is above 900 mV (vs SHE); at 25^0C, it is 325 mV (vs SHE); and in the range of temperatures from 25^0 to 50^0C, it undergoes small changes.

While E_c shifts to more active values with increase in temperature for the austenitic stainless steels,[26] for aluminium[28] E_c is not greatly sensitive to temperature in the range 0^0 to 40^0C. Working with nickel in alkaline chloride solutions, Postlethwaite[29] found that the effect of raising the temperature is to stimulate the attack up to 175^0C but above this value the trend is reversed, the critical potentials move to higher values, and both the induction period and critical Cl^- concentration

increase. The attack changes from pitting at 25°C to more general attack at elevated temperatures.

Until now, the dependence of E_c upon temperature for the various metals and alloys has not been explained.

2.3.6 Effect of Metallurgical Condition of Metal

Forchhammer and Engell[26] studied the effect of cold working on the E_c value for different austenitic steels in 3% NaCl solution. They found that E_c does not vary much for the cold worked samples in comparison with annealed ones, but in the first case, the number of pits is higher and the pits are smaller.

Tomashov et al.[30] found that a 18 Cr - 14 Ni steel with 5% Si is not susceptible to pitting in the solution treated state, and that sensitizing it for 2 hrs. at 650°C strongly impairs its resistance to pitting corrosion. Thus, working with pure metals eliminates the problems associated with carbide precipitation during sensitization.

In many cases, though tempering of steel increases the number of pits, possibly due to precipitation of carbides, their depth is smallest.

2.3.7 Effect of the Oxide Film

Kinetics of film growth is different in the presence of chloride ions than in the absence of those ions. The growth in the presence of chloride ions results in nonlimiting thickness of the oxide layer.

Ambrose and Kruger[31] studied the changes of optical properties of the passive film on a high purity iron during pitting using an ellipsometer and measuring the corrosion current. They found that the breakdown is observed by simultaneously following changes in optical phase retardation and current at constant potential. The thickness of the film is not

the sole factor in influencing the time to breakdown. Their results indicate that adsorption and complete penetration by Cl^- to the metal surface is necessary to initiate pitting. In further support of these conclusions, the recent work of McBee and Kruger[32] points to the mechanism for passive film breakdown on iron that requires a penetration of chloride ion via lattice defects, possibly anion vacancies.

Bianchi et al.[33] studied the susceptibility of 19 Cr - 10 Ni steel to pitting corrosion in $AlCl_3$ + LiCl glycerol-ethanolic solutions. They found that Cl^- content weakly influences the pitting corrosion process of the naturally oxidized samples (in air at 25°C for 2 hrs) whilst it markedly increases the pit nucleation on the samples oxidized at 300°C for the same time. According to them, this difference in behaviour is due to the defect nature of the oxide film. High susceptibility to pitting is connected with n-type conductivity while low susceptibility to pitting corresponds to p-type conductivity of the oxide film.

2.4 Sites for Nucleation of Pits

There is, perhaps, no general agreement regarding the favoured sites for the nucleation of pits. Different workers have shown different sites as those favouring pit nucleation. In general, it has been clearly pointed out that pits nucleate at imperfections - whether these be in the metal or in the passive film.[34,35,36] These imperfections, or weak spots, have been shown to be scratches,[4,21] dislocations[37] and structurally disturbed regions such as grain boundaries[21,30,38] and slip traces.[35] Inhomogeniety in composition, microsegregation of solute and dominant residual impurities,[39] inclusions[40,41] and precipitation of complex carbides[30] also

causes pitting. It is believed[39] that segregations cause a sufficient decrease of the cathodic overvoltage to bring the corrosion potential to the value at which Cl^- ions lead to pitting corrosion.

In an investigation[38] of the pitting corrosion of 13 Cr - Fe alloy, it was observed that during the initial period pits belonging to different grains develop with different rates. Both prolonged corrosion and high potentials of anodic polarization bring about pitting of the grain as well.

Pit nucleation at imperfections in the passive film does not seem too improbable in view of the fact that for pitting corrosion to occur a 'border-line passivity' is essential. Pearson et al.[42] while studying the pitting corrosion of aluminum in tap water, were unable to relate the starting points of individual pits to any particular feature of the metallurgical structure or of the metal surface. Nevertheless, it seems reasonable to suppose that the passive film around a defect, such as a dislocation where the lattice is strained, is imperfect. Naturally enough, such sites are those favouring pit nucleation.

It has been generally assumed[40] that a certain limited number of points (structural defects or compositional inhomogeneity) are present on the surface of stainless steel where pits nucleate. The investigations of Rosenfeld and Danilov[19] have shown, however, that this is actually not the case. If the pits which are produced initially are opened up and therefore made easily accessible to the passivator, then such pits will passivate and new ones will be originated on the surface. This has been confirmed by their experiments. On reimmersion the number of pits on the surface becomes very high; this number increases continuously as the

initial pits are opened up. Consequently, the concept of a certain limited number of the centres sensitive to pitting corrosion on the metal surface seems doubtful. In reality there are a great number of such centres, but owing to the protective action of the first pits, new pits are not formed.

2.5 Composition changes in Solution during Pitting

A consequence of the localization of the anodic and cathodic reaction is, first of all, a noticeable difference in the composition of the solution near the active area from its composition at other sections of the surface and in the bulk.

The production of acidity at an anode has been definitely established.[4] For a divalent metal like Ni, the existence of various ions can lead to a variety of possible anodic reactions:

$$Ni = Ni^{++} + 2e$$
$$Ni + H_2O = Ni(OH)^{+} + H^{+} + 2e$$
$$Ni + 2H_2O = Ni(OH)_2 + 2H^{+} + 2e$$

Under ideal circumstances, where the reactions occur at such rates as to keep the various ions in equilibrium with one another, the last equation will predominate at about pH 7. At first sight, it may seem that in a neutral liquid, film-repair will prevail, and corrosion will be avoided indefinitely. However, this overlooks the fact that the last reaction automatically generates H^{+} ions. Provided that the acidity formed at the anode is not dispersed into the body of the liquid by stirring or destroyed by cathodically formed alkali, the pH at an anodic point will sink, and conditions will soon become increasingly favourable for destructive corrosion with the formation of soluble products. As a matter of fact, Hoar's[17] theory

of pitting corrosion links the formation and development of pits with the increased acidity of the solution at the active area, as a result of which the metal can pass into the solution in the form of soluble salts, instead of being precipitated as oxides or hydroxides. However, as has already been pointed out, the increased acidity of solution in the pits is the result of the action at the pits, but not the cause for their formation.

According to the results of many investigators,[23] the composition of the solution inside the corrosion pits is characterized by a higher concentration of the aggressive anions and a noticeably lower pH compared with the bulk solution. Available data also indicates that the activity of the metal in the pits is due mainly to the particular aggressiveness of the solution in them. Evans[43] has shown that the products of corrosion flowing out of the pits stimulate the destruction of other regions of the surface. If the corrosion products are removed from the pits by means of rapid stirring or centrifuging, the pits can be passivated.

It is not clearly known in what form and in what proportions the individual components of a given alloy dissolve during pitting. Stolica[44] studied the composition of the solution after measurement of the current vs. time during pitting of Fe - Cr alloys. He found that both Cr and Fe are present in the solution in the same proportion as in the steel.

2.6 Morphology of Pitting Corrosion

The shape, size and distribution of pits can provide a clearer understanding of the basic mechanism accompanying pitting corrosion. Many different kinds of pits have been observed: hemispherical, flat-walled, formless, uncovered, covered etc..

It is still not clear what sort of conditions must be fulfilled to realize the formation of pits of a particular shape. It seems that the shape of the pit depends upon both the conditions existing within the pit - and consequently, upon the composition of the aggressive solution - and properties of the given metal, its composition, structure, etc.

The formation of covered pits indicates that the passive film is scarcely soluble both in the bulk electrolyte and in that within the pit. The formation of flat walled pits indicates that there is no ohmic layer within the pits which tends to maintain equal current density at all points of the pit surface. Formation of hemispherical or partly spherical pits suggests that within the pit there probably occur processes similar to those accompanying electropolishing.

Schwenk[45] observed anisotropic pit growth of 18 Cr - 10 Ni stainless steel in solutions containing Cl^- ions. At low potentials, near E_c, and at a low current density within the pit, flat walled pits, mostly hexagonal, and sometimes square were observed. In another study,[46] pits formed on 16 Cr - Fe single crystals in aqueous solution containing Cl^- ions in the vicinity of E_c had the shape of polyhedra composed of most closely packed {110} and less closely packed {100} crystal planes.

It is not easy to study directly the growth of three-dimensional pits; the most successful attempt has been that of Pearson et al.[42] In their work on aluminum in tap water, they found that the shape of corrosion pits is rather complex, the nature and characteristic appearance of which varies as corrosion proceeds. Short exposure times lead to the formation of tunnels - pits with square cross-section and numerous right-angle turns. In cold worked material the corners of these tunnels are more rounded

than in the annealed material. Pits which result from medium times of exposure show a very definite grain boundary attack. Pits in cold worked material although more numerous, are usually smaller and shallower than those in the annealed material.

These findings received more support from the work of Edeleanu,[47] who simplified the problem by studying two-dimensional pits. He found that pits are markedly crystallographic and the stable surface (i.e. the slowest to corrode) is the (100) plane. However, with increasing current, the crystallographic nature of the pits disappears and as the potential rises markedly, the advancing fronts become virtually circular. Changes in applied current do not alter the rate of pit growth at the place where it is growing, but merely increase the number of such places and the width of the fronts. The rate of pit growth is approximately 0.15 mm/min. At very low currents and when the pits advance on very narrow fronts (a few μm) the pits frequently change direction through right angles.

Edeleanu suggested that the tunnels formed during natural corrosion in Cl^- solutions may sometimes follow dislocation lines. It is naturally not suggested that the dislocations themselves bend through frequent right angles, but merely that the narrow tunnel-like pits follows the dislocation as best as they can by advancing on a narrow front in one of the <100> directions but choosing whichever of the {100} planes has a suitable emerging dislocation.

He also attempted to study the natural growth of pits (i.e. with no applied current). He did not find any difference in the corrosion reaction in this case as compared with the one in which there is an applied current. Even experiments with slightly cold-worked material did not show any obvious differences.

Garz et al.[48] studied the morphology of corrosion pits formed in 0.5 N $NiCl_2$ on {111} , {110} and {100} surfaces of nickel single crystals. The shape of the pits varied. They found, for instance, that a {100} surface yielded a square pit, a {110} face gave a rectangular pit while the shape of pits on the {111} surface varied from triangular to hexagonal. The pits in polycrystalline sample had varying shapes. They stated that faces of high atomic density constitute the facets of pits obtained at high anodic potentials. They observed pit facets to be composed of {310}, {110} and {111} planes.

The most complete study of the morphology of corrosion pits on nickel single crystal has been made by Tokuda and Ives.[49] Pits were formed by passivating the samples in 1 N H_2SO_4 or in 0.5 N $NiSO_4$ + 0.01 N H_2SO_4 for 30 mins at various potentials followed by the incremental addition of chloride ions (as NaCl solution) until pitting was initiated at the chosen potential. The two electrolytes permitted a study of morphological change with acidity. Two reaction rates have been distinguished - low and high - depending on the anodic current during pitting achieved by an appropriate selection of the potential. They found that the morphology of the corrosion pits varies depending upon the surface orientation, acidity of solution and the reaction rates. The pit morphologies are summarized in Figure 4. Pits obtained on {110} surfaces exhibit a dependence on the passivating potential and an independence of the activation potential. The external shape changes from hexagonal to rhombohedral as the passivating potential is increased. Pit shape on {100} surfaces is independent of reaction rate. To account for the observed pit morphologies, they have proposed a model based on the atomistic mechanism of dissolution. It is found that a simulation,

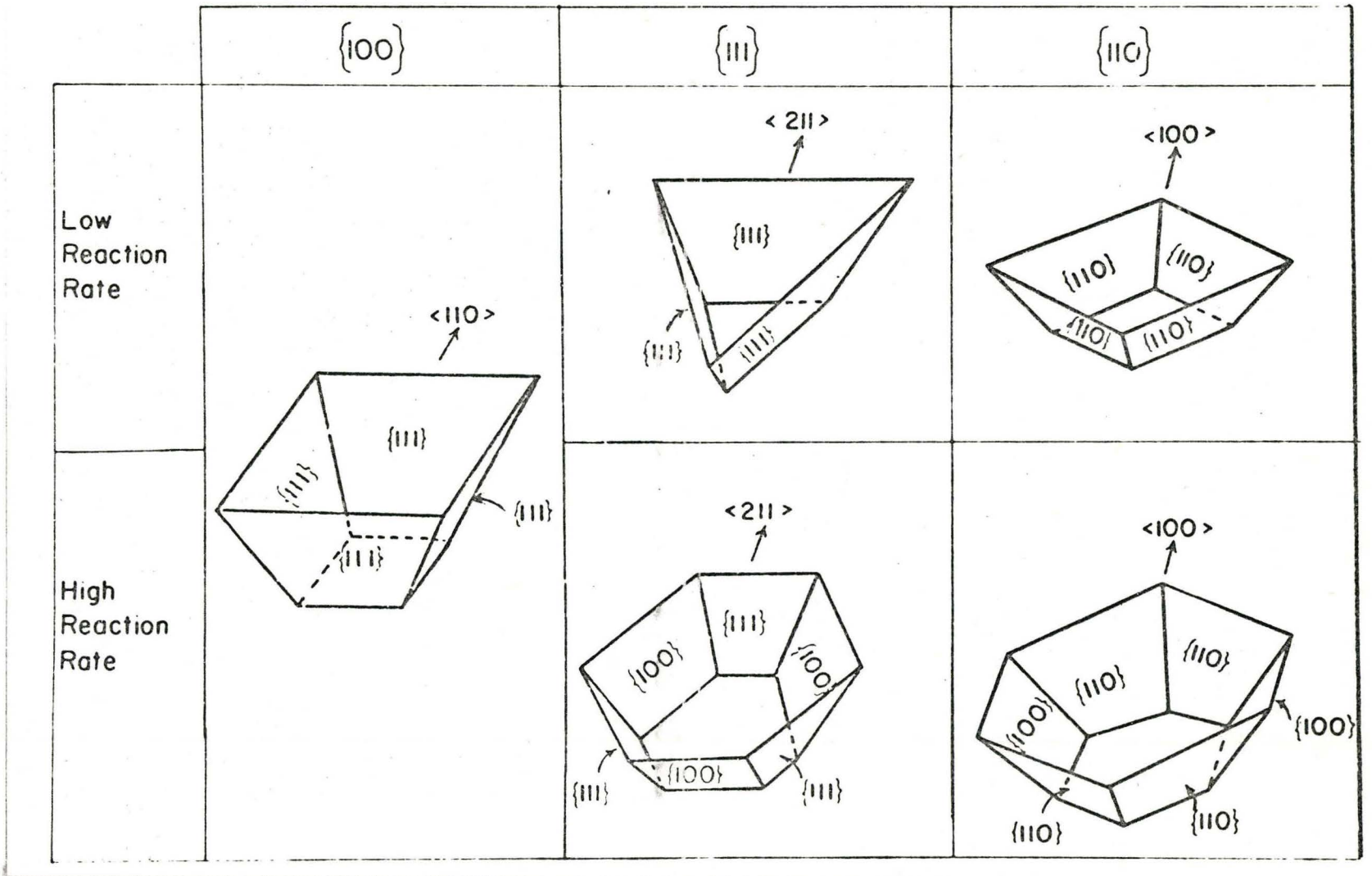

Figure 4. Pit morphologies obtained by simulation for {100}, {110} and {111} fcc surfaces at low and high reaction rates. All simulations assume uniform deepening of a pit until it is arrested and a planar base is formed.[49]

which removes atoms one by one according to the principle that atoms more accessible to the aggressive ions are removed more easily, approximates the morphologies of pits obtained experimentally.

2.7 Kinetics of Pitting Corrosion

2.7.1 Induction Time for Pit Formation

The formation of pits is due to the destruction of passivity. Based on any of the theories of pitting corrosion, it is necessary for the aggressive ion to make its way from the bulk of the solution to the active areas and, finally, to the metal surface. The time necessary to form the first pits, i.e., the induction time, depends upon the concentration of the aggressive ions in the solution. The more the aggressive ions, the shorter is the induction time.

Engell and Stolica[20] found that reciprocal of the induction time, τ, is a linear function of the concentration of Cl^- ions

$$\frac{1}{\tau} = k[Cl^-]$$

Below a certain critical value of Cl^- concentration, pitting does not occur. For mild steel[20] the induction time is potential independent. However, for 18 Cr - 10 Ni steel in 1 N H_2SO_4 + 0.2 N Cl^- solution, Stolica[44] found that the induction time decreases with increasing potential. For the pitting corrosion of nickel in alkaline chloride solutions, it was found[29] that the induction time depends on potential, the Cl^-/OH^- ratio, and the OH^- ion concentration.

Hoar and Jacob[17] measured the induction time of 18 Cr - 8 Ni stainless steel. They supposed that $1/\tau$ is an approximate estimate of the rate of the breakdown process. The slope of the log τ vs. log C_{Cl^-} plots showed that the rate is proportional to the nth power of the Cl^- ion concentration,

where n lies between 2.5 and 4.5. The rate of the breakdown process depends on the halide ion concentration, anode potential and temperature. According to them, the exponent n = 2.5 to 4.5 and a high activation energy show that the transition state in the breakdown process involves 2.5 to 4.5 halide ions and has a very high activation energy. This rules out the pitting corrosion theories which assume simple anion exchange or migration as rate determining stages in the breakdown process.

2.7.2 Galvanostatic Measurements

Rosenfeld and Danilov[50] studied the pitting corrosion rate of 18 Cr - 10 Ni-Ti steel in 0.1 N NaCl by galvanostatic method. They measured the number of pits and their mean and maximum depth. They found that proportionality exists between the number of pits, N, their areas, S, and the current density. The mean radius of the pit changes with time according to the equation:

$$r = at^{0.37}$$

where, t is the time. Hence, the dissolution rate decreases with time.

From the polarization current values and the total area of pits, they calculated the current density in the pits to be:

$$i_p \propto t^{-3/2}$$

Experiments without applied current, yield the value of i_p as:

$$i_p \propto t^{-1/2}$$

Hence, the current density within the pits decreases with time and is not constant as has been assumed by some authors.

Experiments on the nucleation and development of pits in different types of steel have shown that the majority of the pits nucleate within the initial stages. Later, the number of pits is constant. During any

period of time, the majority of the pits have the same size and depth, signifying that the growth rate is the same.

2.7.3 Potentiostatic Measurements

Under potentiostatic conditions, corrosion rate increases temporarily according to the current-time curves. Apart from transient phenomena in the vicinity of the pitting potential (which can be attributed to repassivation effects) the current-time curves have uniformly ascending shapes. Engell and Stolica[20] have shown that the rate of development of pits, characterized by the increase of the current at a constant potential, is given by:

$$i = kt^b$$

where t is the time and k is a constant dependent upon the concentration of Cl^- ions. The exponent b equals 2 when the number of pits, N, is constant in time, and equals 3 when the pit number is proportional to t. The basic assumptions underlining the above equation are that the pits are hemispherical in shape and that the current density in the pit is constant. If this is true, then the radius of the pits, r, should increase proportionately with time.

The validity of the above equation has been confirmed many times. However, the exponent b is not always 2 or 3, and also not always a linear dependence of r upon t and N upon t is observed.

In a study[51] of the pitting corrosion of 16 Cr - Fe alloy in sulfate solutions containing chloride ions, the value of b has been found to depend on the ratio of Cl^-/SO_4^{2-}. The lower this ratio, the higher is the exponent b. For example, at constant potentials, when $Cl^-/SO_4^{2-} = 0.29$, b = 4-5 and $N \propto t^3$; while when $Cl^-/SO_4^{2-} = 0.43$, b = 2 and $N \propto t^2$.

Stolica's[52] observations of the rate of pitting in a 15 Cr - Fe alloy in 1 N H_2SO_4 + 0.32 N Cl^- showed that the radial growth of the largest pit is proportional to time, but the number of pits is approximately proportional to t^n, where $n > 1$.

Apart from the various steels, substantial work has also been done on the pitting corrosion kinetics of nickel. Studying the corrosion of nickel in 1 N H_2SO_4 with additions of Cl^- ions, Gressman[53] found that the value of $b = 3$.

Exponent b smaller than 2 has been noticed by Garz et al.[48] who performed electrochemical and metallographic studies of Ni single crystals anodically polarized in 0.5 M $NiCl_2$. They found that the increase of the current during pitting occurs in agreement with Engell and Stolica's equation, but the exponent b is less than 2 and depends upon the crystallographic orientation. For {100} and {110} planes they obtained b values of 0.6 and 0.3 respectively, whereas for the {111} plane, the value is 1 when the pits are triangular and 1.5 when they are hexagonal. They always obtained crystallographic pits, and not hemispherical ones for which Engell and Stolica deduced the equation.

Investigations[54] of the pitting corrosion of nickel in solutions containing different concentrations of SO_4^{2-} and Cl^- ions at various pH values showed that within the range of equivalent Cl^-/SO_4^{2-} ratios from 0.15 to 2.5, the current increases with t^b, but the values of b are either higher (at a low ratio of Cl^-/SO_4^{2-}) or lower than 1 (at higher ratios of Cl^-/SO_4^{2-}), independent of the pH of the given solution.

Thus, as is evident from the available experimental data, Engell and Stolica's[20] model of hemispherical pits is not valid for all cases of

pitting corrosion. Other models are required which can explain the observed kinetics of pit growth and the resultant morphology of corrosion pits.

CHAPTER III

EXPERIMENTAL PROCEDURE

3.1 Material used

All experiments in the present study have been performed on polycrystalline nickel in various metallurgical conditions. The nickel was graciously supplied by Dr. L. A. Morris, Research Laboratories, Falconbridge Nickel Mines Ltd. A typical analysis is given below.

Element	Analysis in ppm by wt.
O_2	14
N_2	2
H_2	1.5
C	15
P	<2
S	5
Pb	8
Al	<1
Ca	3
Cr	<0.6
Co	60
Cu	8
Fe	40
Mg	<1
Mn	<0.7
Si	5
Ti	<1

The material was received as cold-rolled sheets prepared directly from electrolytic cathode.

3.2 Preparation of Specimen

Samples of 6 mm x 6 mm were cut from the sheet and a lead wire was soldered in the centre on one side. The sample mount consisted of a Teflon tablet 12 mm in diameter and 5 mm thick with a 1 mm diameter hole through it. On one side of this tablet, there was a deep cavity to accommodate the soldered head of the sample. The soldered sample was mounted on this tablet with resin, taking care to see that the mounting was horizontal. The outer periphery of the disc had threads so that it could be screwed onto the specimen holder.

The possibility of the presence of crevices cannot be completely ruled out. As has been pointed out by Wilde,[55] the presence of crevices leads to premature breakdown of passivity and, therefore, is prejudicial to material evaluation. In the present investigation, the test specimen was thoroughly checked under an optical microscope for crevices prior to its insertion into the corrosion cell. After completion of an experiment, the specimen surface was again checked, and in cases where crevice corrosion had taken place the data was disregarded. However, with careful specimen preparation, crevice corrosion did not pose any problem throughout this investigation.

3.3 Description of the Set-up

3.3.1 Corrosion Cell Assembly

The corrosion cell consisted of a cylindrical glass container with a removable top cover (Figure 5). The cell capacity was 300 ml. A thin glass window was incorporated in the bottom of the cell to permit observation and photomicrography in-situ, if required, when the cell was placed

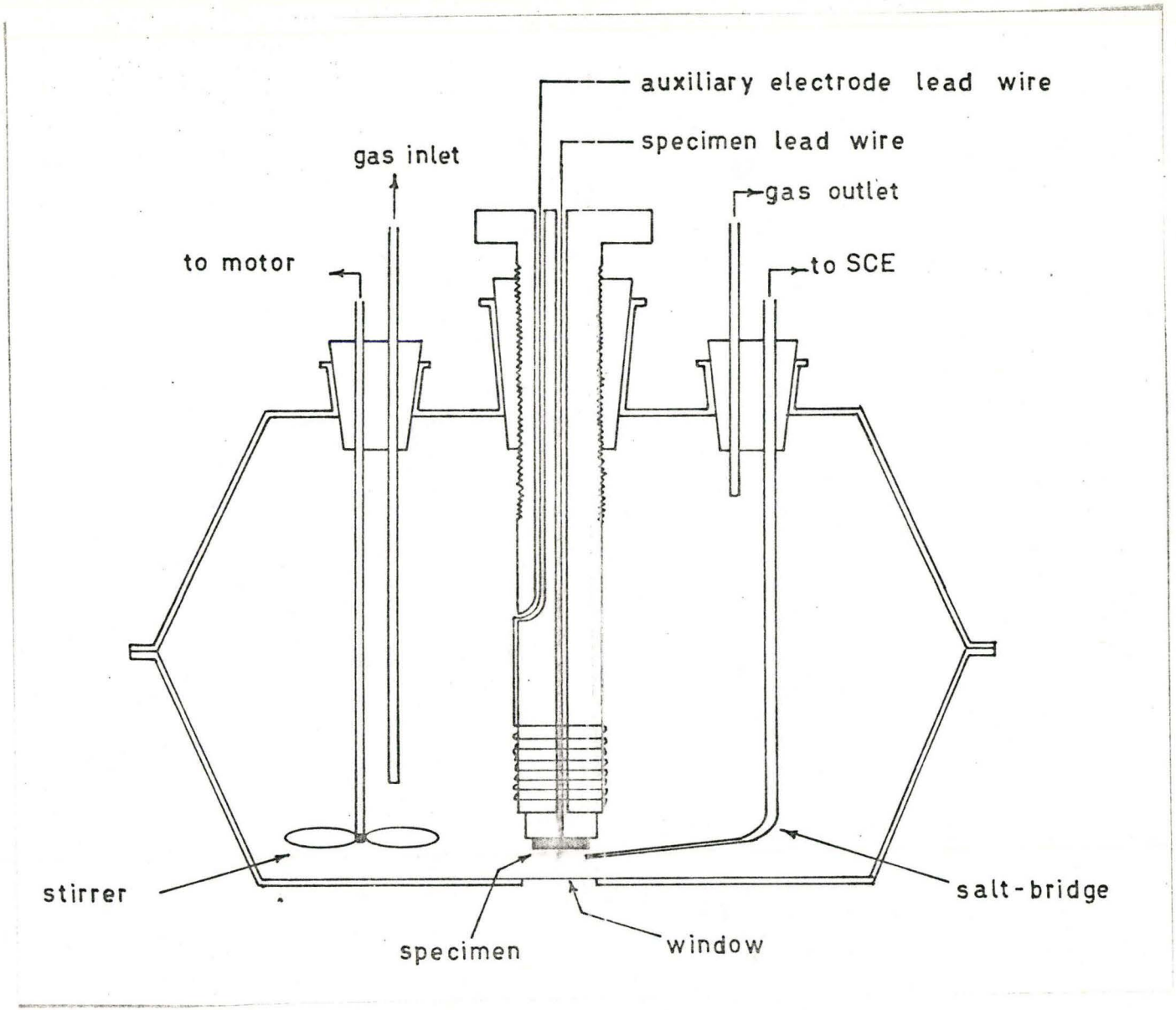

Figure 5. Schematic diagram of the corrosion cell. The window for in-situ microscopic observations is at the bottom.

on the stage of a Zeiss "inverted" Metal Microscope. The top cover was fixed by means of springs. There were openings in the cover to accommodate the specimen holder, salt bridge, gas inlet and outlet and the stirrer.

The specimen holder was made of Teflon and fitted the cell in such a way that it could be raised or lowered by screwing in or out. The specimen could be screwed onto the holder at the lower end. The auxiliary electrode was a Platinum wire wound at the lower end of the holder. The lead wires passed through the holder out of the cell.

3.3.2 Potential Measuring Device

All potential measurements were carried out versus the Saturated Calomel Electrode (SCE) using an agar-agar salt bridge. Care was taken to see that the 'pick-up' end of the salt bridge was very close to the specimen surface. All values of potential reported are as recorded with no correction being made for any junction potentials.

3.3.3 Polarization Circuit

A conventional potentiostatic circuit was used (Figure 6). It consisted of a Wenking potentiostat and a Keithley electrometer for the measurement of potential.

3.3.4 Purification of Nitrogen

The atmosphere within the corrosion cell was maintained inert by bubbling pure dry nitrogen. Pure nitrogen* was further purified by passing it over copper turnings at 400^0C, cooled in a coiled glass water column and dried in 3 N H_2SO_4 before entering the corrosion cell.

---

*Canadian Liquid Air Ltd. 'L-Grade'. Purity - 99.99%; oxygen 20 ppm max., argon 80 ppm; moisture < 10 ppm (dew point - 76^0F)

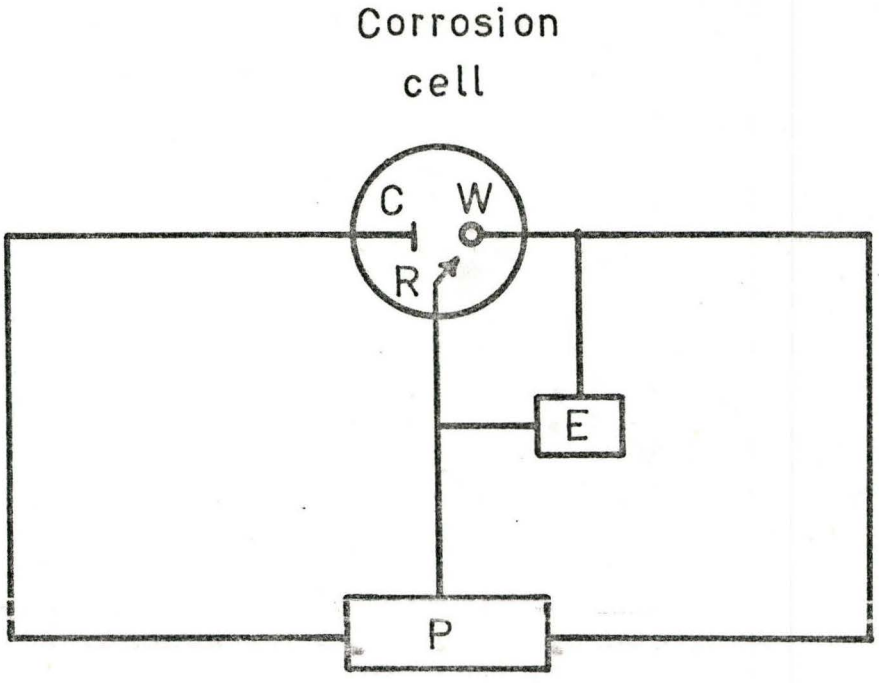

Figure 6. The circuit diagram for potentiostatic studies
W - working electrode (specimen)
C - counter or auxiliary electrode (Pt)
R - reference electrode (SCE)
P - Wenking potentiostat, Model 62TRS
E - Keithley electrometer, Model 610C

3.4 Polishing and Etching of Specimen

Specimens were mechanically polished upto 1μ diamond, followed, when required, by an electropolish in a 60% H_2SO_4 solution at 1 amp/cm^2 for 30 secs. In order to completely eliminate etch pitting, it was found necessary to maintain the solution at 0^0C with vigorous mechanical stirring.[56] A stainless steel strip of the same area as the specimen was used as the cathode.

All specimens when removed from the corrosion cell after completion of polarization had their structure clearly revealed and did not require any etching. However, specimens which were directly subjected to a passive potential had to have their micro-structure revealed by etching in a solution of:

Nitric acid (conc.)	50 ml
Acetic acid (ice-cooled)	50 ml

at room temperature for about 5 secs.

In many cases, electrolytic etching was employed prior to polarization. Specimens were etched in 1 N H_2SO_4 solution at 2 amps/cm^2 for 30 secs using a stainless steel cathode.

3.5 Metallurgical Treatments

Two types of metallurgical treatments were given - annealing and cold working. Annealing was done in two ways - in air and in vacuum. For vacuum annealing, the nickel sheet was cut into strips and sealed in a quartz tube under vacuum ($< 10^{-5}$ torr) before placing in the furnace. In both cases, the annealing was carried out in crucible furnaces. The starting material for grain growth anneals was the 1 mm thick, 'as received'

nickel sheet. The temperatures and times used to obtain the various grain sizes are given in Table 1.

Table 1

Grain Size (Av. Gr. Dia.) mm	Temperature °C	Time* hrs.
0.025	500	4
0.035	775	5
0.150	950	72
0.250	1000	77
0.330	1000	100

Following annealing and prior to rolling, the sheet was descaled by grinding off the oxide layer, since all commercial methods of descaling did not succeed. It is important to completely remove the scale prior to cold working, since the penetration of any scale into the metal during rolling will lead to sites susceptible to pitting.

Cold working in the material was induced by rolling. The sheet was cut into strips and rolled to various degrees of cold work, defined as percentage reduction in thickness.

3.6 Determination of Grain Size

The measurement of the grain size was performed as per the ASTM non-ferrous grain size standard.[57] In this method, the grain size of non-ferrous metals and alloys is rated by comparing the microstructure of the unknown specimen, at a magnification of 75X, with standard grain size charts. The grain size is then designated as the average grain

*Time mentioned is from power 'on' to 'off' and does not include the time for furnace cooling.

diameter in mm. For the present measurements, in order to eliminate any ambiguity that may arise due to the presence of the disturbed metal layer left after mechanical polishing, particularly in small grain size specimen, after polishing up to 1μ diamond, the specimens were immersed in the following solution[58]

Nitric Acid (conc.)	30 ml
Sulfuric Acid (conc.)	10 ml
Orthophosphoric acid	10 ml
Acetic Acid (ice-cooled)	50 ml

for 100 secs at 80°C. The thickness reduction in solution is about 12 μm/min.[58] The structure was then revealed by chemical etching.

3.7 Preparation of Solutions

All solutions were prepared from reagent grade materials meeting A.C.S. Specifications using distilled water. The potassium chloride solution used for the SCE was especially prepared for the purpose by Fisher Scientific Company and saturated at 20°C.

3.8 Polarization Techniques

Two types of polarization techniques were employed:

i) "Potentiostatic polarization" - Specimens were anodically polarized from -300 mV to different potentials, depending upon the nature of the experiment. In all cases, the potentiostatic steps were 25 mV/min and an inert atmosphere of dry nitrogen was maintained within the corrosion cell. The polarization solution was 1 N H_2SO_4 containing varying quantities of 1 N NaCl. Prior to use, the solution was deaerated by bubbling pure dry nitrogen for an hour, deaeration being carried out in the corrosion cell.

ii) "Potentiostatic activation" - Specimens were directly subjected to a passive potential in 1 N H_2SO_4 solution and maintained in that condition

for a certain period of time. They were activated by the addition of either saturated NaCl solution (saturated at 25^0 C) or 1 N NaCl solution at a chosen potential.

In both techniques, the polarizing solution was 1 N H_2SO_4 with additions of varying quantities of NaCl (saturated or 1 N), the concentration of Cl^- ions being expressed as volume of NaCl (sat. or 1 N)/100 or 150 ml 1 N H_2SO_4. 150 ml of the solution was used for each test run. The temperature of the solution in all cases was 24 ± 1^0C.

3.9 Sectioning of Specimen

Specimens were sectioned perpendicular to the pitted surface for the determination of pit shapes. In order to preserve the inner details of the pit and to avoid distortion, after polarization copper was electrodeposited for 1-2 mins on the specimens from the following solution

Copper sulfate as $CuSO_4.5\ H_2O$	200 gms/litre
Sulfuric Acid (conc.)	50 gms/liter

at a current density of 0.1 amp/cm^2 using a Pt-anode. The specimens were then metallographically mounted and sectioned.

3.10 Photomicrographic Observations

Photomicrographic observations were made on two types of microscopes:

i) Optical microscope

ii) Scanning electron microscope

All photomicrographic observations of anodic potentiostatic polarization studies were performed after the completion of the experiment.

CHAPTER IV

RESULTS

The two techniques adopted for the present investigation have been termed 'potentiostatic polarization' and 'potentiostatic activation'. The difference in experimental procedures has already been explained. A significant consequence of the two techniques was that the surface film was thicker in the latter case. Whereas the second method was found suitable to study the nature of pit development, for reasons discussed later, it was found unsuitable for susceptibility and anodic dissolution studies.

The variables of this study were polarization technique, metallurgical condition of nickel, grain size and chlorine ion concentration. On the basis of the electrochemical data, optical and scanning electron microscopic observations, the following studies are reported:

i) Effect of grain size and cold work on the pitting susceptibility of nickel

ii) Effect of chlorine ion concentration on the anodic dissolution behaviour of nickel

iii) Distribution of pits

iv) Shape and size of pits

v) Nature of pit development

Except in cases where it is specifically mentioned, all experiments on annealed material were carried out on nickel which had been annealed in air.

4.1 Electrochemical Studies

The addition of Cl^- ions to a solution containing a potentiostatically passivated annealed nickel electrode resulted in an increase of the anodic current. Figure 7 shows the anodic current density as a function of time after the addition of Cl^- ions. Microscopic examination of the specimen surface revealed a large number of pits. Thus, pitting corrosion is accompanied by an increase of the anodic current density. An obvious question arises regarding the sites of pit nucleation. It may be seen from Figures 8(a) and 8(b) that pits nucleate at the grain boundaries, particularly at grain boundary intersections.

4.1.1 Pitting Susceptibility of Nickel

4.1.1 (a) Effect of Grain Size

If in a homogeneous and strain free material pits nucleate at the grain boundaries, then the formation of pits is expected to be a direct function of grain size. Thus, the smaller the grain size, the larger will be the grain boundary area, and greater will be the susceptibility for pitting.

Specimen of four grain sizes were potentiostatically polarized in a solution containing 2 ml 1 N NaCl/100 ml 1 N H_2SO_4. The anodic polarization curves for the four grain sizes are shown in Figure 9 and the anodic dissolution parameters are summarized in Table 2. It can be seen that while all specimens upto a grain size of 0.150 mm exhibit an active-passive transition, specimen with a grain size of 0.330 mm does not.

For the specimens that exhibit an active-passive transition, it is to be noted that as the grain size increases from 0.025 mm to 0.150 mm, the 'activity' of the specimen (as evident from the values of E_{pp}, I_c

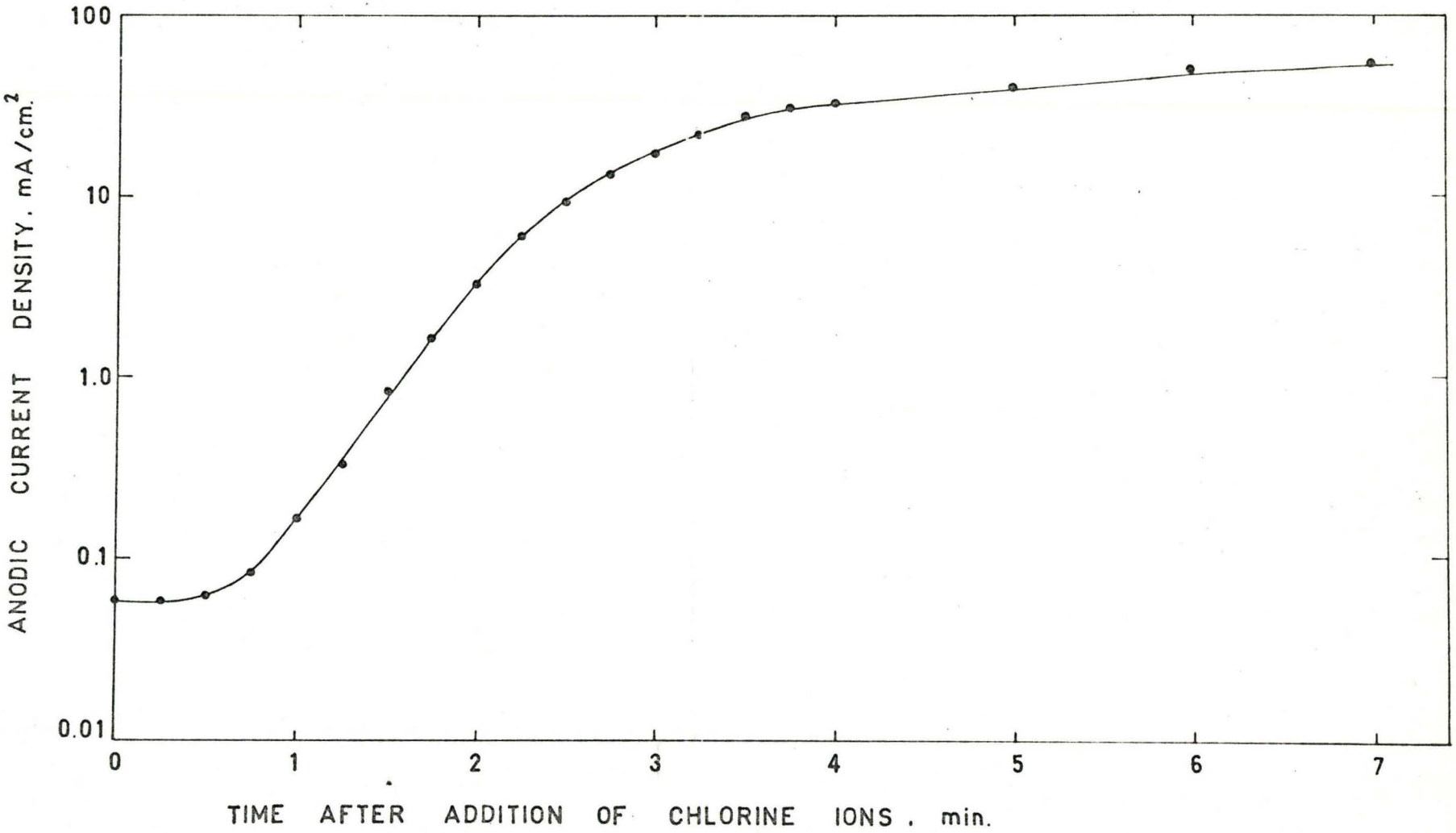

Figure 7. Anodic current density as a function of time after addition of chlorine ions for a potentiostatically passivated polycrystalline nickel electrode.
Passivation - 150 ml 1 N H_2SO_4 at 550 mV for 30 mins.
Activation - 3 ml sat. NaCl/150 ml 1 N H_2SO_4 at 650 mV
Note that there is an induction period before the anodic current density increases.

Figure 8(a). Surface of specimen of figure 7 after pitting corrosion. Un-etched. 80X

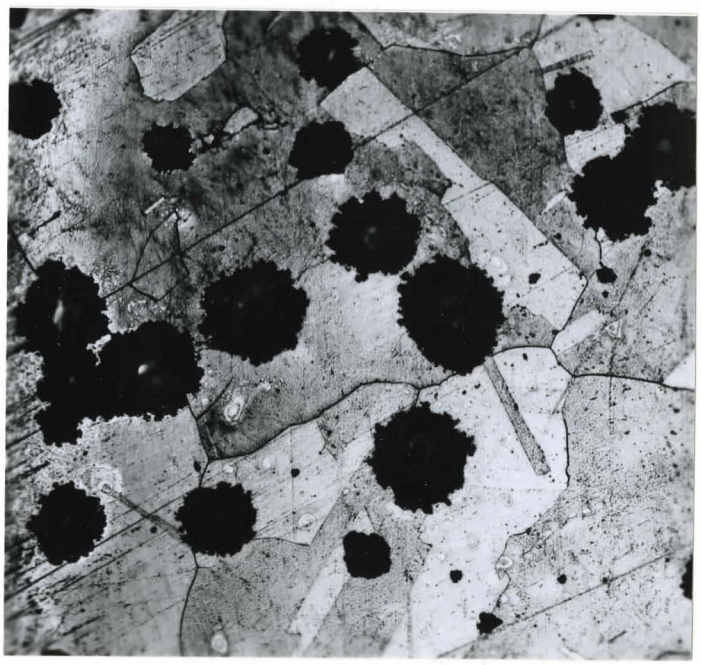

Figure 8(b). Same as in figure 8(a). Etched. 80X. Note that pits are formed at the grain boundaries

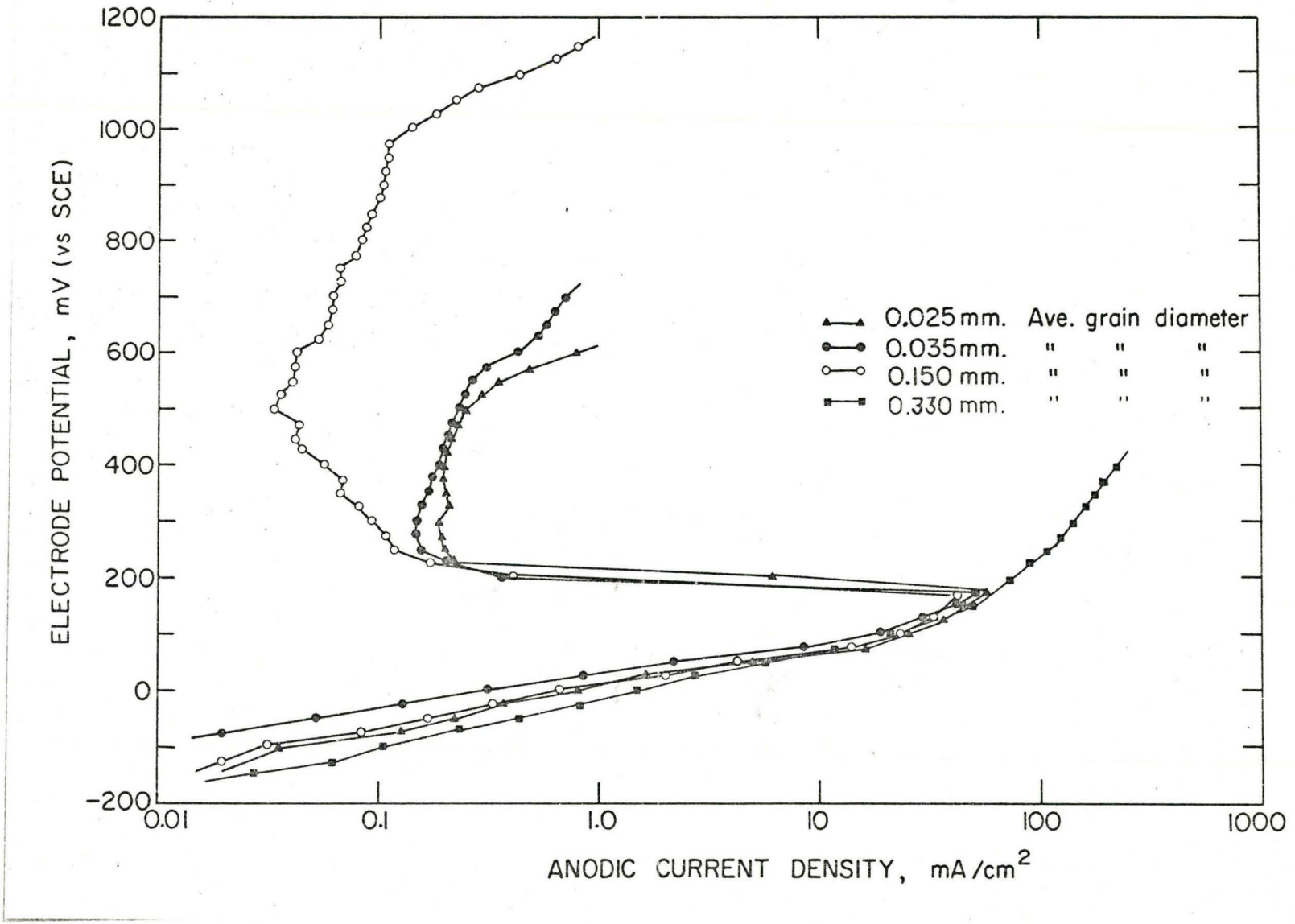

Figure 9. Anodic polarization curves for polycrystalline nickel of varying grain size (air grown) in 2 ml 1 N NaCl/100 ml 1 N H_2SO_4.

Table 2

Anodic dissolution parameters for polycrystalline nickel of varying grain size in 2 ml 1 N NaCl/100 ml 1 N H_2SO_4

Specimen	ASTM non-ferrous grain size standard Average grain diameter mm	E_{pp} mV vs SCE	I_c mA/cm^2	I_p mA/cm^2	E_c mV vs SCE	Passive Range mV vs SCE
G-1	0.025	+175	54.7	0.189	+500	+325
G-2	0.035	+175	50.0	0.153	+575	+400
G-3	0.150	+150	43.6	0.042	+975	+825
G-4	0.330	No 'passive' region				

and I_p) decreases. It is apparent from the data presented that the more active specimen exhibits a greater susceptibility for pitting.

The surface of the specimens after completion of polarization are shown in Figure 10 to 13. It is interesting to note that in specimen G-1 (Figure 10) apart from the presence of individual pits at the grain boundaries, there is deep grain boundary grooving. In specimen G-2 (Figure 11), this grain boundary grooving is again present, but is less severe than in specimen G-1. There is, however, no evidence of this phenomenon in specimen G-3 (Figure 12). Another interesting feature is that for the same area of specimen surface, the less susceptible specimen exhibits a smaller number of pits.

A deviation from the expected behaviour exists for specimen G-4 with a grain size of 0.330 mm. It does not exhibit an active-passive transition. Instead the anodic current density shows a continuous increase with potential. Microscopic examination of the specimen surface reveals a mixture of attack consisting of general corrosion in some areas, pitting within the grains and deep grain boundary corrosion (Figure 13).

It can, therefore, be seen that a significant difference exists in the electrochemical behaviour and consequently, the nature of metallographic attack on the surface of the specimens with grain sizes of 0.150 mm and 0.330 mm. Since the experimental procedure after grain growth was the same for every specimen, it was felt that the observed difference could be due to the grain growth procedure. The required grain sizes in the above cases had been obtained by annealing in air (Table 1). Thus, for a second set, grain growth was carried out by annealing in vacuum ($<10^{-5}$ torr). When a specimen of grain size 0.330 mm (grain growth carried out by annealing

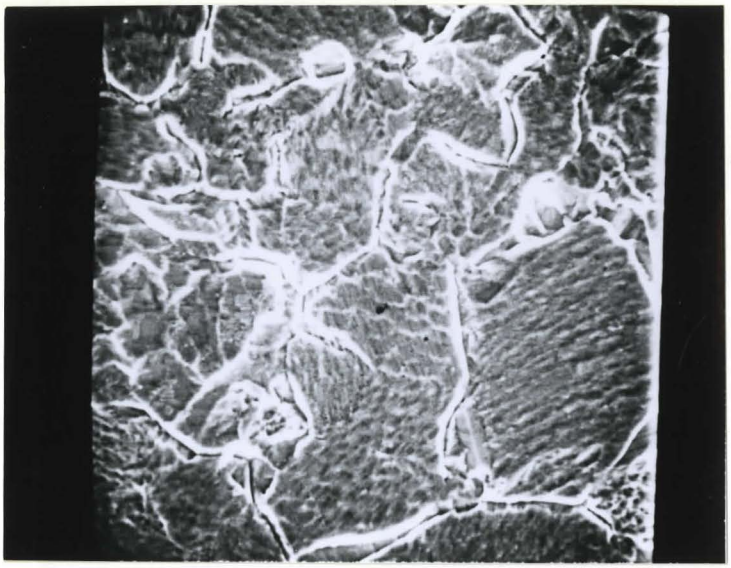

Figure 10. Pits at the grain boundaries, 1050X. Specimen G-1. Average grain dia. = 0.025 mm. Note the deep grain boundary grooving

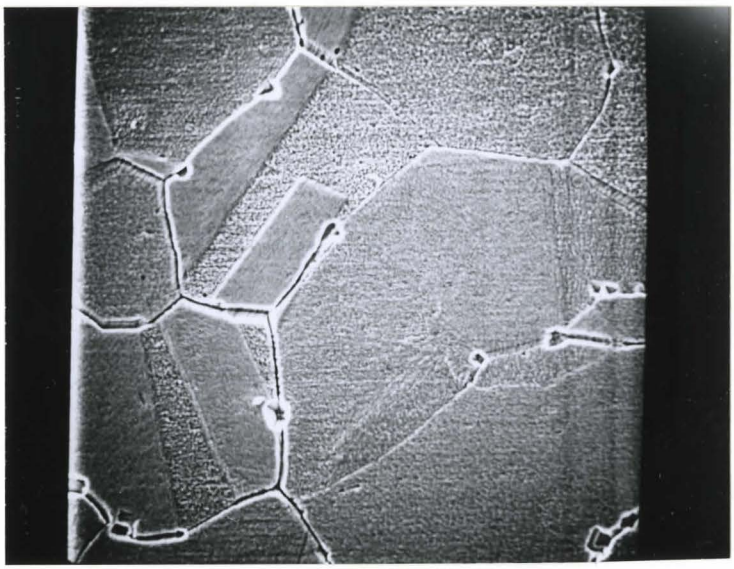

Figure 11. Pits at the grain boundaries, 560X. Specimen G-2. Average grain dia. = 0.035 mm. Note that the grain boundary grooving is again present, but is less severe than in specimen G-1.

Figure 12. Pits at the grain boundary, 200X. Specimen G-3. Average grain dia. = 0.150 mm. Note that grain boundary grooving is absent.

Figure 13. Attack on surface of specimen, 80X. Specimen G-4. Average grain dia. = 0.330 mm. Note that the attack is a mixture of general corrosion, pitting and deep grain boundary corrosion.

in vacuum) was potentiostatically polarized in 2 ml 1 N NaCl/100 ml 1 N H_2SO_4, the specimen exhibited an active-passive transition (Figure 14). Pits were formed within the grain interiors only and almost no attack existed along the grain boundaries (Figure 15). In-situ microscopic observations revealed that the majority of the pits were formed in the active region, i.e. before the onset of passivity. This was a general observation in the case of vacuum annealed specimens and was not observed for air annealed ones.

4.1.1 (b) Effect of Cold Work

Since pitting corrosion is a direct consequence of a localized anodic reaction, it depends upon the anodic-cathodic site distribution. It should remain unchanged for any particular specimen, if the site distribution remains unaltered. It would, therefore, be expected that any process which can change the distribution of these sites would affect pitting corrosion. For a specimen of the same grain size, the site distribution may be altered by cold working.

The effect of cold work on the pitting susceptibility of nickel was tested for specimen of grain size 0.250 mm with varying amounts of cold work. The anodic polarization curves obtained are shown in Figure 16 while the anodic dissolution parameters are summarized in Table 3. It may be noted that, with the exception of specimen C-4, an increase in the degree of cold working increases the critical current density, I_c. However, without exception, the current density required to maintain passivity increases with increase in cold work. It is interesting to note that the primary passive potential and the critical potential for the

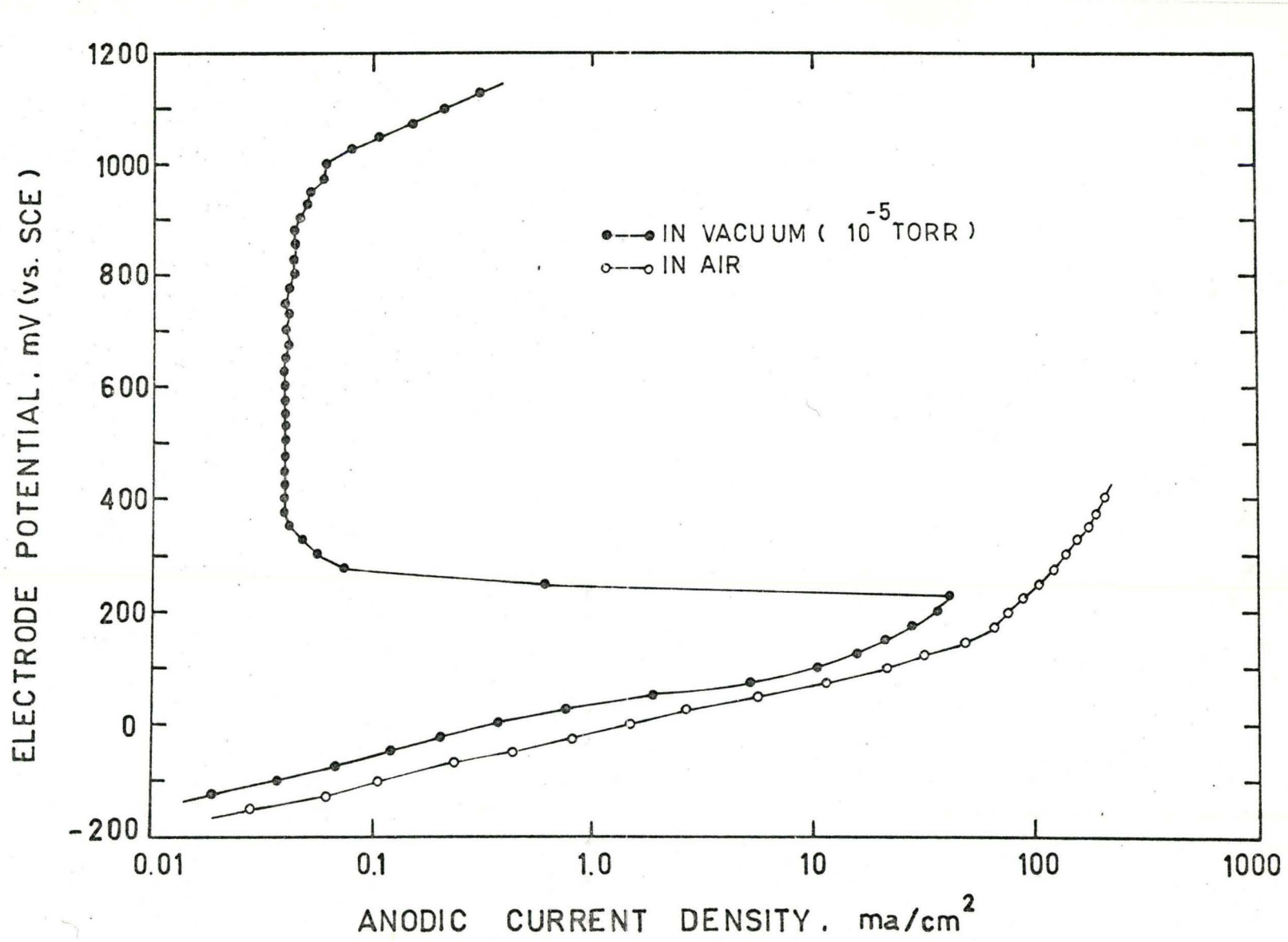

Figure 14. Anodic polarization curves for polycrystalline nickel of the same grain size (0.330 mm), grown in different atmosphere in 2 ml 1 N NaCl/100 ml 1 N H_2SO_4.

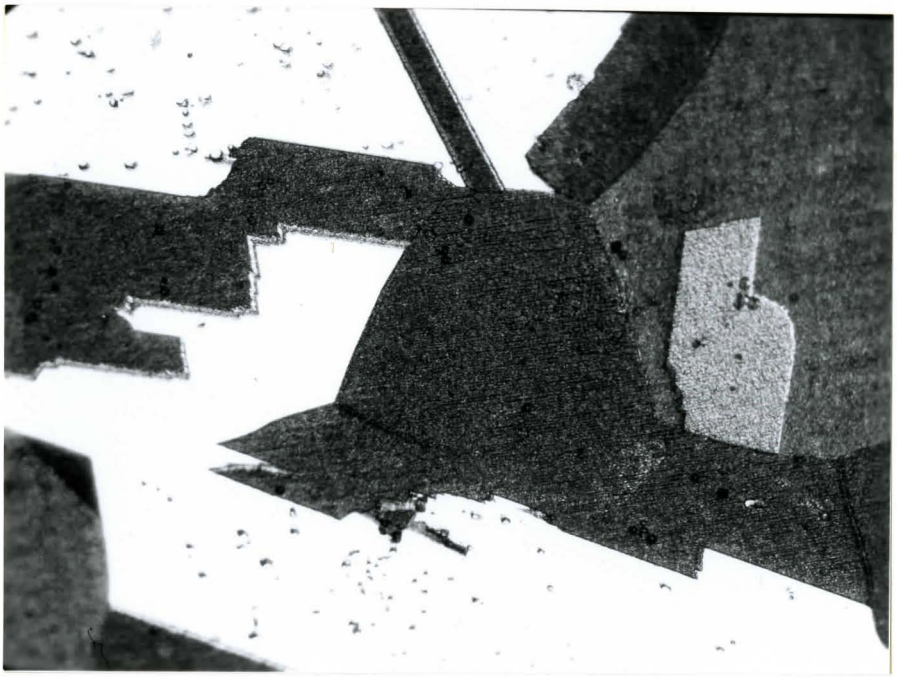

Figure 15. Surface of specimen of grain size. 0.330 mm (vacuum grown) after potentiostatic polarization in 2 ml 1 N NaCl/100 ml 1 N H_2SO_4. 160X. Note that pits are formed only within the grains and no attack exists along the grain boundaries.

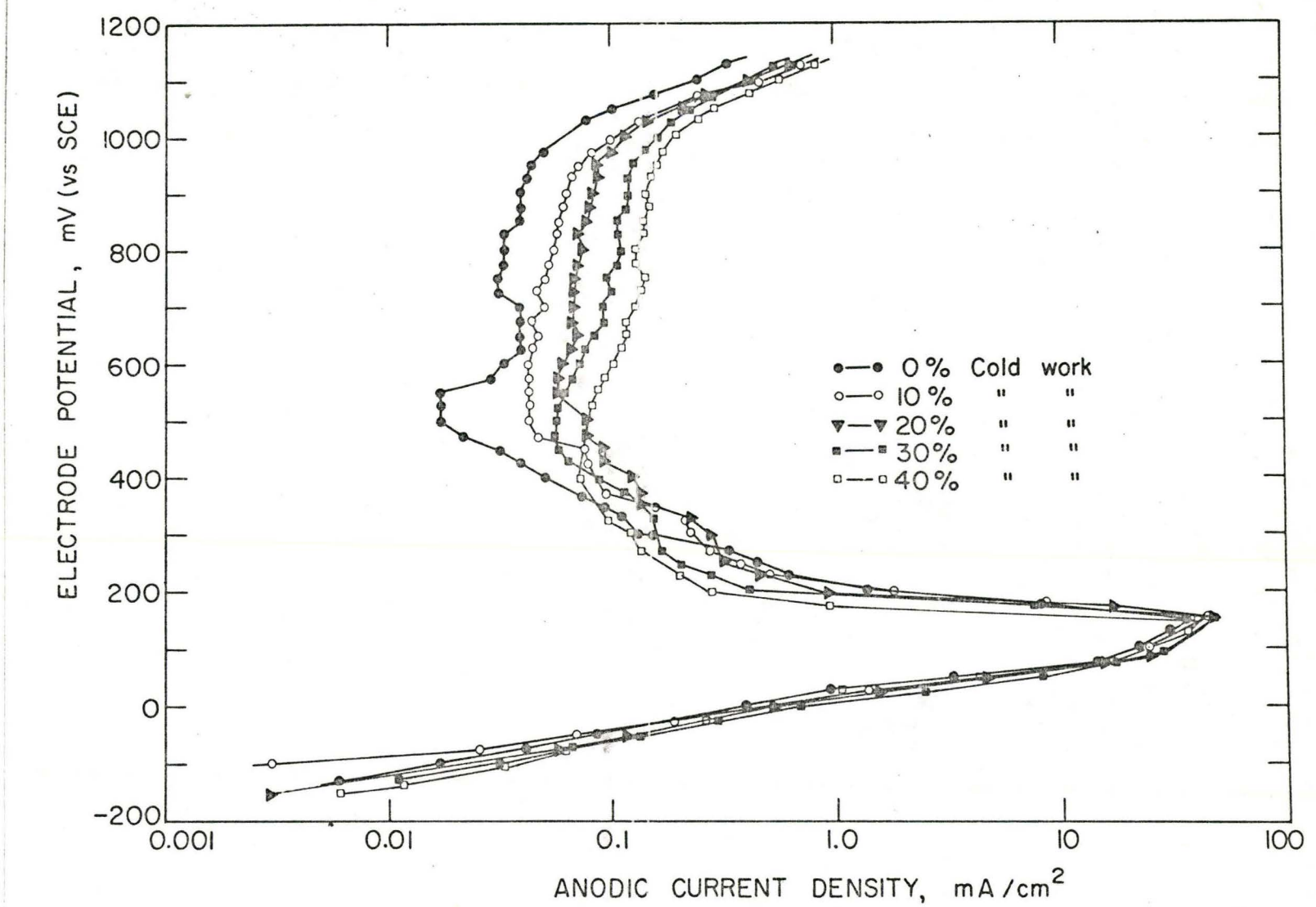

Figure 16. Anodic polarization curves for polycrystalline nickel with varying amounts of cold work in 2 ml 1 N NaCl/100 ml 1 N H_2SO_4. Grain size = 0.250 mm, grown in air.

Table 3

Anodic dissolution parameters for polycrystalline nickel with varying amount of cold work in 2 ml 1 N NaCl/100 ml 1 N H_2SO_4
Grain grown in air

Specimen	Amount of Cold Work %	E_{corr} mV vs SCE	E_{pp} mV vs SCE	I_c mA/cm^2	I_p mA/cm^2 lowest recorded value	I_p mA/cm^2 at 800 mV	E_c mV vs SCE
C-0	0	-160	+150	36.1	0.017	0.033	+950
C-1	10	-120	+150	44.7	0.042	0.056	+950
C-2	20	-220	+150	45.0	0.056	0.075	+950
C-3	30	-145	+150	45.0	0.056	0.111	+950
C-4	40	-240	+150	37.5	0.072	0.128	+950

breakdown of passivity do not exhibit any dependance on the degree of cold work. It can, therefore, be concluded that cold working does not have any effect on the pitting susceptibility of nickel. Microscopic examination of the specimens after removal from the polarization cell revealed pits to be nucleated not only along the grain boundaries but also within the grains. The number of pits within the grains did not change significantly with cold work but pitting along the grain boundaries tended to become continuous. The anodic Tafel slopes, β_a, and the slopes in the transpassive region, β_t, are given in Table 4.

When the above experiment was repeated with specimen with the same grain size and degree of cold work, but with the grain growth having been carried out in vacuum ($<10^{-5}$ torr), similar results were obtained. Figure 17 shows the anodic polarization curves and Table 5 contains the anodic dissolution parameters. In comparison to the results obtained for air annealed specimen, it may be noted that, except for minor differences, the values of I_c and I_p are of the same order of magnitude; the value of E_c is exactly the same. However, the value of E_{pp} is higher. Pits were formed within the grains and only a counted few nucleated at the grain boundaries. There was no significant change in the number of pits with increasing cold work. In-situ microscopic observations revealed that most of the pits were formed before passivity set in. The anodic Tafel slopes and the slopes in the transpassive region are reported in Table 4.

4.1.2 Effect of Chlorine Ion Concentration on the Anodic Dissolution Behaviour of Nickel

In all the studies that have been conducted, the specimens were 'activated' by the addition of Cl^- ions. Whatever is the mode by which

Table 4

Anodic "Tafel" slopes and "transpassive" slopes for polycrystalline nickel with varying amount of cold work in 2 ml 1 N NaCl/100 ml 1 N H_2SO_4

Amount of Cold Work %	Annealed in Air		Annealed in Vacuum	
	Tafel βa mV/decade	Transpassive βt mV/decade	Tafel βa mV/decade	Transpassive βt mV/decade
0	70	160	95	152
10	65	140	95	172
20	70	160	95	142
30	72	200	92	157
40	72	160	92	180

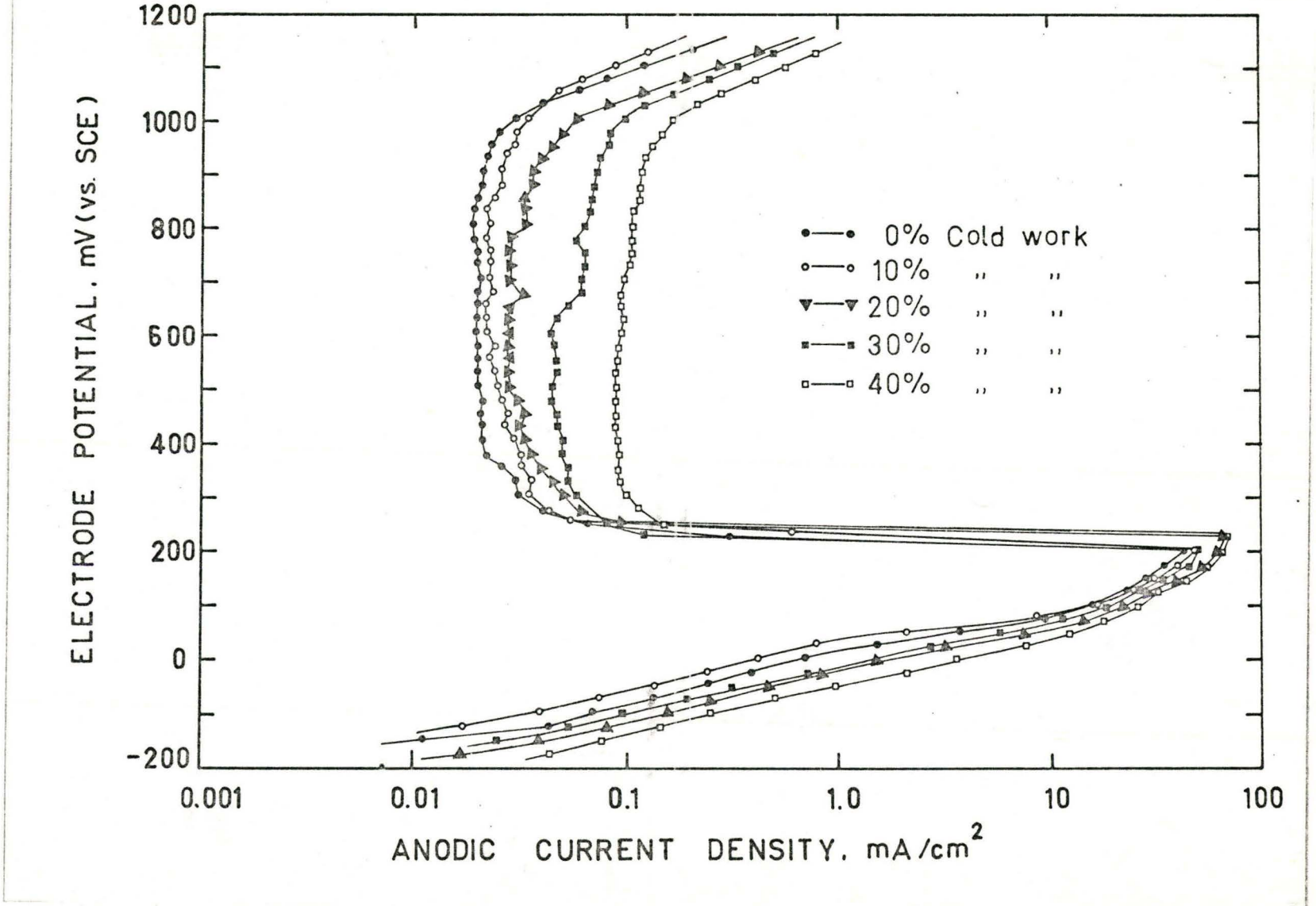

Figure 17. Anodic polarization curves for polycrystalline nickel with varying amounts of cold work in 2 ml 1 N NaCl/100 ml 1 N H_2SO_4. Grain size = 0.250 mm, grown in vacuum (<10^{-5} torr).

Table 5

Anodic dissolution parameters for polycrystalline nickel with varying amount of cold work in 2 ml 1 N NaCl/100 ml 1 N H_2SO_4
Grain growth in vacuum (<10^{-5} torr)

Specimen	Amount of Cold Work %	E_{corr} mV vs SCE	E_{pp} mV vs SCE	I_c mA/cm^2	I_p mA/cm^2 lowest recorded value	I_p mA/cm^2 at 800 mV	E_c mV vs SCE
C'-0	0	-170	200	41.9	0.019	0.019	+950
C'-1	10	-180	200	46.1	0.022	0.023	+950
C'-2	20	-245	225	66.1	0.028	0.033	+950
C'-3	30	-260	200	47.2	0.044	0.064	+950
C'-4	40	-345	225	69.4	0.032	0.108	+950

the Cl^- ion acts, its importance in the destruction of passivity cannot be doubted. The effect of the change in the Cl^- ion concentration on the anodic dissolution behaviour of nickel is presented below.

Figure 18 shows the specimen surface after anodic polarization in a solution containing 2 ml 1 N NaCl/100 ml 1 N H_2SO_4. The pits are seen along grain boundaries, particularly at grain boundary intersections. There seems to be almost no localized attack within the grain interiors.

When the concentration of Cl^- ions in the polarizing solution is increased to 4 ml 1 N NaCl, the attack begins to spread out. It can be seen from Figure 19(a) and 19(b) that the attack within the grains is very crystallographic in nature.

A further increase of Cl^- ions to 8 ml 1 N NaCl intensifies the corrosion, but not to the extent where the pitting attack along the grain boundaries cannot be distinguished (Figure 20(a) and 20(b)). In fact, as the Cl^- ion concentration increases, the surface area covered by general attack increases. When the polarizing solution contains 10 ml 1 N NaCl, the attack over the entire specimen surface becomes so intense that grain boundary attack cannot be distinguished. In any particular grain, the attack is very crystallographic in nature (Figure 21(a)). Even over the entire specimen surface, there is a remarkable regularity of the crystallographic attack (Figure 21(b)). In the solutions mentioned above, all specimens exhibited an active-passive transition and a critical potential for the breakdown of passivity, E_c, was observed. Figure 22 contains the anodic polarization curves and Table 6 summarizes the anodic dissolution parameters and also contains remarks on the morphological details of the specimen surface. The horizontal bars in the curve for specimen A-4 in

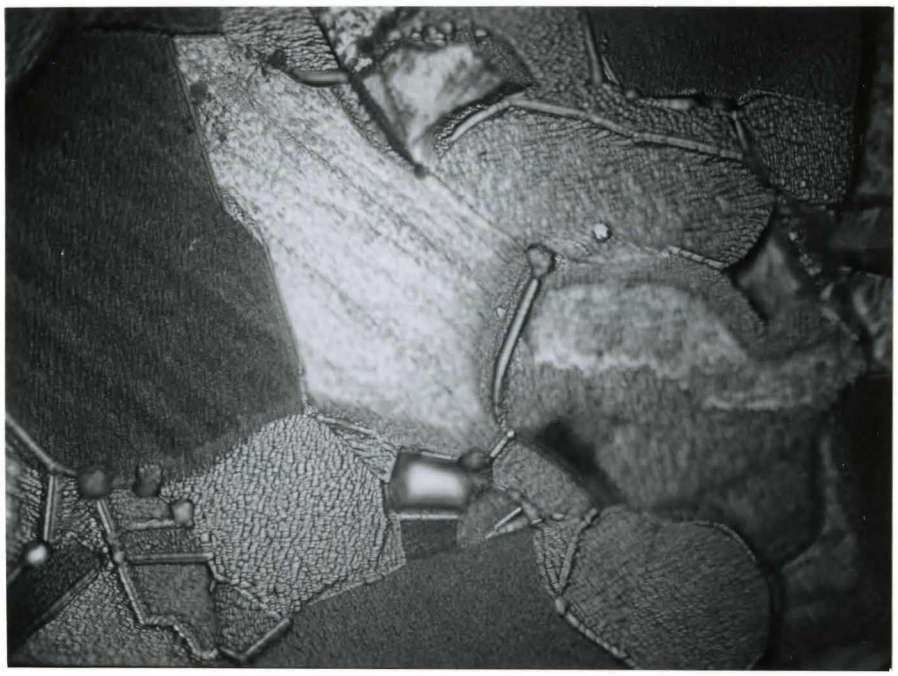

Figure 18. Surface of specimen A-1 polarized in 2 ml 1 N NaCl/100 ml 1 N H_2SO_4, 160X. Pits are formed at the grain boundaries and no attack is seen within the grains.

Figure 19(a). Surface of specimen A-2 polarized in 4 ml 1 N NaCl/100 ml 1 N H_2SO_4, 160X. Pits are still formed at the grain boundaries, but the attack spreads to the grains as well.

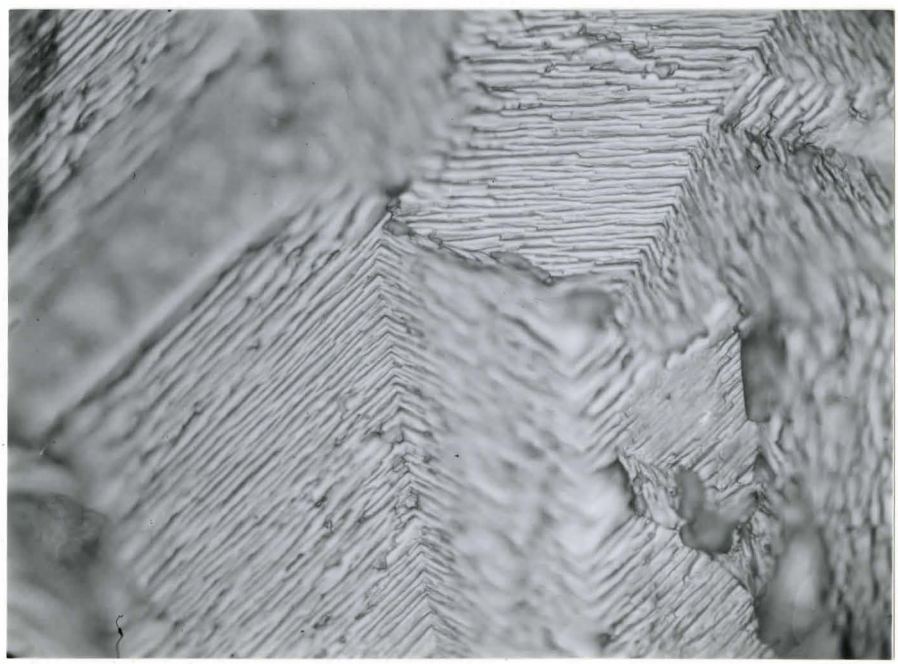

Figure 19(b). Magnified view of the attack, 400X. The attack within the grains is very crystallographic.

Figure 20(a). Surface of specimen A-3 polarized in 8 ml 1 N NaCl/100 ml 1 N H_2SO_4. 400X. The pitting attack along the grain boundaries can still be distinguished from the attack within the grains.

Figure 20(b). Magnified view of the grain interior attack. 620X. The appearance of the surface is typical of general corrosion.

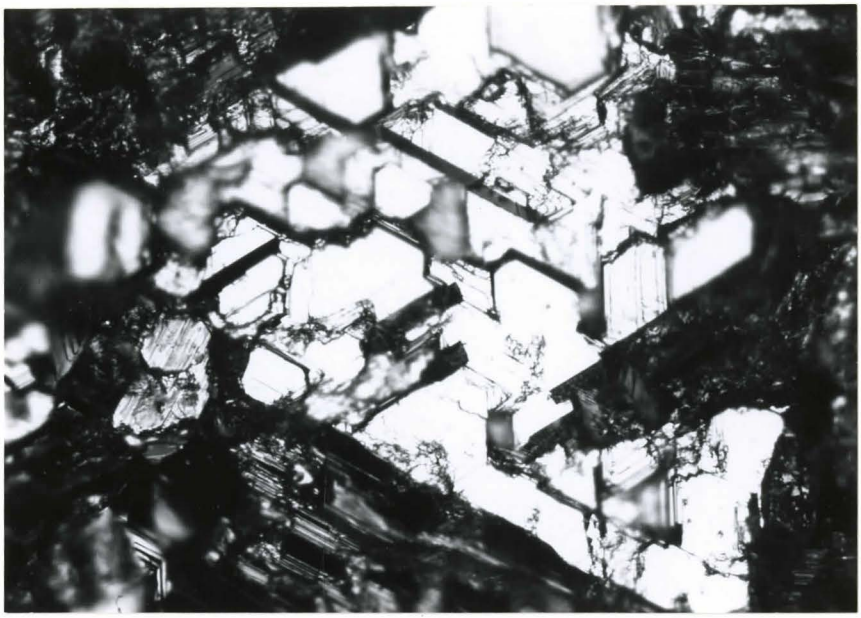

Figure 21(a). Surface of specimen A-4 polarized in 10 ml 1 N NaCl/100 ml 1 N H_2SO_4. 248X. The attack along the grains and the grain boundary cannot be specifically distinguished.

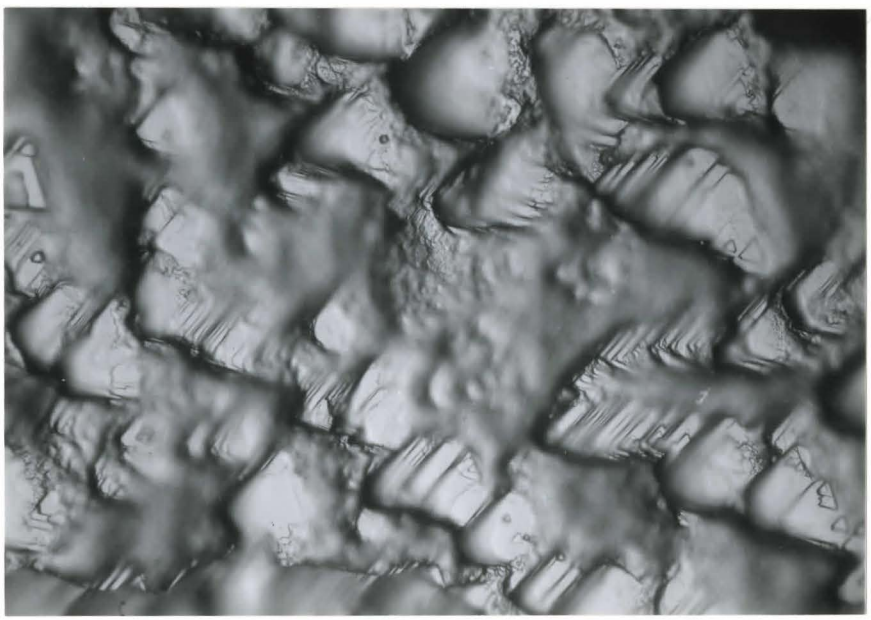

Figure 21(b). Magnified view of attack on surface. 400X. The attack is crystallographic and typical of heavy general corrosion.

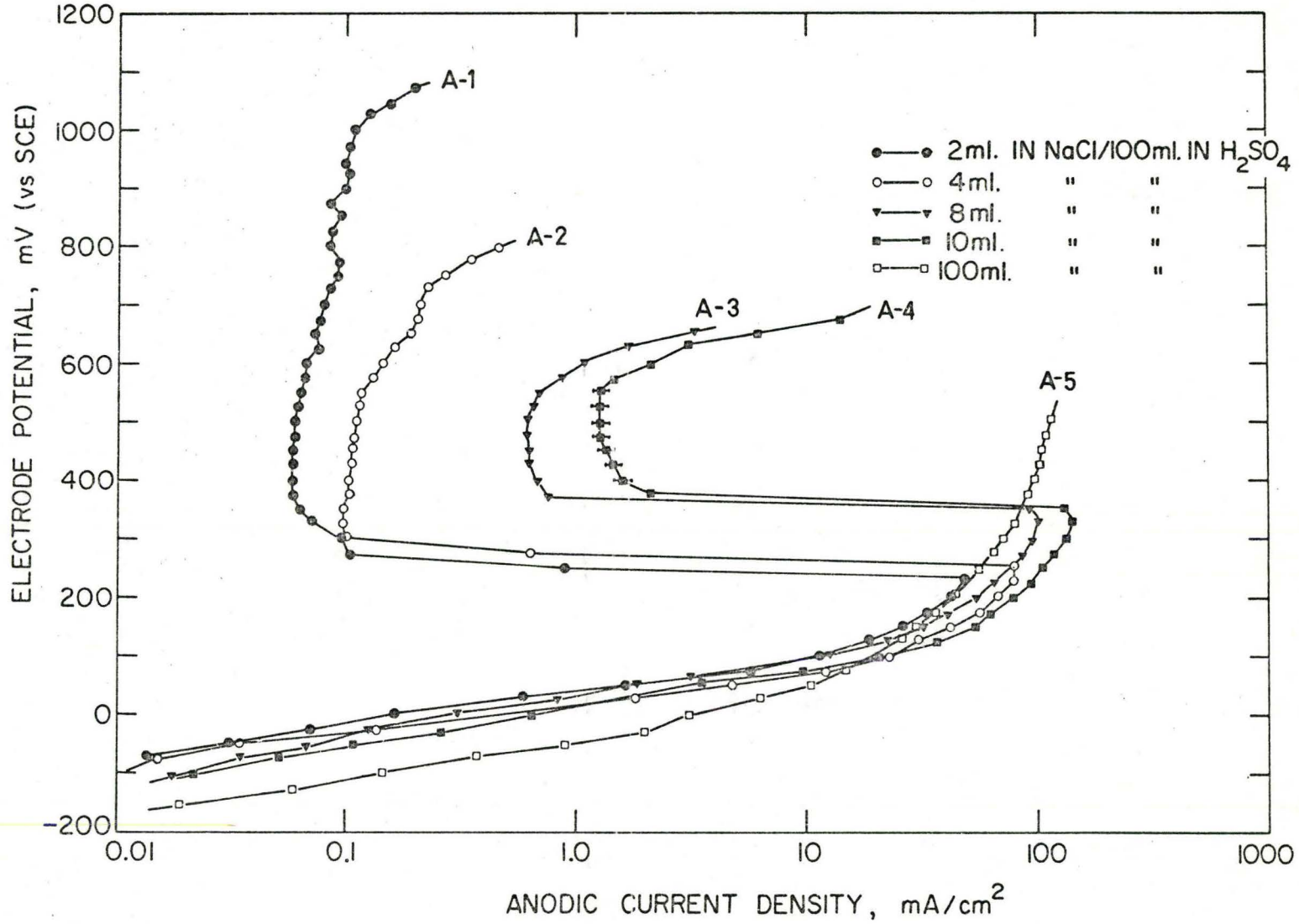

Figure 22. Anodic polarization curves for polycrystalline nickel in solutions of varying chlorine ion concentration. Grain size = 0.035 mm, grown in air.

Table 6

Anodic dissolution parameters for polycrystalline nickel in solutions of varying chlorine ion concentration

Specimen	Chlorine ion concentration ml 1 N NaCl/100 ml 1 N H_2SO_4	E_{pp} mV vs SCE	I_c mA/cm^2	I_p mA/cm^2	E_c mV vs SCE	Morphological appearance of surface
A-1	2	+225	48.4	0.058	+1000	Pits along grain boundaries particularly at grain boundary intersections. No attack on grain interiors.
A-2	4	+250	78.9	0.102	+700	Pits along grain boundaries. Attack on grain interior; very crystallographic in nature.
A-3	8	+325	102.7	0.621	+550	Same as before, but attack more intense. Pitting along grain boundaries still distinguishable.
A-4	10	+325	140.0	1.280	+550	Very intense attack. Corrosion between grains and boundaries indistinguishable Attack very highly crystallographic in nature.
A-5	100	No "passive" region				Highly corroded surface. Nature of attack same as in previous case, but more intense and less crystallographic.

the passive region, signify the occurrence of fluctuations in the anodic current density, the plotted points representing mean values.

It is to be noted from Figure 22 that the specimen polarized in a solution containing 100 ml 1 N NaCl/100 ml 1 N H_2SO_4 does not exhibit an 'active-passive' transition. Instead, the anodic current density increases continuously with increasing potential. Figures 23(a) and 23(b) are photomicrographs of this specimen. Except for showing a surface which is more corroded, they exhibit a remarkable resemblance to Figures 21(a) and 21(b) from the surface of the specimen which exhibited a 'passive' region.

4.2 Corrosion Morphology

4.2.1 Distribution of Pits

The data presented earlier show that under potentiostatic polarization, depending upon the condition of the nickel and the polarizing solution, the distribution of pits and, in some cases, the nature of attack varies. A summary of the pit distribution will be presented at the end of this section.

When a specimen with a grain size of 0.330 mm (air grown) is potentiostatically activated at 800 mV in a solution containing 10 ml 1 N NaCl/150 ml 1 N H_2SO_4 (passivated at 550 mV for 30 mins in 150 ml 1 N H_2SO_4), pits are nucleated not only along the grain boundaries, but also within the grains (Figure 24). It can be seen that the pits in the grain interiors are small, while those along the grain boundaries are larger. In-situ microscopic observations showed that the pits along the grain boundaries nucleated before those in the grains. The smaller pits are obviously those with a smaller life. It is to be remembered that a specimen from the same

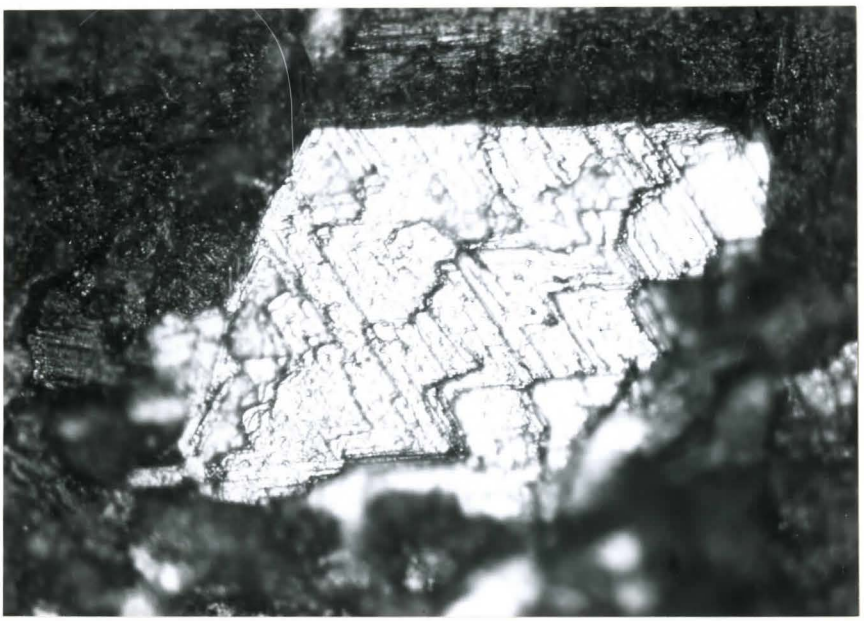

Figure 23(a). Surface of specimen A-5 polarized in 100 ml 1 N NaCl/100 ml 1 N H_2SO_4. 248X. The attack is uniform over the entire surface.

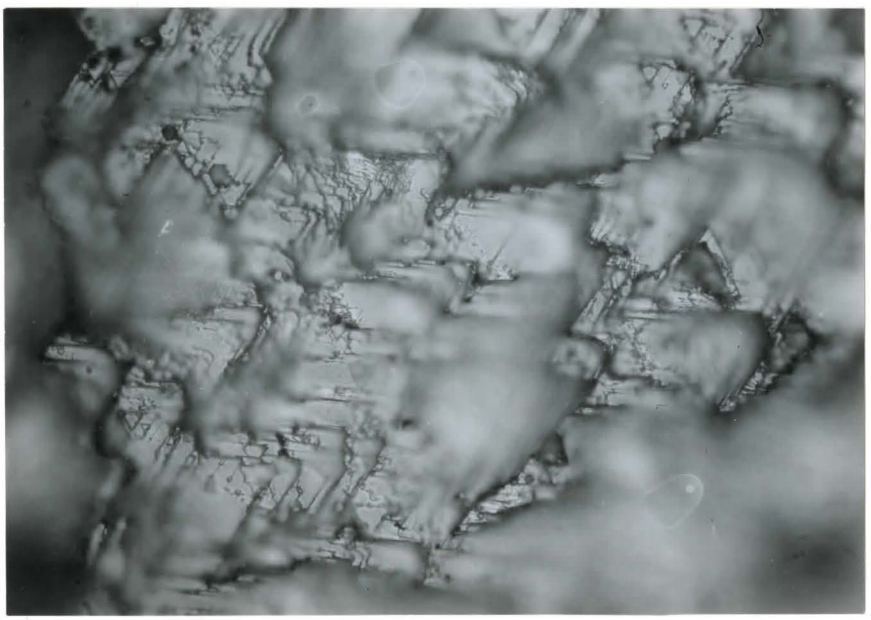

Figure 23(b). Magnified view of attack on surface. 400X. The attack is crystallographic and bears a remarkable resemblance to that in figure 21(b).

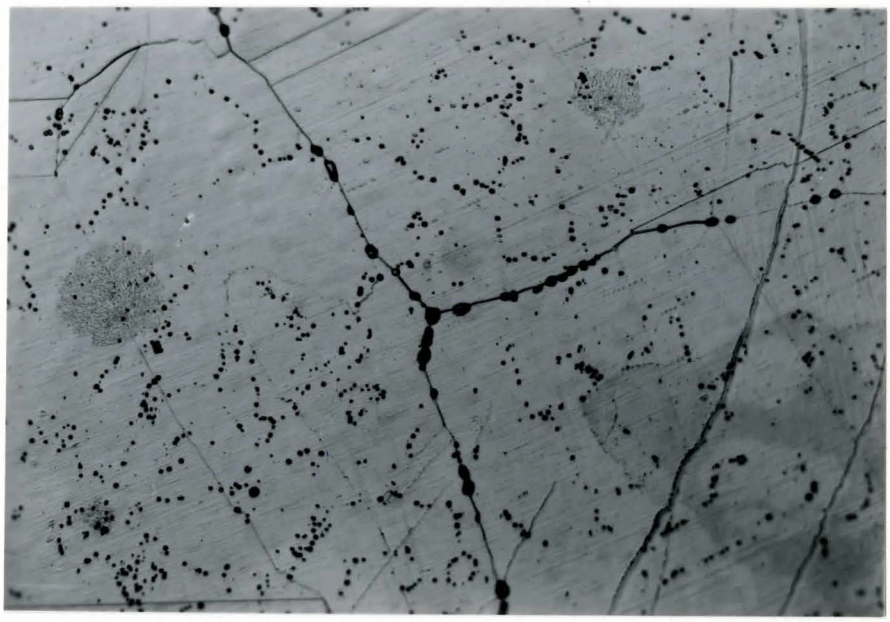

Figure 24. Surface of specimen of grain size 0.330 mm. (air grown) after potentiostatic activation. 160X. Passivation - 150 ml 1 N H_2SO_4 at 550 mV for 30 mins. Activation - 10 ml 1 N NaCl/150 ml 1 N H_2SO_4 at 550 mV. Pits are formed at the grain boundaries as well as within the grains.

lot when potentiostatically polarized showed a mixture of attack (Figure 13).

Potentiostatic polarization of a 90% cold worked specimen in a solution containing 2 ml 1 N NaCl/100 ml 1 N H_2SO_4 yielded a typical anodic polarization curve (Figure 25). It may be seen from the curve that the critical potential for the breakdown of passivity is very low - about +375 mV (vs SCE). After this, the anodic current density rise with potential is continuous, but slow. Microscopic examination of the specimen revealed a dark surface with a few pits and uniform general corrosion (Figure 26). The number of these pits was about 50% more than those formed by the potentiostatic activation technique. The pits were extremely shallow and no crystallographic facets existed in their interior. Pit distribution was quite random, and no correlation could be made between their starting point and any particular feature of the specimen surface.

Potentiostatic activation at 550 mV by the addition of 8 ml sat. NaCl/150 ml 1 N H_2SO_4 of a specimen with a grain size of 0.035 mm (after passivation in 1 N H_2SO_4 at 550 mV for 30 mins) yielded pits along the grain boundaries. Those at the grain boundary intersections grew into other grains too. There was no attack within the grain interiors. The anodic current density was found to increase continuously with time. An exactly similar experiment with a specimen with 90% cold work yielded a similar trend for the anodic current increase with time, but a significant change in the distribution and number of the pits. The pits tended to cluster together and their number was approximately 4 times less than in the annealed specimen. There was almost complete absence of general corrosion of the surface. For the same period of time, pits in the annealed material were larger and deeper than those in the cold worked material.

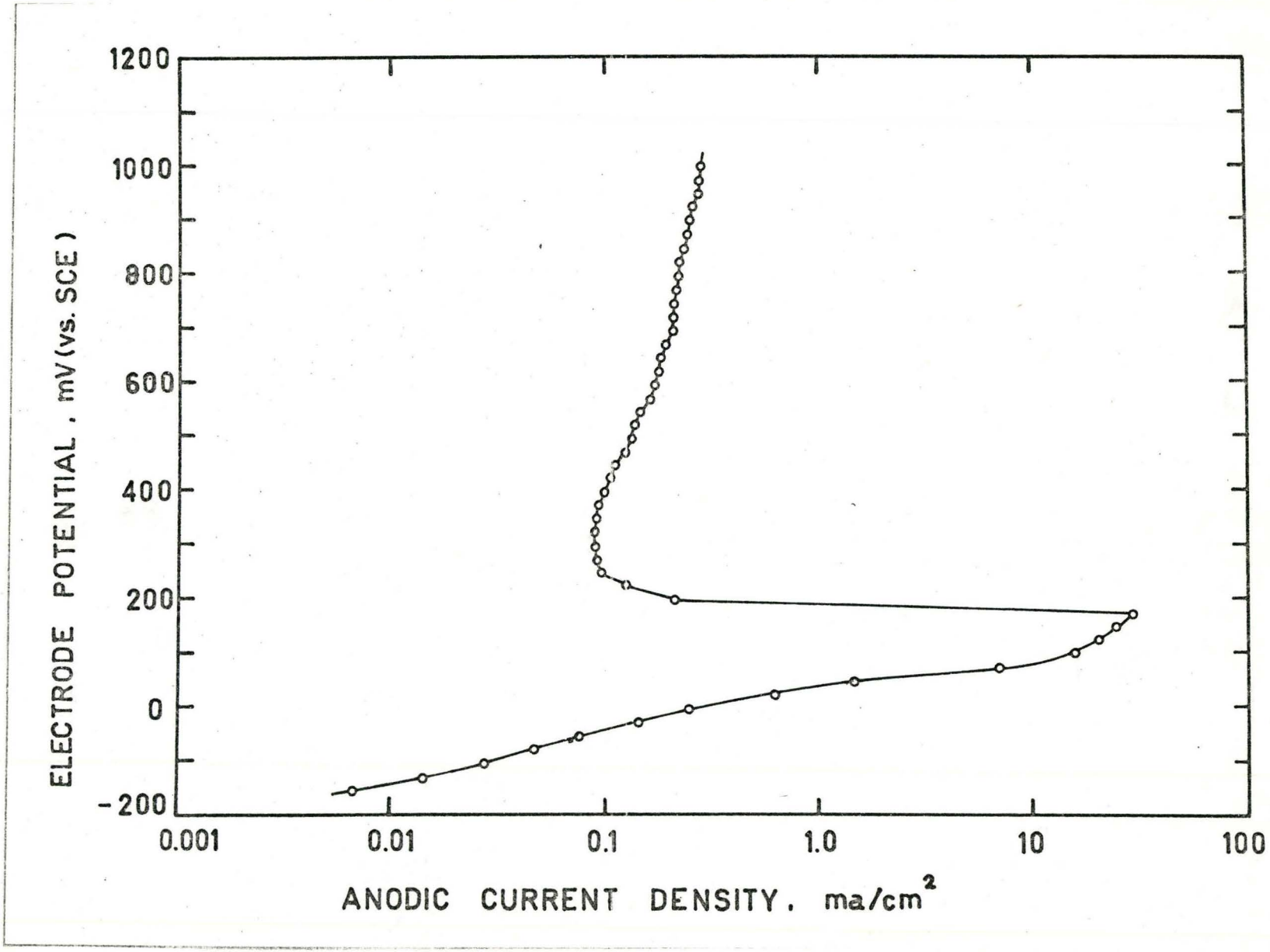

Figure 25. Anodic polarization curve for polycrystalline nickel with 90% cold work in 2 ml 1 N NaCl/100 ml 1 N H_2SO_4.

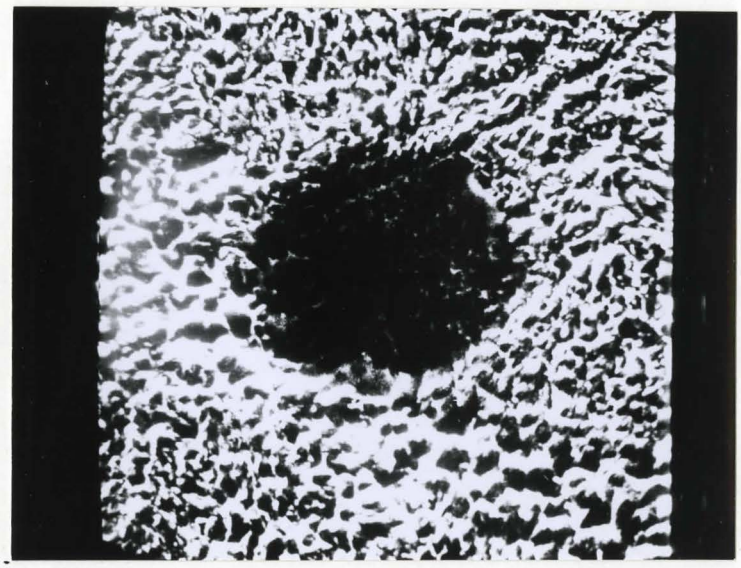

Figure 26. Surface of specimen with 90% cold work polarized in 2 ml 1 N NaCl/100 ml 1 N H_2SO_4, 1100X. The pit is shallow and circular, and there is considerable general corrosion of the surface.

On the basis of the results presented so far, the following observations can be made regarding pit distribution:

i) Under potentiostatic polarization and grain growth performed in air, specimens with grain size up to 0.150 mm show pits along the grain boundaries while those with a grain size of 0.250 mm show pits along the grain boundaries as well as within the grains. A specimen with a grain size of 0.330 mm exhibits a mixture of attack comprizing general corrosion, pitting and grain boundary corrosion.

When the grains are grown in vacuum, then under potentiostatic polarization, specimen with grain sizes of 0.250 and 0.330 mm pit only within the grains.

ii) Under potentiostatic activation and grain growth performed in air, a specimen of grain size 0.035 mm shows pits only at the grain boundaries while a specimen of grain size 0.330 mm shows pits within the grains as well as at the grain boundaries.

iii) For a specimen with 90% cold work, pit distribution is random and independent of the polarization technique.

4.2.2 Shape and Size of Pits

An analysis of the pit shape in the annealed and cold worked material under the two modes of polarization is presented below.

Despite the fact that the critical potential for the breakdown of passivity did not change with increasing cold work, changes were observed in the morphology of the pits in the different specimen. Figures 27 to 31 show the changes in pit morphology with increasing cold work. A comparison of the shape of the pits with those reported in other works[49,59] suggests that the grain orientation is {100}. The grain size of this specimen is

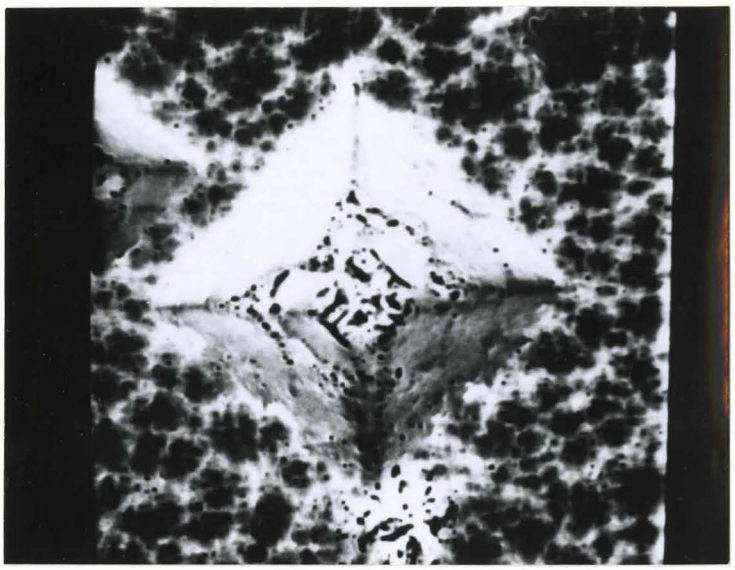

Figure 27. Morphology of pit formed on grain of {100} orientation. 5500X. The pit facets are assumed to comprise of {111} faces. Pit size = 9.50 μ.

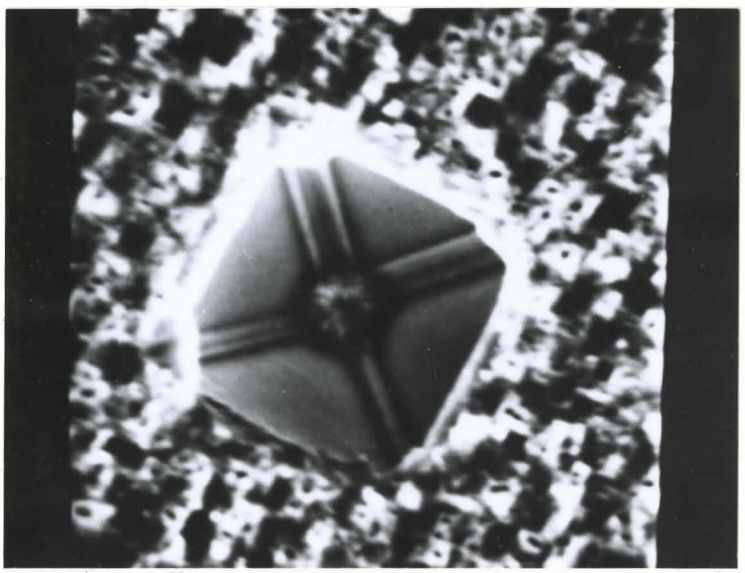

Figure 28. Morphology of pit formed on grain of {100} orientation with 10% cold work. 5200X. Another set of facets are seen. These are probably of the type {hh0}. Pit size = 7.73 μ.

Figure 29. Morphology of pit formed on grain of {100} orientation with 20% cold work. 4900X. The initial facets can still be distinguished. Pit size = 7.18μ.

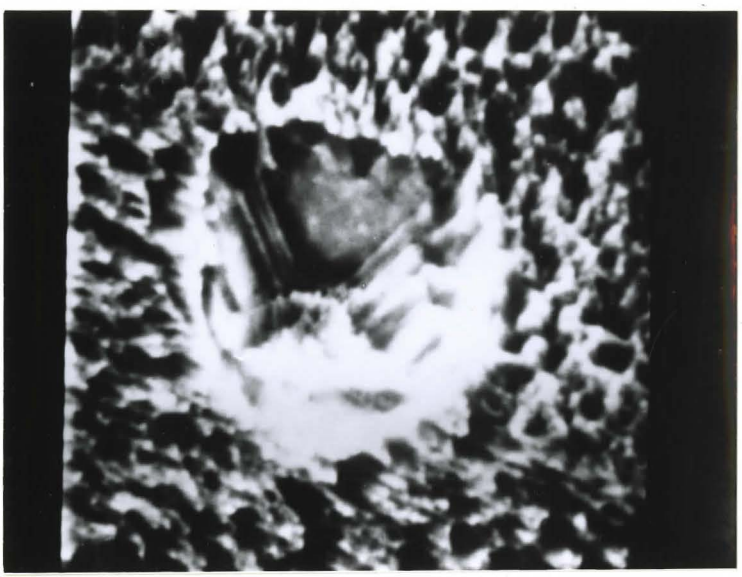

Figure 30. Morphology of pit formed on grain of {100} orientation with 30% cold work. 5300X. The pit shape has changed considerably. Pit size = 7.62 μ.

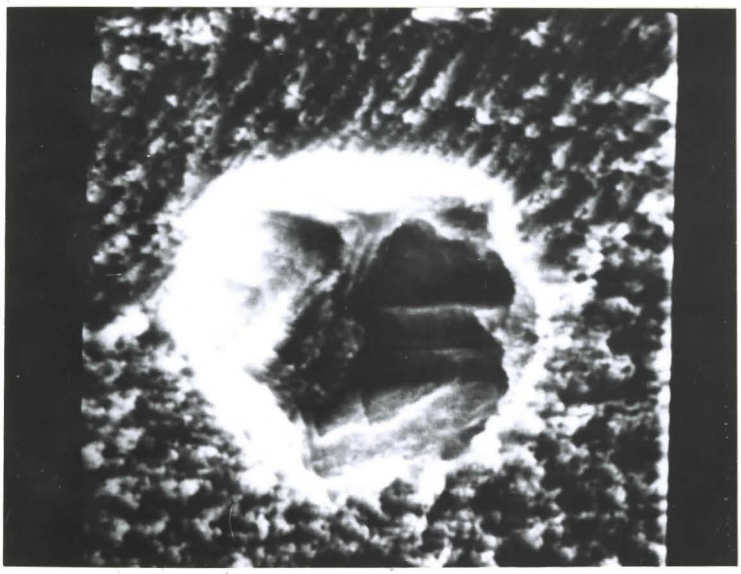

Figure 31. Morphology of pit formed on grain of {100} orientation with 40% cold work. 6600X. The exterior of the pit has become almost circular and no regular crystallographic facets exist in the pit interior. Pit size = 6.86 μ.

0.250 mm. It can be seen that with no cold work the pit is shaped like a blunted pyramid with a square base. When the specimen is cold worked to 10%, the external shape of the pyramid remains the same with a slight blunting of the corners. But on the inside, there is rounding off at the side intersections and appearance of a separate strip joining two sides. On increasing the cold work to 20%, the pyramid still maintains its initial characteristics but they are much more distorted (Figure 29). A further increase of cold work breaks up the pyramid significantly. By comparing Figures 27, 30 and 31 it can be seen that not only have the sides broken up completely, but also the shape is no longer a square; it has changed to circular. The size of these pits decreases and their depth increases with cold work. Pits formed in specimens with 90% cold work by both polarization techniques were always circular.

Another interesting observation of the same study is summarized in Figures 32 to 35, which shows the morphology of pits formed, presumably, in a grain of {111} orientation (grain orientation has been obtained by comparison of pit shape with previous works[49,59]). It can be seen that with increasing cold work there is an appearance of steps in the pits. It may be noted that these pits exhibit an increase of growth rate both in size and depth, with cold work.

Figure 36 and 37 show the difference in pit morphology of an isolated pit at the grain boundary in annealed and 30% cold worked specimens respectively. While the facets of the pit with no cold work are characteristic of each grain, this is not the case with the one with 30% cold work. The pit in the former case has two facets belonging to one grain and three belonging to the other, thereby forming a pentagon; the pit in the latter

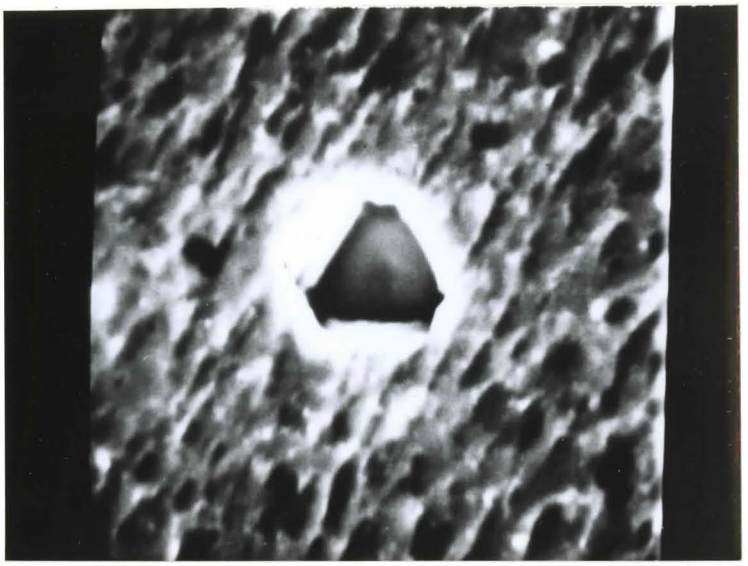

Figure 32. Morphology of pit formed on grain of {111} orientation. 5300X.

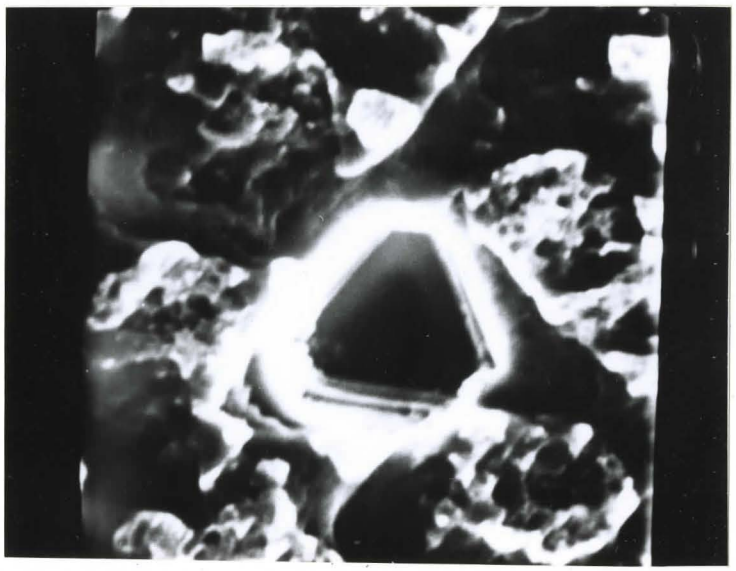

Figure 33. Morphology of pit formed on grain of {111} orientation with 10% cold work. 5200X. A few steps can be seen in the pit.

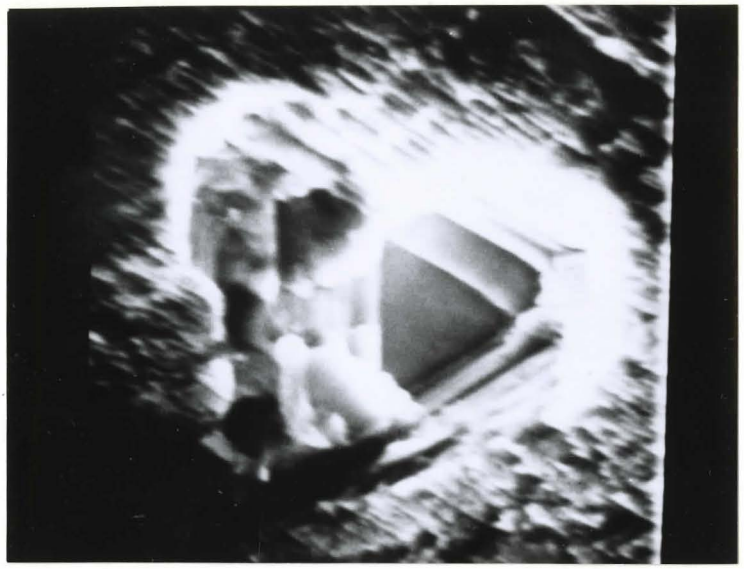

Figure 34. Morphology of pit formed on grain of {111} orientation with 20% cold work. 4900X. The number of steps in the pit has increased. The pit facets are assumed to be composed of {111} faces.

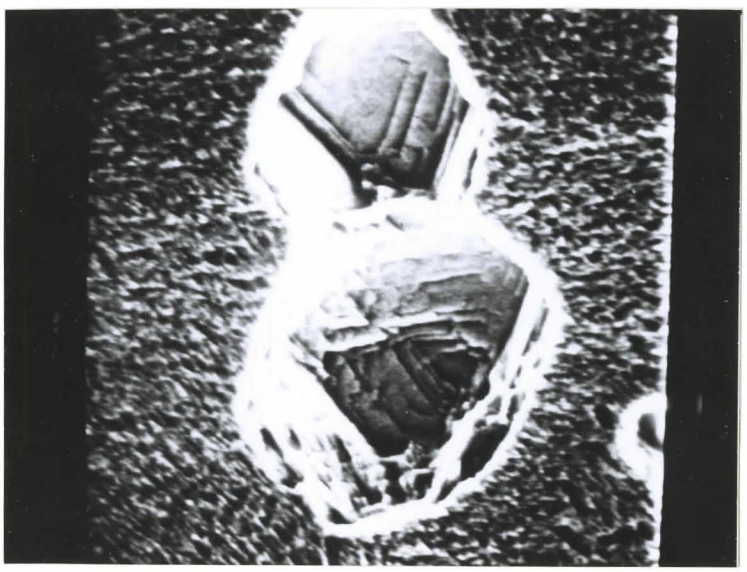

Figure 35. Morphology of pit formed on grain of {111} orientation with 30% cold work. 2100X. The pit is deeper and many more steps have formed.

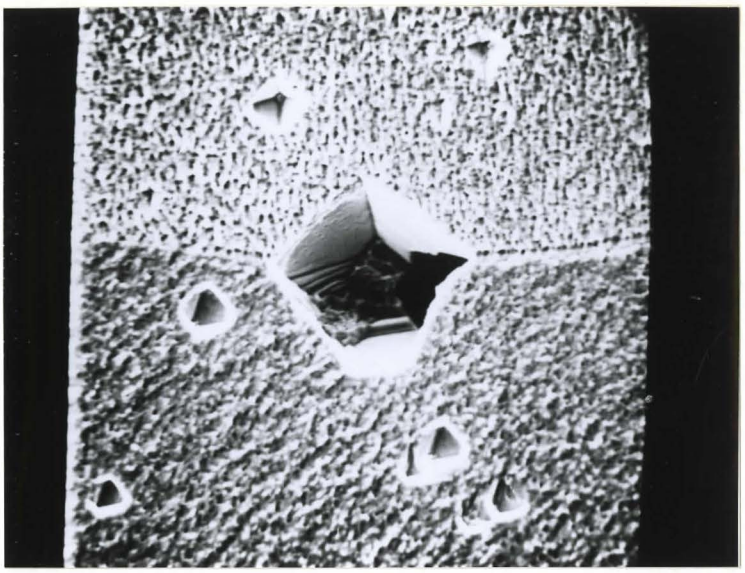

Figure 36. Morphology of an isolated pit at the grain boundary in an annealed specimen. 1100X. The pit facets belong to the pit characteristic of each grain.

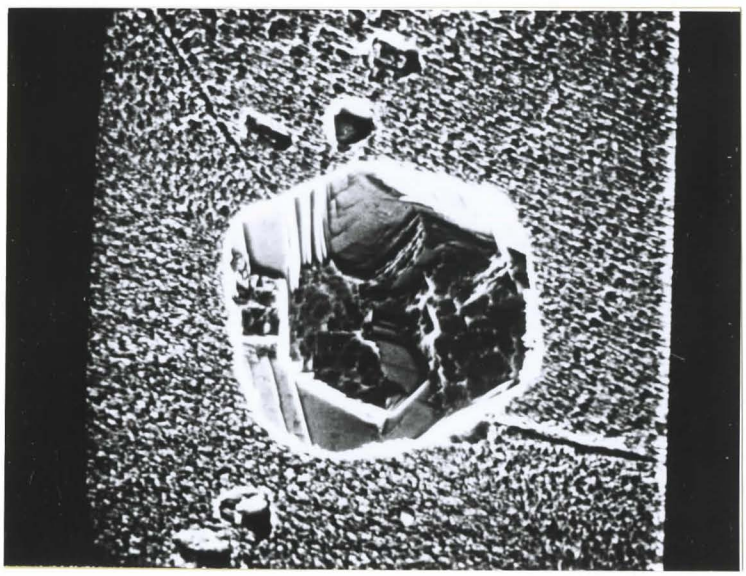

Figure 37. Morphology of an isolated pit at the grain boundary in a specimen with 30% cold work. 1100X. The pit facets do not belong to any grain and no regular crystallography exists in the interior.

case is almost circular.

Scanning electron microscopic observations of the interior of pits in the annealed material after potentiostatic activation are shown in Figures 38 and 39. In contrast to the micrographs just presented, it can be seen that a significant difference exists in the morphology. During the earlier stage of its growth, the facets of the pit belong to the characteristic morphology of each grain (Figure 38). The pit shown in Figure 39 was observed to nucleate at a grain boundary intersection and, at this stage, has grown into many grains. It may be seen that the interior is crystallographic but complex and steps are present. The presence of steps in pits formed in the annealed material by the potentiostatic activation technique was found to be general.

No significant change was observed in the morphology of pits in the 90% cold worked material tested by the two polarization techniques. In both cases, the pit interior appeared mottled at low magnifications (Figure 40 (a)), and no distinct crystallographic facets were present within the pits (Figure 40(b)).

At this stage, it may be mentioned that pits with covering films were formed only in specimen which had been "potentiostatically activated". Many times in the annealed material, despite the fact that the film showed a small break, the pit underneath was large and deep.

Although scanning electron microscopic observations can yield much useful information regarding the shape of pits, they are incapable of providing any information about covered pits or those with branches which tunnel sideways into the metal. This difficulty can be overcome by sectioning the specimen. Sectioning experiments were performed on completely annealed

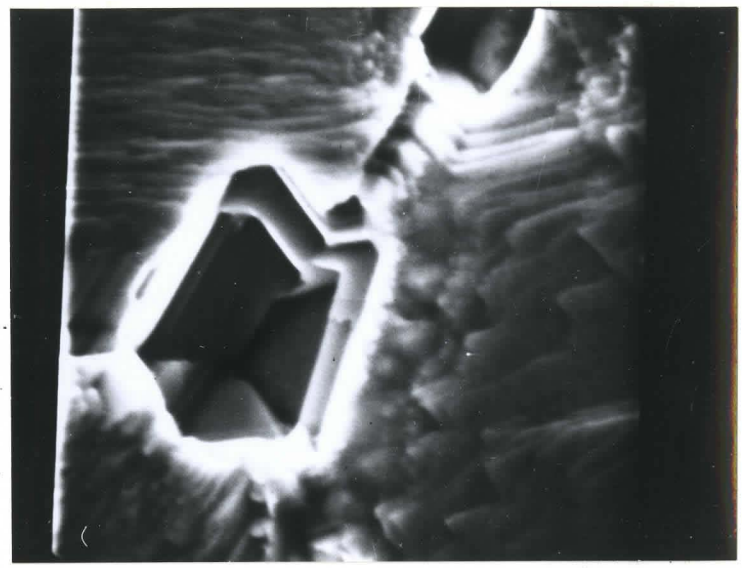

Figure 38. Pit at the grain boundary of a specimen tested by the potentiostatic activation technique. 5100X.
Passivation - 150 ml 1 N H_2SO_4 at 550 mV for 30 mins.
Activation - 8 ml sat NaCl/150 ml 1 N H_2SO_4 at 550 mV.

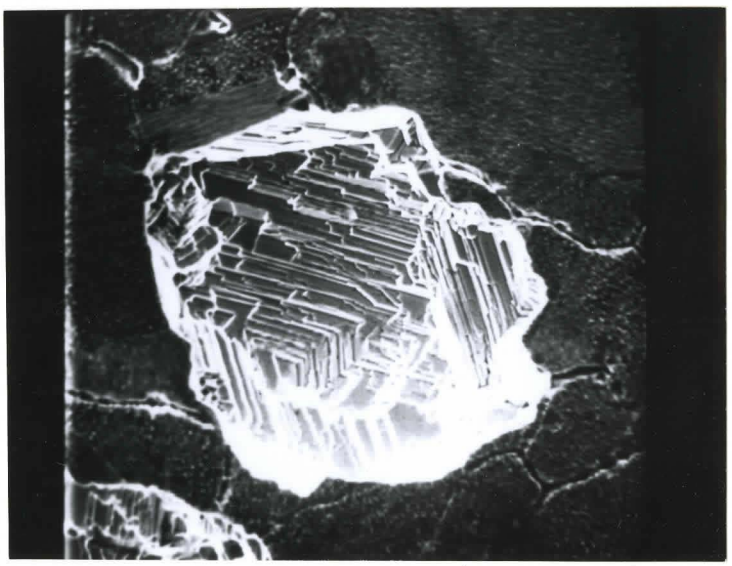

Figure 39. A large pit in the specimen of figure 37. 540X. Note the presence of steps in the pit. The pit was observed to nucleate at a grain boundary intersection and, at this stage, has grown into many grains.

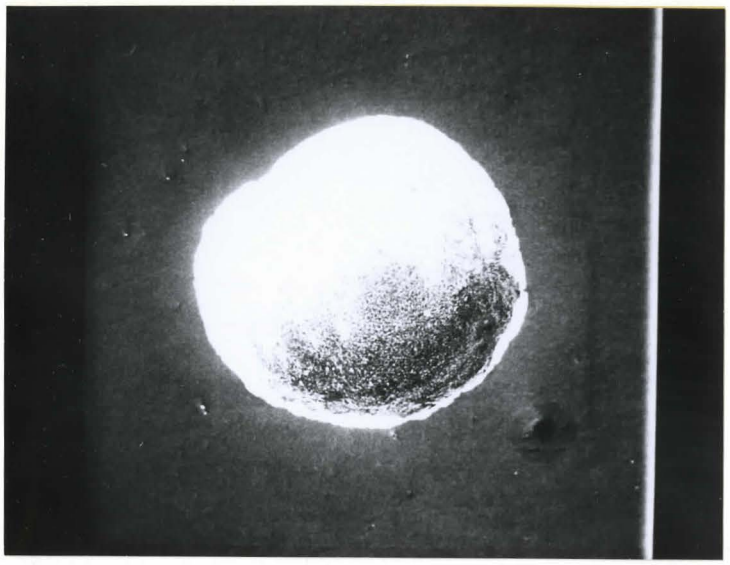

Figure 40(a). Shape of pit formed in a 90% cold worked specimen after potentiostatic activation. 110X.
Passivation -150 ml 1 N H_2SO_4 at 550 mV for 30 mins
Activation - 5 ml sat NaCl/150 ml 1 N H_2SO_4 at 550 mV
The pit is very shallow and the bottom appears mottled. Note that no general corrosion can be seen.

Figure 40(b). Magnified view of pit interior. 5400X.
No distinct crystallographic facets are present.

and 90% cold worked specimens after being subjected to potentiostatic activation only. The results are presented in Figures 41 to 48.

The shape of pits found in cold worked material may be divided into three categories:

i) Conical pits - The conical pits grow into the metal (presumably with the area near the vertex as the anode) (Figure 41). The number of such pits is extremely small.

ii) Saucer pits - Most pits exhibit a smooth shallow rounded shape. Two kinds of such pits have been found:

Type 1 - these exhibit only a single impression (Figure 42)

Type 2 - these result from the combination of two (or more) shallow impressions (Figures 43(a) and 43(b))

Type 1 pits are more predominant than those of type 2.

iii) Tunnel pits - The number of such pits observed was very small, and owing to their configuration within the metal surface, no photomicrographic observation was possible. However, in this case, the pit started as a circular impression, grew some way into the metal and then changed direction. Often, further growth of the pit was not in the same plane. Such pits showed the presence of a white corrosion product at the ends of the tunnels.

Figure 44 shows an early stage of pit development. The attack on the metal is directed along the surface - in a direction of the grain boundary of the heavily cold worked material.

Sectioning experiments on annealed material yielded similar shape of pits but of differing size (Figure 45 to 47). However, no instance of any tunnel pits were recorded. A careful examination of these figures reveals that there is attack at the grain boundaries intersecting the surface.

Figure 41. 'Conical' pits in a 90% cold worked specimen. 80X. The number of such pits was very small.

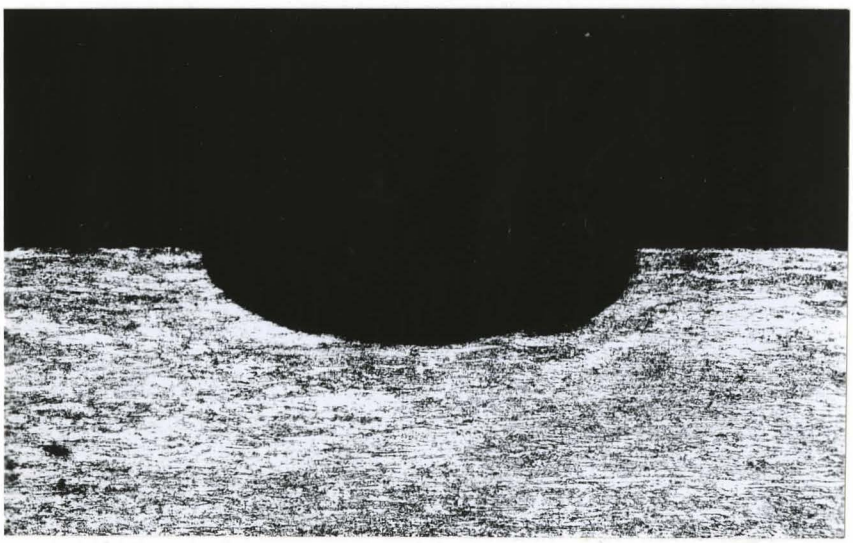

Figure 42. 'Saucer' pit (type 1) in a 90% cold worked specimen. 80X. The pit has a circular top view. Most pits were of this type.

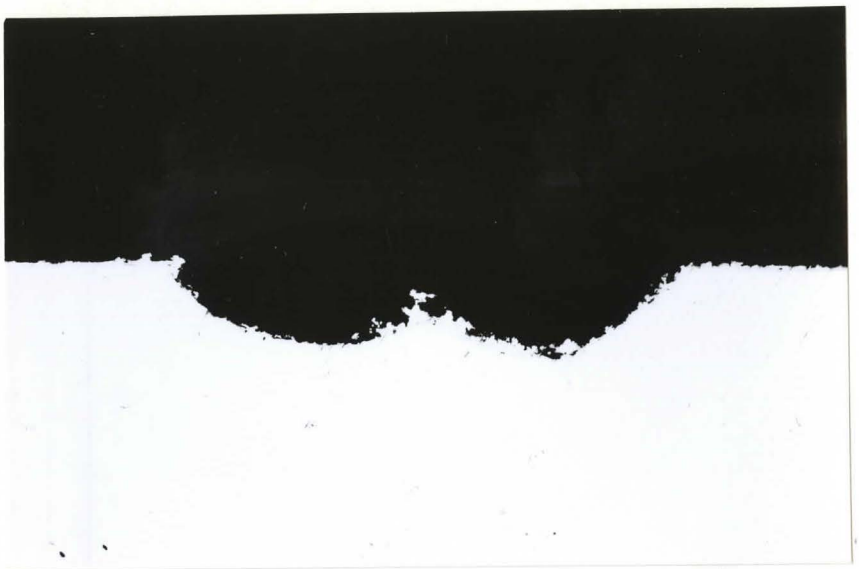

Figure 43(a). 'Saucer' pit (type 2) in a 90% cold worked specimen. Unetched. 80X. The pit is a combination of two shallow impressions.

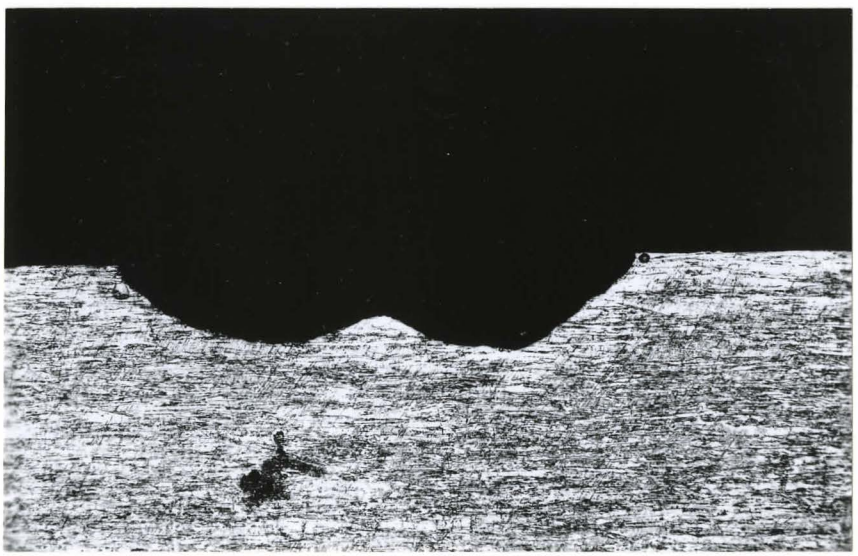

Figure 43(b). Same as in 42(a). Etched. 80X.

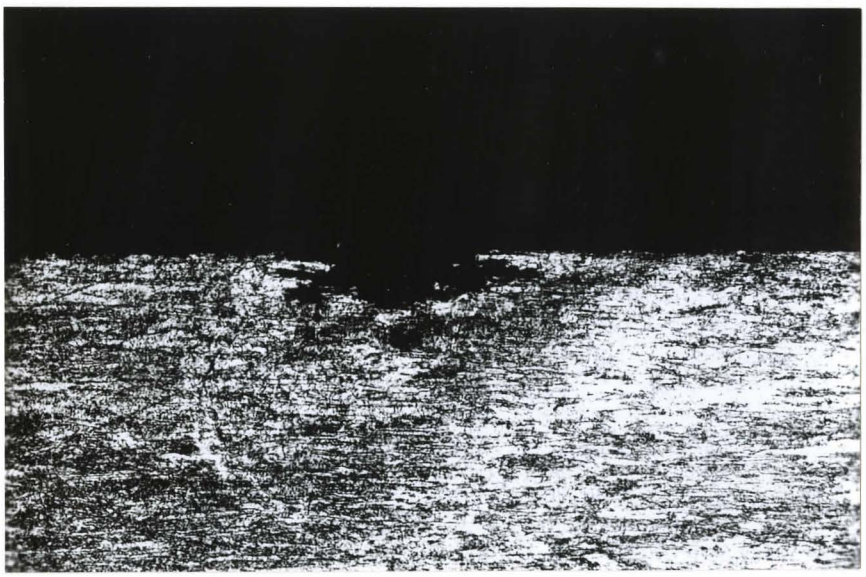

Figure 44. Early stage of pit development in a 90% cold worked specimen. 124X. Note that the attack is directed parallel to the surface - in a direction of the grain boundary of the heavily cold worked material.

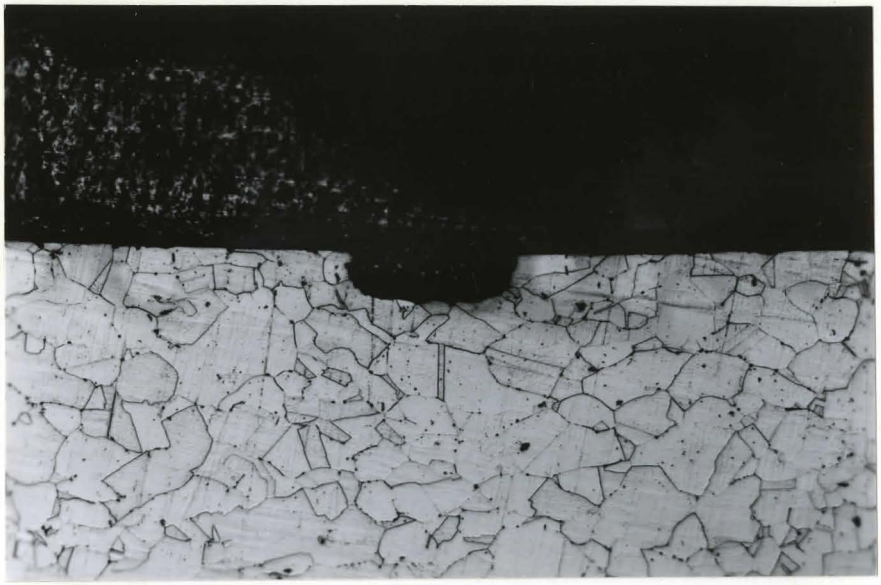

Figure 45. Saucer pit (type 1) formed in an annealed specimen. 160X. Most of the pit showed this shape.

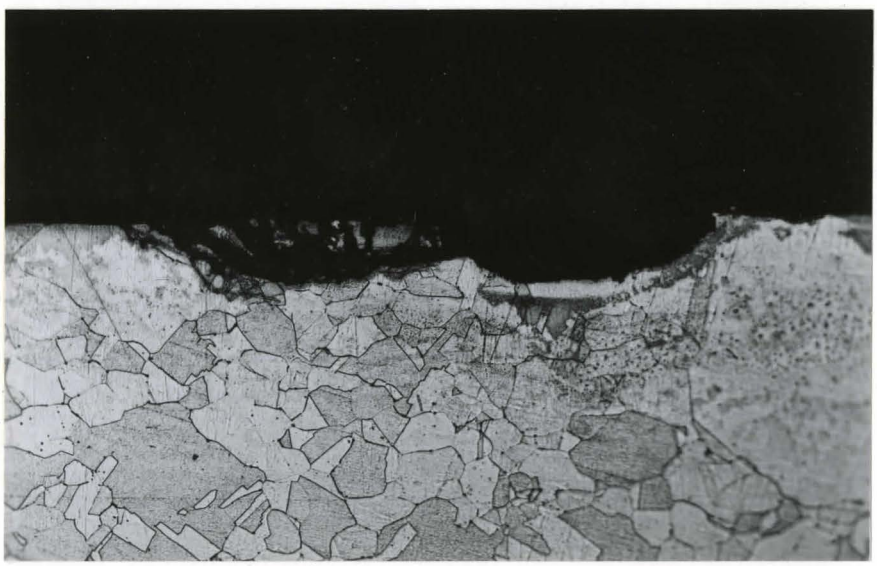

Figure 46. Saucer pit (type 2) formed in an annealed specimen. 160X.

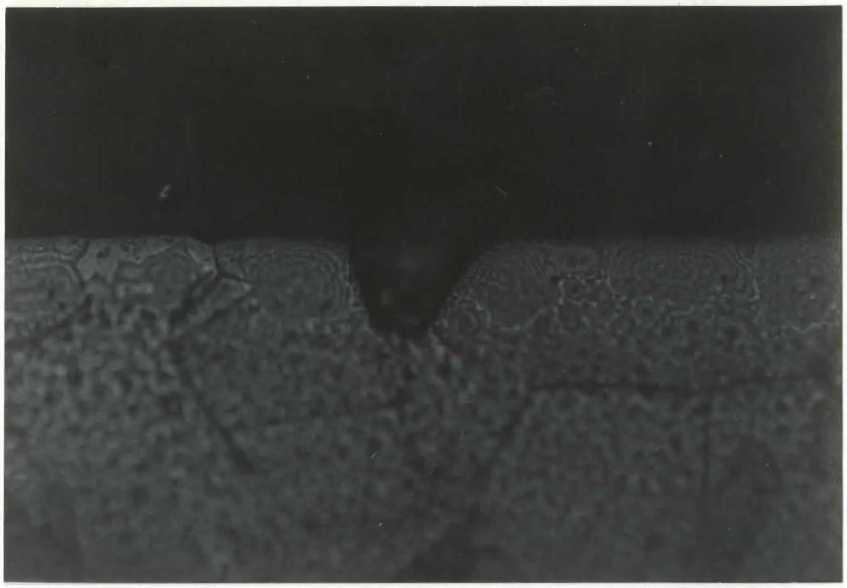

Figure 47. Shape of pit formed in an annealed specimen (dark field). 620X. The pit is very small and its appearance suggests that it was bound by low index crystallographic facets.

Figure 48. Grain boundary attack in an annealed specimen (dark field). 400X. The attack starts at the grain boundary but deeper into the material, becomes trans-granular. In this case, eventually a conical pit would have formed.

Whatever be the mode of polarization, for the same solution and period of time, the pits in the cold worked material were always smaller and shallower than those in the annealed one. Thus, the smallest pit size which could be seen in sectioning was controlled by the pits in the cold worked material. Since, the growth rate of the pits in the annealed material was very high, while that in cold worked material was rather low, in the time required to grow pits large enough to be visible in sectioning in cold worked material, the pits in the annealed material penetrate through the metal surface and nothing definitive can then be known about their size and shape. It is for this reason that the shape of pits reported in sectioning are not on the basis of a constant time. Although formed under the same conditions, the pits in cold worked material (Figures 41-44) are at long times, while those in annealed material (Figures 45-48) at short times.

The attack on the material tends to stay along the grain boundaries. It is to be noted from Figure 48 that the attack starts from the specimen surface along the grain boundaries and proceeds as such deeper into the metal until it encounters a large grain. There, instead of following the grain boundary, which is almost at right angles to its length, it proceeds straight into the grain. The similarity in the attack along grain boundaries in the cold worked and annealed material may be seen in Figures 44 and 48.

4.2.3 Nature of Pit Development

Throughout this study, no attention has been paid to the actual mechanism of pit initiation and growth. One is left wondering as to whether a discontinuity pre-exists in the passive surface film and the chlorine ions merely accelerate the dissolution process at these points, or they themselves trigger a burst in the film and then promote dissolution, or some altogether different process is followed. In order to provide at least

partial answers to these questions, a study was conducted to observe pit development at very early stages.

For reasons discussed later, 90% cold worked material was tested by the 'potentiostatic activation' technique.* The results are presented in Figures 49 to 52. Microscopic examination of the specimen surface (after passivation and prior to the addition of Cl^- ions) at magnifications upto 10000X did not reveal any breaks in the surface film. After the addition of Cl^- ions, the formation of the pit is characterized by a hump in the surface film which is initially very small (1.06μ) and then grows (1.6μ) (Figures 49 and 50). With time the hump grows further (3.0μ) and finally a break occurs in the surface film. The two types of breaks that have been found are shown in Figures 51 and 52. In most cases the film break was around the edge of the hump and very few instances were observed where the break was across the hump. If the hump is removed, the pit surfaces inside cannot be seen as the pit is full of a white corrosion product (Figure 53). The break in the hump is probably due to the excess of the corrosion product accumulated in the pit. If the test specimen is left in a desiccator for a few days and then re-examined, multiple breaks are often observed in the surface film (Figure 54). These breaks are probably associated with covered pits or pits which grew very close to each other.

---

*Specimens were passivated in 1 N H_2SO_4 at 550 mV for 30 mins and then activated by the addition of 10 ml 1 N NaCl/150 ml 1 N H_2SO_4 at 550 mV. Specimens were removed from the corrosion cell after different periods of time to study pit development. The micrographs (Figures 49 to 52) are not of the same pit. Figure 49 and 50 are from one specimen while Figure 51 and 52 are from another specimen.

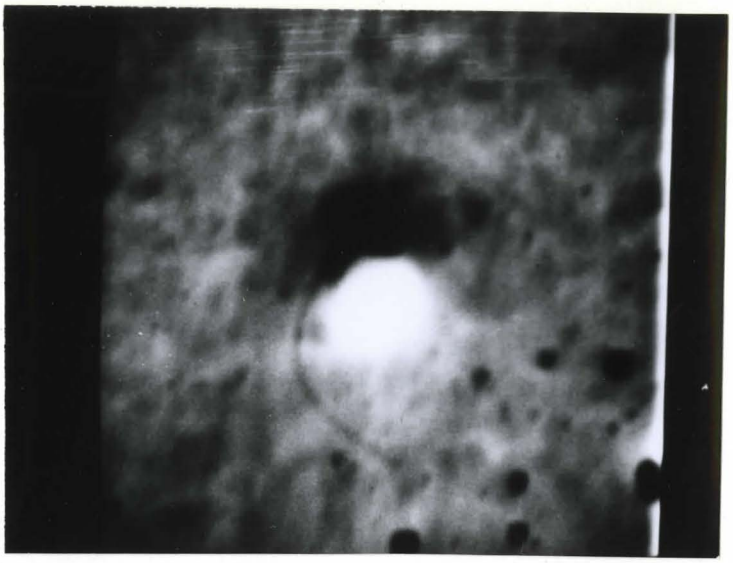

Figure 49. Sequence of pit development in a 90% cold worked specimen. 13000X.
Potentiostatic activation technique.
Passivation - 150 ml 1 N H_2SO_4 at 550 mV for 30 mins
Activation - 10 ml 1 N NaCl/150 ml 1 N H_2SO_4 at 550 mV
Hump size - 1.06 μ.

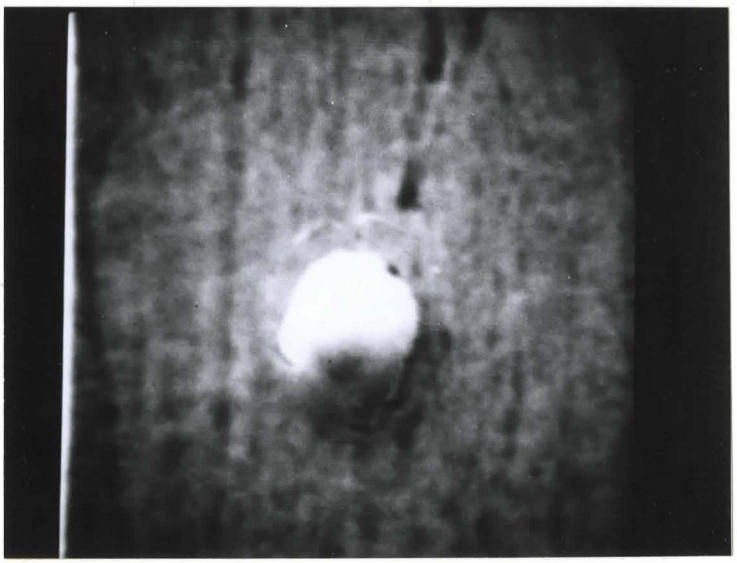

Figure 50. Development of pit in a 90% cold worked specimen. 11000X. Another pit in specimen of figure 49. Hump size - 1.63 μ. Note that the hump tends to break at the edges.

Figure 51. Development of pit in a 90% cold worked specimen. 5300X. Hump size - 3.0 μ. The hump has broken at the edges. In most instances such breaks were found.

Figure 52. Development of pit in a 90% cold worked specimen. 5300X. Another pit in specimen of figure 51. Hump size - 3.0 μ. The break has occurred across the hump. Very few such breaks were found.

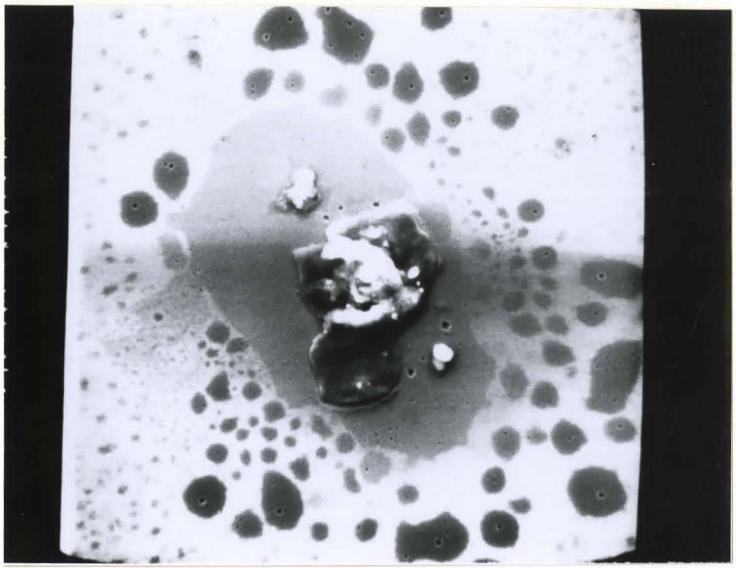

Figure 53. Inside of a pit formed in a 90% cold worked specimen by the potentiostatic activation technique. 500X. The pit is full of a white corrosion product.

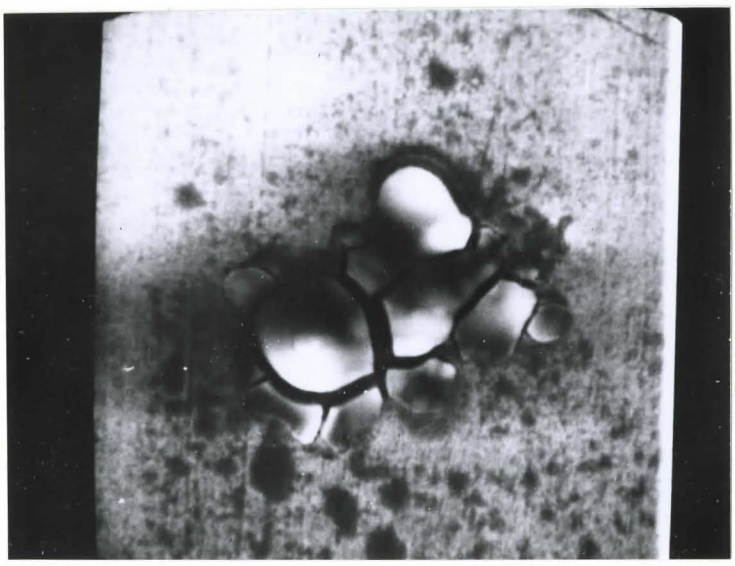

Figure 54. Surface of a 90% cold worked specimen tested by the potentiostatic activation technique and left for 2 days in a desiccator. 2000X. Multiple breaks occur in the surface film. These breaks are probably due to covered pits or pits which grew close to each other.

CHAPTER V

DISCUSSION

5.1 The Nature of the Passive Film on Nickel

Very little is known about the thickness of the passive nickel films. Tronstad[60] estimated 50-80 Å for nickel passivated anodically in acid sulfate solutions using his optical method. Pfisterer et al.[61] report only 15 Å for the passive films on very thin nickel foils. Arnold and Vetter[62] determined a thickness of about 50 Å from oscilloscopic coulometric measurements.

The formation of the passive film proceeds by the anodic dissolution of nickel. An oxide film is formed. The oxides in this film have been identified to range from NiO to Ni_2O_3; their formation depending only upon the potential and pH of the solution.[63] For instance, in alkaline solutions it has been shown[64] that the final oxidation state on the nickel electrode corresponds to a non-stoichiometric oxide, NiO_x, (where x = 1.7 - 1.9). Recently, Yahalom and Weisshaus[65] observed a film covering the pits formed in phosphate buffer solution by Cl^- ions in thin nickel foils. From the electron diffraction data they concluded that the film was NiO.

The constituents of the passive film in acid solutions are evidently quite different. Sato and Okamoto[63] proposed that the potential for the onset of passivity was the potential for the transformation from NiO to the higher oxide Ni_3O_4 when the concentration of the nickel in solution was small. Polarization to higher potentials led to oxidation and conversion of this oxide (Ni_3O_4) to Ni_2O_3. Thus, the passive oxide film may be taken

to consist of either a single higher oxide Ni_3O_4 or the duplex oxide NiO and Ni_3O_4. In cases where the nickel electrode is directly subjected to a passive potential in an acid solution (the 'potentiostatic activation technique') the passive film has been shown[66] to be composed of NiO.

The observations of this study have shown that covered pits were formed only when a specimen was tested by the potentiostatic activation technique and, in such cases, the passive film was observed to flake off at pit sites. The formation of covered pits indicates that the passive film is either insoluble or sparingly soluble in the solution within the pits and in the bulk electrolyte. On the other hand, under potentiostatic polarization the complete breakdown of the passive film at potentials more positive than the critical potential in solutions of high Cl^- ion concentration, and particularly the fluctuations in the anodic current density in the passive region, indicate that the passive film is probably soluble in the bulk electrolyte. This is further supported by the fact that no covered pits were formed when specimens were potentiostatically polarized and in-situ microscopic observations did not show any flaking off of the passive film. The differing behaviour of the passive film in potentiostatic activation and potentiostatic polarization is indicative of the fact that the passive film formed in the two cases is evidently quite different. Based on different evidence, Tokuda and Ives[21] also arrived at the same conclusion.

While the rate of film formation and the rate of film destruction are in competition with one another in chloride containing solutions, the film destruction phenomenon is totally absent in non-chloride containing solutions. Thus, films formed in the former case may be expected to be thin while those formed in the latter case to be much thicker. This is

clearly borne out by the observations of this study. It is possible that maintaining a specimen at a passive potential for a period of time leads not only to the direct formation of an oxide film, but also to the precipitation of some salt, probably a sulfate, which can hydrolyze in water:

$$NiSO_4 + 2\ H_2O = Ni(OH)_2^{*}\downarrow + H_2SO_4$$

The probability of the formation of $NiCl_2$ cannot be completely overlooked. But, since the solubility of $NiCl_2$ is more than $NiSO_4$,[67] it dissolves away before it can hydrolyze. Thus, the presence of Cl^- ions tends to retard the repair of the passive film, thereby disturbing the stationary state and promoting dissolution.

5.2 Nature of Film Breakdown

Numerous theories may be found in the literature on the mechanism of pitting corrosion. Though there has been considerable agreement between the different workers regarding the growth mechanism and many of the morphological aspects of pitting, very little agreement exists on the nucleation processes. This problem manifests itself in two ways: first, the favoured sites for pit nucleation, and secondly, the mechanism of nucleation.

The results of this investigation show that in a completely homogeneous and strain free polycrystal, pits nucleate at the grain boundaries, particularly at grain boundary intersections. This may be taken to mean that the passive film is weaker along the grain boundaries than elsewhere. Since the passive film forms by the anodic dissolution of the base metal, this implies that the passive film inherits the structural imperfection of the metal surface thereby generating certain 'susceptible spots' for pit

---

*$Ni(OH)_2 \equiv NiO.H_2O$

nucleation. As has been pointed out by Smialowska,[68] there are two possible ways in which these spots can help pit nucleation. Once the critical concentration of the Cl^- ions is reached in the pitting solution, they either penetrate the metal surface at these weak spots or react at them chemically. For a localized breakdown of the passive film, the concentration of the Cl^- ions present in solution must be small.

The existing theories regarding the mechanism of pitting corrosion require the existence of a protective film or a passive state as a precursor to the onset of pitting. However, recently Hodge and Wilde[69] found that a pure nickel specimen did not passivate in 1 N NaCl + 1 N H_2SO_4 solution and the anodic current density increased continuously with potential. From an examination of the structure of the specimen, they concluded that the metal had undergone severe pitting corrosion.

The results that have been presented here clearly show that with increasing Cl^- ion concentration in the polarizing solution, the attack on the specimen surface, which is initially along the grain boundaries begins to spread out. That the attack in the grain interiors, by virtue of being crystallographic in nature, is pitting is an incorrect conclusion. The grain interior attack cannot be pitting because with active pitting in progress at the grain boundaries, the area surrounding these (i.e. the grain interiors) must be cathodic in nature. The passive film within the grain interiors may break at some points to give pits, but that cannot account for a uniform crystallographic attack within almost all grains. It is possible that there is general corrosion of the grain interiors, which is much less intense in nature and where the grain interior is still cathodic to the grain boundary and thereby to the growing pits.

The processes occurring on the specimen surface may be viewed to be as follows:

Until the onset of passivity, the Cl^- ions may be considered to play a negligible role. This is evident from the initial stages of the polarization curves (Figure 22) where no significant difference exists between them in the various solutions. However, as the specimen dissolves anodically and the oxide film forms, the presence of the Cl^- ions becomes increasingly important. At all subsequent stages, there exists a competition between the formation of the film by anodic dissolution and its destruction by Cl^- ion adsorption. Naturally, higher the concentration of the Cl^- ions in solution, greater is the tendency of film destruction.

When the concentration of the Cl^- ions is low, the passive film formation far exceeds the film breakdown, and the specimen exhibits a clear active-passive transition. However, owing to the fact that there exists a slight lattice mis-match at the grain boundaries, the passive film is weaker here than in the grain interiors. Thus, once the critical potential is reached, the film breaks down at the grain boundaries and pitting corrosion occurs.

As the concentration of the Cl^- ions increases, the rate of film breakdown fast approaches the rate of film formation. Once a particular concentration of Cl^- ions is reached, any weaknesses in the passive film resulting from grain boundaries in the metal cease to be of any importance and the passive film breakdown is controlled by the Cl^- ion availability. The passive film in such cases could be expected to be extremely thin and the passive region of the polarization curve rather small. In all such specimens, it is to be expected that once passivity sets in, the passive film

does not remain intact. Instead, it breaks and reforms, thus giving rise to a fluctuating anodic current - as was experimentally observed for specimen A-4 (Figure 22). The process of competitive breakdown and reformation of the film continues until the critical potential, E_c, is reached where the film breaks down completely and general corrosion occurs. Since the concentration of the Cl^- ions in solution is high, their availability is the same over the entire specimen surface and this aids the complete breakdown of the film.

The morphology of the attack depends on the concentration of the Cl^- ions. However, once the critical concentration is reached the morphology becomes independent of the Cl^- ions in the polarizing solution. Thus, despite the fact that specimen A-4 undergoes an active-passive transition and exhibits a critical breakdown potential, the attack on the surface is not pitting but general corrosion.

When the concentration of the Cl^- ions is very high, theoretically film breakdown far exceeds film formation. This tendency is so high that, if at all, the film forms for a few micro-seconds and breaks down instantaneously. Since, the critical potential for the breakdown of passivity decreases while the primary passivation potential increases with increase in Cl^- ion concentration (Table 6), a stage is reached when the passive region no longer exists and the active dissolution of the metal continues. Since, the recorded anodic current is the sum of all local cell action on the surface, and the current density calculations are based on the original area of the specimen, the anodic current density shows a continuous increase with potential. The attack on specimen A-5 (Figures 23(a) and 23 (b)) can, therefore, be considered 'general corrosion' and not pitting.

It is, therefore, evident that electrochemical data should be supplemented by metallographic observation for a complete appreciation of the pitting phenomenon. As has been seen, though a difference exists in the anodic polarization behaviour of specimen A-4 and A-5, the nature of attack in both is the same.

That a high concentration of Cl^- ions can lead to general corrosion has also been shown by Smialowska,[68] who has found that after pitting the amount of Ni estimated analytically in the solution is higher than that calculated mathematically from the volume of pits formed. The excess Ni has been attributed by her to be due to general corrosion. It may be pointed out that this excess, which has been solely attributed to be due to general corrosion, also incorporates the Ni derived from the dissolution of the passive film.

The presence of Cl^- ions is known to stimulate film breakdown and promote pit formation. The exact mode by which the Cl^- ions act has been the subject of controversy. Figure 7 shows that after the addition of Cl^- ions to a passive nickel electrode, a certain time period is required before an increase in the anodic current density is observed and the first pits are formed. This observation of an induction or incubation period has been previously noted for many materials[20,21,44,45] including nickel.[29] The induction period has been interpreted as the time required for the passage of the Cl^- ions from the bulk of the solution to the passive film and their transport through it (passive film) to the metal surface.

When the nickel is subjected to a passive potential in a non-chloride containing solution, a protective film is formed. It is assumed that this film is uniform over the entire specimen surface. However, as has been

pointed out earlier, certain susceptible or weak spots exist in the passive film. Thus, once the Cl^- ions are added, they are adsorbed and at these spots they penetrate through the passive film to the film/metal interface. At the metal surface they react with the nickel leading to the formation of pits. The passive film remains structurally intact and no breaks occur. The process of adsorption and penetration continue and as the pit grows, more and more of the corrosion product forms. The volume of the corrosion product is more than that of the pit and the excess in the volume is compensated for by the appearance of a hump in the passive film (Figure 49). (Passive films are known to possess substantial ductility.[70]) However, with further growth of the pit, a stage is reached when the passive film can no longer 'stretch' and it breaks (Figures 51 and 52). The corrosion products are washed away and the pit becomes exposed to the bulk electrolyte. From now on, there is a decrease in the corrosion rate (designated as the rate of change of the anodic current density with time). This implies that the overall activity of the pits decreases. This is due to the fact that as the pits open up, they become equally accessible to the passivating ions as to the aggressive ones.

The observations quoted above go a step further in establishing that the Cl^- ions do not react chemically at the weak spots. For, if this was the case, then with time the base metal would have been exposed and no hump in the passive film would have appeared. Thus, passage of the Cl^- ions from the bulk of the solution to the passive film, followed by complete penetration through it to the metal surface is required to initiate pitting corrosion. Recent ellipsometric studies[31,32] have shown this to be true for pit initiation on iron single crystals.

Since the pits are very small, it is rather difficult to remove the corrosion product within them and, therefore, no analysis of the nature of the corrosion product has been possible. Nevertheless, on the basis of the ions present in solution and the fact that the Cl^- ions penetrate to the metal surface, the corrosion product may be taken to be a mixture of $NiCl_2$ and $NiSO_4$, probably richer in the former constituent.

5.3 Pitting Susceptibility

No comprehensive definition of 'pitting susceptibility' is available in the literature. Loosely, it has been spoken of as 'the tendency of a metal or alloy towards (to undergo) pitting corrosion'.[22] Among the methods that have been used to measure the pitting susceptibility of materials are:

i) Following passivation, recording the relative anodic current density as a function of time after Cl^- ion addition.[21]

ii) Measurement of the number and size of pits formed during a fixed time.[33]

iii) Determination of the minimum Cl^- ion concentration required to initiate pitting.[52]

iv) Comparison of the relative critical breakdown potential, E_c.[26]

Regarding the use of the increase in the relative anodic current as a function of time as a measure of pitting susceptibility, it is pointed out that the anodic current increase obtained after the addition of Cl^- ions is the average over the entire specimen surface. It is possible that two specimens have the same number of pits, but their rate of growth may be different. Specimen 1 may have a few pits with a higher growth rate. Thus, the overall anodic current will also be high. On the other hand, specimen 2 may have pits with a similar and lower growth rate resulting in a lower

overall anodic current. In the long run, such a specimen will experience failure by pitting more readily than the previous one. Since the pitting susceptibility is related principally to the number of active sites for pitting and not to the rate of pit growth,[21] to conclude that the first specimen is more susceptible to pitting will be wrong. Thus, the relative anodic current is not a proper measure of the pitting susceptibility. It represents more adequately the 'intensity of attack' rather than the 'susceptibility of attack.'

As far as the second method is concerned, it would be believed that the more susceptible specimen will exhibit a greater number and deeper pits. So far, more susceptible specimens have, generally, exhibited more pits, but they need not always be deep.[26] The third method, namely, determination of the minimum Cl^- ion concentration required to initiate pitting, is a suitable one, but it has not been widely used, probably because it is tedious and time consuming.

The most commonly used measure of pitting susceptibility is the relative critical breakdown potential, E_c. This potential characterizes the resistance of metals to pitting corrosion and, therefore, may be considered as a measure of the susceptibility of different metals and alloys to pitting corrosion in aggressive environments. Below E_c, at more negative potentials, the metal is in the passive state, and above E_c active and passive states coexist on the metal surface and pitting corrosion occurs. Thus, the more positive is E_c, the more resistant is the metal to pitting corrosion and lower is its pitting susceptibility. However, as has already been pointed out, this may be so in less aggressive solutions, but a total reliance on the electrochemical data only can lead to erroneous conclusions

for highly aggressive solutions.

5.3.1 Effect of Gas Absorption

The extent of pitting depends upon the active anode/cathode site ratio, being higher if this ratio is large and vice versa. The observations of this study show that as the grain size decreases from 0.150 mm to 0.025 mm the pitting susceptibility of nickel (as evident from the shift in E_c to more active values, see Table 2, and the increase in the number of pits formed per unit area of the specimen surface) increases. If the potential anodic areas are taken to be distributed along the grain boundaries, with the specimen size being the same in each case, this implies that a specimen with a smaller grain size has a larger grain boundary area and consequently, a higher anode/cathode site ratio. Thus, such a specimen will exhibit a greater susceptibility for pitting (when compared with a specimen of a larger grain size).

If the above proposition is to be generally valid, then every specimen should exhibit an 'active-passive' transition and with increasing grain size, E_c should shift towards more noble values and fewer pits should be formed, all along the grain boundaries. However, the results presented show quite the contrary. An air-annealed specimen with a grain size of 0.250 mm does exhibit a 'passive' region, but pits are formed along the grain boundaries as well as within the grain interiors. When the grain size increases to 0.330 mm, the specimen does not show a 'passive' region and a mixture of attack comprizing general corrosion, pitting and grain boundary corrosion is obtained. On the other hand, when the grain growth is carried out in vacuum, specimen of both grain sizes (0.250 mm and 0.330 mm) show an 'active-passive' transition. No change is observed in the value of E_c and, in both

cases, pits appear within the grains only. It is, therefore, evident that the discrepancies mentioned above are not a consequence of the grain size effect, but are due to something else.

It will be seen from Table 1 that the larger grain sizes were grown by annealing at high temperatures for long periods of time. With regard to air annealing, therefore, solubility (and diffusion) of nitrogen and oxygen become an important factor and must be taken into consideration.

The solubility of oxygen in nickel[71] is 0.014 wt. % at 1000°C; the solubility of nitrogen in nickel is extremely small. The value[72] at 1600°C and 1 atm. pressure of nitrogen is 0.001 ± 0.001 wt. %, the limits of experimental error being as much as the solubility itself. The solubility of nitrogen in solid nickel has been estimated[73] as <0.0004 wt %. There is also evidence[71,74] that nitrogen is insoluble in pure nickel even upto 1400°C. Moreover, the heat of formation at 298°K of the oxide and nitride are found to be:[75]

$$(\Delta H_{298})_{NiO} = -57.5 \mp 0.5 \text{ kcals/mole}$$

$$(\Delta H_{298})_{Ni_3N} = +0.2 \mp 1.0 \text{ kcals/mole}$$

Thus, it is evident that the nitride of nickel is not stable and that the solubility of nitrogen in nickel is negligible as compared to that of oxygen. Therefore, only oxygen diffusion will be considered in the present analysis.

Despite the fact that oxygen diffuses easily into f.c.c. metals, quantitative data on the diffusion of oxygen in nickel does not exist. The only work found in the literature[76] deals with the diffusion of oxygen in (110) single crystals. The temperature dependence of the diffusion coefficient has been derived as:

$$D_O = 2.3 \times 10^{-5} \exp\left(\frac{-11500}{T}\right), \text{ cm}^2/\text{sec}$$

On the basis of this equation, the diffusion coefficient of oxygen in nickel and the distance to which it can penetrate the metal surface at the temperatures and times of annealing can be calculated (Table 7):

Table 7

Temperature of Annealing	Diffusion Coefficient of Oxygen, D_o	Time	Distance to which oxygen can diffuse $x = \sqrt{D_o t}$
°C	cm^2/sec	hrs.	μm
500	8.5×10^{-12}	4	3.5
775	4.0×10^{-10}	5	26.9
950	1.9×10^{-9}	72	220.0
1000	2.8×10^{-9}	77	280.0
1000	2.8×10^{-9}	100	320.0

It can be seen from Table 7 that the diffusion coefficient of oxygen at the temperatures of annealing is appreciable and that for the durations of annealing, oxygen diffuses to substantial depths. In the last case, this depth is slightly less than half-thickness of the specimen used.

The oxygen diffusion results in the formation of a main scale and an oxygen-rich region where the concentration is not high enough for the formation of the oxide. The main scale is completely removed in polishing and despite repeated polishing a substantial thickness of the region with dissolved oxygen remains. It is the presence of this region that exhibits enhanced reactivity and prevents the metal from being passivated (Figure 14, lower curve). Thus, depending upon the distribution of oxygen, the nature of attack on the specimen surface will vary. Areas which have a uniform concentration of oxygen will show general corrosion; areas where the concentration varies drastically (or where the oxygen is present in discrete

areas) will exhibit pitting, while the grain boundaries will always show deep corrosion.

5.3.2 Effect of Site Distribution

The distribution of anodic and cathodic sites is initially random over the entire specimen surface and both types of sites are present along the grain boundaries as well as within the grains. Which of these sites become activated depends upon the conditions existing at the metal/solution interface during polarization.

An explanation must now be sought for the shift in the pitting susceptibility from the grain boundary (for specimens upto grain size of 0.150 mm) to the grain interior (for specimens with grain size greater than 0.250 mm). It is assumed here that specimens which show enhanced reactivity along the grain boundary when annealed in air will continue to do so even when annealed in vacuum.

To start with, it is assumed that a certain concentration of active anodic sites exists per unit area of the grain interior and per unit length of the grain boundary, and that this concentration is independent of the grain size. Then, by virtue of the presence of these sites, a certain chemical potential or reactivity will be associated with the grain interior as well as the grain boundary. In the case of a specimen with small grains, the total length of the grain boundary is high. Thus, on the average, the total grain boundary reactivity exceeds the total grain reactivity. If the passive film is taken to form according to the 'dissolution-precipitation mechanism',[77] then areas which are more active will passivate more readily. However, since these areas exhibit a greater reactivity, the current required to maintain passivity at them will be high, and once the conditions for breakdown are achieved, chlorine will adsorb more readily at these areas than elsewhere.

Thus, areas which are first to be passivated will also be the first to be activated. Thus, in a small grain size specimen, the grain boundaries are more readily passivated and once the conditions for breakdown of passivity are established, the passive film breaks preferentially along the grain boundaries and pits are formed (Figure 10, 11 and 12). On the other hand, when the grains of the specimen are large, the total grain boundary length is smaller and fewer anodic sites are present along it. Thus, the total grain reactivity exceeds the total grain boundary reactivity. For such a specimen, therefore, the grain interiors are not only the first to be passivated but also the first to be activated. This activation results in film breakdown in the grain interiors. Large grain size specimens thus show pits only within the grains (Figure 15).

If the critical breakdown potential, E_c, is taken as a measure of the pitting susceptibility, the results presented show that no change is observed in the value of E_c with increasing cold work, regardless of whether the annealing is performed in air or in vacuum. From the anodic Tafel slopes (Table 4) it is evident that for air annealed specimen an increase in cold work tends to slightly increase the reactivity of the metal. However, this increase is significant only in the earlier stages of cold working and no change in β_a is observed beyond 10% cold work. For vacuum annealed specimens, the Tafel slopes are higher (which means that the metal is less reactive) and in this case very little difference exists in the slopes over the entire range of cold working. Electrochemically, these facts may be taken to mean that despite cold working, the primary dissolution mechanism and the characteristics of the passive film are similar in each case. It may, therefore, be concluded that cold working upto 40% does not significantly alter the anodic-cathodic site distribution over the specimen surface and, consequently,

has no effect on the pit nucleation characteristics of nickel. That cold working upto a certain stage does not alter the site distribution has also been found for α-brass.[78*]

It will be noted from Tables 3 and 5 that the value of the primary passivation potential, E_{pp}, is higher for vacuum annealed specimens. This is in support of the dissolution-precipitation mechanism of passivity[77]. Since the vacuum annealed specimens show lower reactivity, they need to be polarized to higher potentials before the passive state can set in.

The slopes in the transpassive region do not provide any specific information. They cannot be regarded as a measure of the growth rate of the pits because of the multiple events occurring on the surface. Pits that had nucleated grow, new ones nucleate and some of the older ones passivate. However, the transpassive slopes, β_t, do provide an idea of the overall corrosion of the specimen in that potential region. Within limits of experimental error, it may be seen that β_t does not significantly change with cold work. This is consistent with the earlier conclusion that cold working does not affect the pitting corrosion characteristics of nickel.

The formation of pits in the active region is consistent with the concept of a 'balance' between film formation and solution discussed earlier, but is in direct conflict with the idea that pitting cannot occur at potentials more active than some critical potential.[23,45] However, as the results show, pitting can and does occur[79] at potentials lower than the critical potential.

---

*In this case, it was found that cold working upto 26.5% did not at all change the cathodic/anodic site distribution and only beyond 32% cold work did an observable change occur. Thus, if this limit were 32% for an alloy, it could be expected to be higher for a pure metal.

The critical potential thus does not entirely describe the electrochemical conditions required for pitting corrosion. Therefore, considerable caution must be exercized in interpreting data based on critical potentials to assess the pitting susceptibility of metals and alloys.

5.4 Corrosion Morphology

The destruction of passivity at discrete points on a metal surface gives rise to enhanced dissolution, resulting in the formation of pits. On single crystal faces of metals, these pits have shapes which are characteristic of the atomic arrangement of that surface and where the facets of the pits are composed of the most stable planes, normally those of high atomic density. The slowest dissolving crystallographic orientations are maintained in the dissolution shape.

Owing to the small size of the grains and, consequently, the pits themselves, no determination of the grain or pit facet orientations have been done. Instead, these have been obtained by comparison with previous works.[49,59] It is assumed that the facets of the pit formed on {100} grains (Figure 27) as well as that on the {111} grains (Figure 32) comprize the {111} planes.

Often pits have sides which are composed of low-index facets, and their profiles reflect the crystallography and orientation of the surface in which they lie. The most probable mechanism governing the development of such pits is one involving orientation-dependent dissolution. The kinematic theory of crystal growth and dissolution as outlined by Frank[80] is capable of predicting the pit shape provided the orientation dependence of dissolution rate is known. The reciprocal of the normal dissolution rate as a function of orientation can be plotted on a polar diagram yielding a

polar 'reluctance' diagram. From this polar reluctance diagram, the pit shape can be predicted using the method outlined by Frank and Ives.[81]

The changes in pit morphology with cold work will now be discussed on the basis of Frank's theory.[80] Since no dissolution rate data was obtained, arbitrary values will be assumed. Since the facets of the pit maintained in the dissolution shape in a {100} grain are {111}, they are the slowest to dissolve. Hence, their 'reluctance' will be the highest. Let us assume that this reluctance is 3 (arbitrary units, TL^{-1}), while that of the {hh0} planes in 2.5 units. Let us assume that the polar reluctance diagram for a <100> zone has the shape shown in Figure 55(a) (though maximas will be present as shown, the exact shape of the curve will depend upon the relative dissolution rates of the various planes). Then, by the method of Frank and Ives,[81] the pit shape can be shown to be the outer curve in Figure 55(a).

The introduction of cold work increases the reactivity owing to the increase in the dislocation density. The effect of an increase in the dislocation density on a high-index plane is not so significant. Its reactivity is not increased as it already has enough steps which act as sites for removal of atoms. But on a low-index plane, where very few such sites are present, the increase in dislocation density drastically increases its reactivity and thus its dissolution rate. Hence, its dissolution reluctance decreases. In the present case, the reluctance may decrease to 2.5 units, so that it now equals that of the {hh0} planes. Thus, this time the dissolution shape will have eight facets as shown in Figure 55(b). This process continues, so that with increase in cold work the dislocation density increases. This increases the dissolution rate of different planes, so that

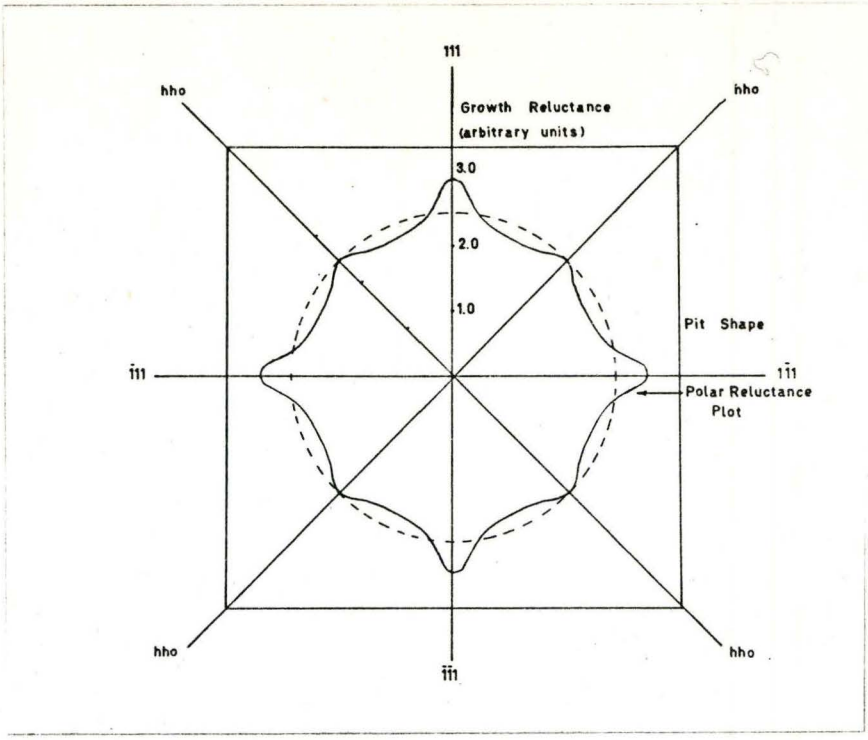

(a)

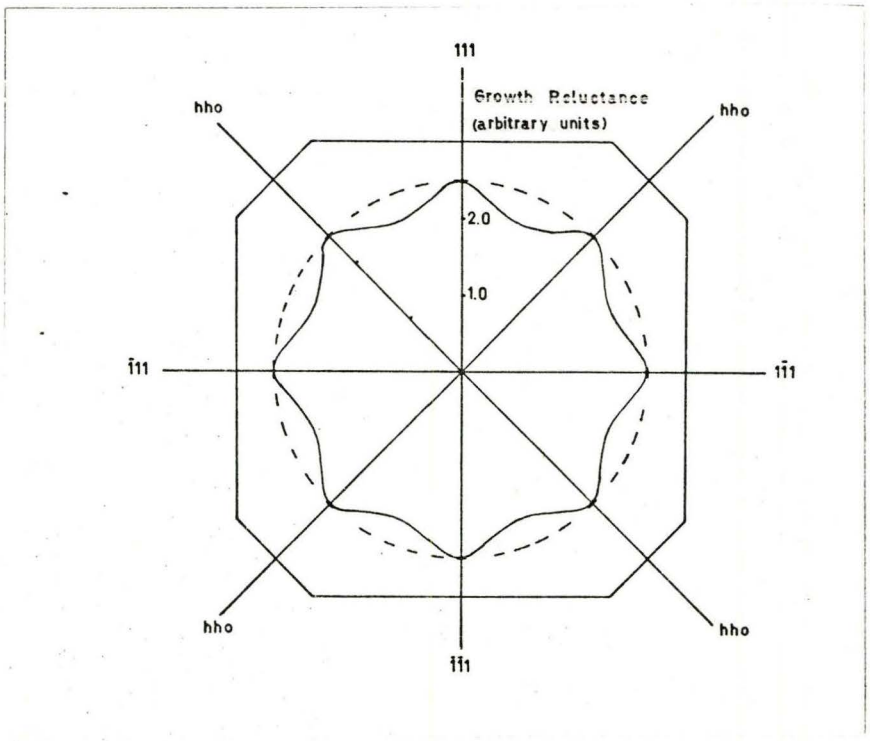

(b)

Figure 55. Polar reluctance diagram for a <100> zone. Arbitrary values have been assumed for the growth reluctance. The exact shape of the curve between the maximas will depend upon the relative dissolution rates of the various planes.

their reluctance decreases. More and more planes are thus revealed in the dissolution shape. In other words, as the cold work increases, the dissolution within the pit which was initially anisotropic, tends to become isotropic. This isotropy in dissolution manifests itself in two ways - first, the exterior shape of the pit becomes circular and secondly, the regular crystallographic facets within the pits tend to disappear (Figure 30 and 31). It would, therefore, be expected that when the cold work is very high, the polar reluctance diagram will be circular, so that the pit shape will be spherical and have no distinct crystallographic facets. This has been found to be experimentally true (Figure 26 and 40). The changes in pit morphology at the grain boundary (Figure 36 and 37) also serve to illustrate that isotropy in dissolution sets in with cold work and is independent of the location of the pit.

On the basis of the transpassive slopes, it was concluded in the last section that cold working does not significantly affect the pitting corrosion characteristics of nickel. On the other hand, it is assumed here that cold working increases the reactivity (and thereby the dissolution rate) of the low-index planes within a pit. It must be pointed out, however, that since the polarization curve is plotted on a semi-logarithmic scale, it tends to visually compress the anodic current density values thereby increasing the slope and showing a lower overall reactivity. Moreover, a phenomenon which is present on a microscopic scale may not be observable on a macroscopic scale,so that even though the reactivity of the low-index surfaces increases due to increase in cold work, the effect is small and unnoticeable in an overall current measurement.

A possible explanation for the appearance of steps within pits may be based on surface effects. The formation of a stepped or faceted surface is known to be a common surface phenomenon. The effect is believed to be a consequence of kinetic as well as thermodynamic factors. The kinetic argument states that a high-index surface has kinks and ledges which act as active sites for selective adsorption and removal of atoms. An adsorbed foreign atom tends to anchor the motion of the ledges, while the removal of atoms from kinks results in the formation of terraces. In the steady state, the surface consists of terraces and ledges. The thermodynamic viewpoint embraces the fact that a high-index plane is also one of high energy. It, therefore, breaks down into facets minimizing the total surface energy. Thus, cold working may mis-orient the pit facets from their normal {111} orientation to a high-index plane, so that the final dissolution shape shows the presence of facets or steps (Figures 33 to 35). With regard to the absence of steps in the pits on the {100} grains, it must be pointed out that the absence of steps on a macroscopic scale does not, necessarily, imply their absence on a microscopic (atomistic) scale too.

The difference in pit deepening between the annealed and cold worked material gives rise to the differing size of pits in the two materials. Since the attack tends to be directed along the grain boundaries, it is evident that with the grain boundaries being almost parallel to the surface in the cold worked material, a shallower pit will result. On the other hand, the equiaxed grain structure in the annealed material permits corrosion to proceed isotropically so that much deeper pits are formed.

Apart from the presence of crystallographic pits, non-crystallographic pits, such as saucer or conical ones, were also observed. The

formation of non-crystallographic pits indicates that the dissolution is tending to be isotropic. When hemispherical pits are formed, it may be assumed that dissolution is completely isotropic. Whatever be the cause of this isotropy in dissolution, it is obvious that it is a result of the situations existing at the metal/solution interface which tend to maintain the current density within the pit the same at every point. In the cold worked material, this situation is caused by the condition of the metal and the appearance of multiple facets in the dissolution shape, whereas in the annealed material the equiaxed grain structure permits isotropic dissolution so that the pit grows into many grains and on a macroscopic section it appears to be hemispherical. Hoar[82] believes that in some cases pits that begin as approximately hemispherical expand to a 'saucer' form or to an 'inverted bubble' form - the mode of growth being evidently influenced by the ease with which the local metal dissolution undermines the still passive surface. If, for some reason, the upper inside periphery of the hemispherical pit is rendered inactive, then the local metal dissolution will be confined to the bottom part of the pit and eventually result in the formation of a conical pit. Since such conditions would be difficult to achieve, it is evident that very few conical pits will be formed. Sectioning experiments have shown this to be true.

A correlation will now be sought between the nature of film breakdown and the type of pits produced. It is suggested that humps in the passive film with breaks around the edges are associated with hemispherical pits while those with breaks across them are associated with conical pits. This statement receives support from the fact that there are very few instances of both conical pits and the incidence of films with breaks across their hump.

At the present stage, it is not clear whether the nature of film breakdown leads to the formation of a particular shape of pit or whether the type of film breakdown is a consequence of the particular pit shape. Probably the latter is correct. For, assuming that before a break occurs in the passive film, the pit has achieved its shape (either hemispherical or conical), then due to the growth of the pit, a flow of corrosion products will be set up within the pit (Figures 56(a) and 57(a)). As a result of this, in a hemispherical pit, the points of maximum tension will be the edges of the hump (thick arrow in Figure 56(a)) while in a conical pit they will be across the hump (thick arrow in Figure 57(a)). The tension experienced by the film will eventually result in its rupture as shown in Figure 56(b) and 57(b).

5.5. Technological Consequences

All studies on the pitting susceptibility of nickel were performed by the 'potentiostatic polarization' technique and the reason why this technique was considered more appropriate for susceptibility studies has already been mentioned. It may be pointed out that although this technique has been widely used for material evaluation, the situation more commonly encountered in industrial practice is closer to the 'potentiostatic activation' technique. In any industrial situation, pit nucleation is no doubt important, but once the pits have nucleated, their growth kinetics become more important than the nucleation of fresh pits. The kinetics of pit growth can well be studied by the 'potentiostatic activation' technique.

If the change in the anodic current density/unit time, i.e. $\frac{dI_a}{dt}$, be taken to represent the pit growth kinetics, then in combination with the critical potential, E_c, four situations can arise:

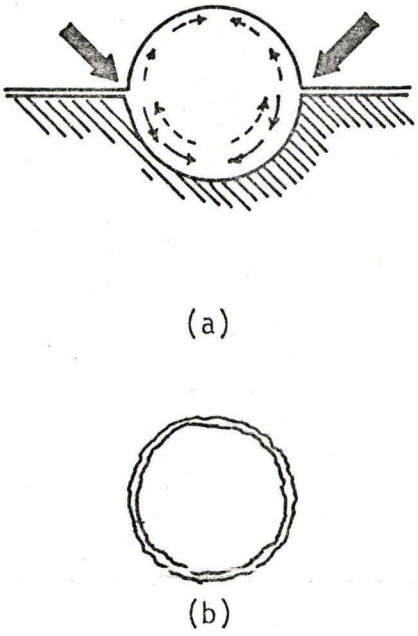

Figure 56

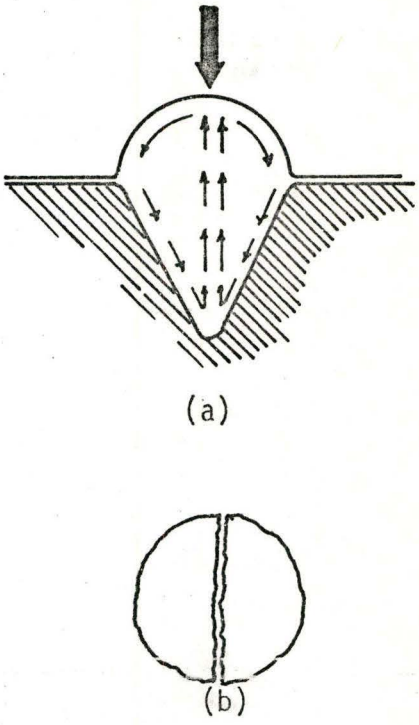

Figure 57

(a) Flow of corrosion products within the pit.
(b) Nature of film breakdown

Note: The thick arrows designate points of maximum tension.

Critical Potential E_c	Pit Growth Kinetics dI_a/dt	Acceptability Index
High	Low	1
Low	Low	2
High	High	3
Low	High	4

The practically most acceptable or desirable situation (expressed as an 'acceptability index'; most acceptable-1, least acceptable-4) clearly will be the one where the critical potential is high (more positive or noble) while the pit growth is slow.

The nucleation of pits prior to the onset of passivity and the significant variation in the distribution of pits (and also the intensity of attack) of two differently treated pieces of the same material even when there is no change in the critical potential suggests that the interpretation of the critical potential must be done with extreme caution and with certain reservations.

A very thin oxide film is known to be present on most metals.[43] The two stages involved in corrosion fatigue are[83] - (i) film breakdown, and (ii) conjoint fatigue and corrosion. The breakdown of the film gives rise to pits and cracks generally start at sharp pits (or crevices) in the surface.[84,85] In view of the above facts, the consequences of the variation in the shape of pits needs to be emphasized. Conical pits, wherever they may be present, will act as stress-raisers. Thus, from the corrosion fatigue viewpoint, a material with more flat bottomed pits is likely to perform better than one with fewer conical pits. It may, however, be pointed out

that in many cases[84] during the initial stages of corrosion fatigue, pits tend to be hemispherical, but they then change to saucer-like depressions. With time, a sharp root-like projection forms at the bottom of the pits, and eventually fissures develop leading to failure.

It is, therefore, emphasized that the evaluation of a material for an application where pitting corrosion may be incurred should take into consideration the value of the critical potential, the pit growth kinetics and the morphology of attack.

On the basis of the above criteria, suitable materials will be those with a high breakdown potential, low pit growth rate and flat bottomed (hemispherical or saucer) pits. Many elements are known to have a beneficial effect on the breakdown potential.[22] Thus, alloying nickel with elements such as chromium, molybdenum, iron etc. will increase the value of the breakdown potential. However, the pit growth kinetics and pit morphology needs to be studied before any firm recommendations can be made.

CHAPTER VI

CONCLUSIONS AND SUGGESTIONS FOR FUTURE WORK

6.1 Conclusions

i) The nature of the passive film formed under "potentiostatic activation" and "potentiostatic polarization" is quite different. The film is thicker in the former case.

ii) Passage of the chlorine ions from the bulk of the solution to the passive film, followed by complete penetration through it to the metal surface is required to initiate pitting corrosion.

iii) The concentration of chlorine ions present in solution must be small for a localized breakdown of the passive film and for pitting corrosion to occur. High chlorine ion concentrations lead to general corrosion.

iv) Cold working upto 40% does not affect the critical breakdown potential of nickel, though the distribution of pits varies.

v) In the latter stages of growth, the shape of corrosion pits is mostly hemispherical or saucer type in annealed as well as cold worked nickel. Few conical pits are formed. Hence, nickel may perform well in corrosion fatigue.

vi) Electrochemical data must be supplemented by metallographic observations for a complete appreciation of the pitting phenomenon.

vii) The critical potential does not entirely describe the conditions required for pitting corrosion. Hence, considerable caution has to be exercized in interpreting data based on critical potentials to assess the pitting susceptibility of metals and alloys.

6.2 Suggestions for Future Work

At the outset only, one immediately asks the question - "Why at all is more work necessary on the corrosion behaviour of nickel and/or its alloys?" The answer is rather straightforward. Ever since their discovery, stainless steels have been regarded as alloys with excellent corrosion resistance and, therefore, have been used quite extensively for applications where corrosion can be encountered. However, even with all their assets, their performance in sea water can at best be rated satisfactory. On the other hand, cupro-nickel* and Hastelloys** have excellent resistance to corrosion in marine atmospheres.[5] This is also true for underground corrosion where either the soil is poorly aerated or has dissolved salts containing chloride. In both the above cases, the material fails by pitting corrosion. Even though pitting corrosion may be suppressed by cathodic protection, the hydrogen produced by the cathodic reaction can be harmful in the case of stainless steels (hydrogen embrittlement) in applications where stress is also a factor. Such a problem will not arise with nickel or its alloys. Hence, for applications in sea water, underground, fluid compressor tubes, centrifugal pump parts etc. nickel alloys hold a promising future.

On the basis of the results reported in this investigation, the following aspects of the localized corrosion of nickel may be studied:

i) The effect of various alloying elements, such as copper, molybdenum, chromium, iron, silicon etc. on -

a) the critical potential for the breakdown of passivity, E_c.

b) the pit growth kinetics, $\frac{dI_a}{dt}$

---

* 70% Cu, 0.45% Fe, balance Ni.

**Trademark of the International Nickel Company for alloys containing Ni, Mo, Cr with small additions of Cb, Fe etc.

c) the corrosion morphology

Material evaluation may be made using the suggested criteria.

An interesting and rewarding investigation will be the study of various heat treatments to obtain different metallurgical structures (and consequently, higher strength) and their effect on the subsequent corrosion behaviour of the alloys.

ii) Test of the alloys found suitable using the suggested criteria in corrosion fatigue.

iii) Studies on the inhibition of pitting corrosion.

A suitable inhibitor may be determined by analyzing the role played by the inhibitor ion during pitting inhibition. This may be done by obtaining anodic and cathodic galvanostatic polarization curves under the conditions of application

a) without inhibitor

b) with inhibitor

and comparing the values of the anodic and cathodic Tafel slopes, β_a and β_c.

Finally, a study may be performed on the effect of the inhibitor on the pit initiation and growth kinetics and subsequent corrosion morphology.

REFERENCES

1. M. G. Fontana and N. D. Greene, 'Corrosion Engineering', p. 28, McGraw Hill Book Co., New York (1967).
2. H. H. Uhlig, 'Corrosion Handbook', p. 253, John Wiley & Sons, Inc., New York (1958).
3. H. H. Uhlig, 'Corrosion and Corrosion Control', p. 14, John Wiley & Sons, Inc., New York (1967).
4. U. R. Evans, 'The Corrosion and Oxidation of Metals', p. 2, Edward Arnold Ltd., London (1960).
5. N. D. Tomashov, 'Theory of Corrosion and Protection of Metals', p. 329, The MacMillan Co., New York (1966).
6. M. Faraday, cited in 'Passivity and Protection of Metals against Corrosion', N. D. Tomashov and G. P. Chernova, p. 12, Plenum Press, New York (1967).
7. G. Tammann, Z. Anorg. Chem., 107, 236 (1919).
8. I. Langmuir, J. Chem. Soc., 62, 517 (1940).
9. I. N. Stranski, Z. Electrochem., 45, 393 (1929); 46, 25 (1930).
10. A. Russell, Nature, 115, 455 (1925).
11. H. H. Uhlig, Trans. Electrochem. Soc., 85, 307 (1944).
12. H. H. Uhlig, Z. Electrochem., 62, 700 (1958).
13. J. Osterwald and H. H. Uhlig, J. Electrochem. Soc., 108, 515 (1961).
14. G. Tammann, Z. Anorg. Chem., 169, 151 (1928).
15. T. P. Hoar, R. B. Mears and G. P. Rothwell, Corr. Sci., 5, 279 (1965).
16. T. P. Hoar, Corr. Sci., 7, 341 (1967).
17. T. P. Hoar and W. R. Jacob, Nature, 216, 1299 (1967).
18. Ja. M. Kolotyrkin, J. Electrochem. Soc., 108, 209 (1961).

19. I. L. Rosenfeld and I. S. Danilov, Corr. Sci., 7, 129 (1967).

20. H. J. Engell and N. D. Stolica, Z. Phys. Chem., 20, 113 (1959).

21. T. Tokuda and M. B. Ives, Corr. Sci., 11, 297 (1971).

22. Z. Szklarska-Smialowska, Corrosion, 27, 223 (1971).

23. Ja. M. Kolotyrkin, Corrosion, 19, 261t(1963).

24. H. P. Leckie and H. H. Uhlig, J. Electrochem. Soc. 113, 1262 (1966).

25. H. Böhni and H. H. Uhlig, J. Electrochem. Soc., 116, 906 (1969).

26. P. Forchhammer and H. J. Engell, Werkst. u. Korr., 20, 1 (1969).

27. H. H. Uhlig, Trans. AIME, 140, 422 (1940).

28. T. P. Hoar, Corr. Sci., 7, 341 (1967).

29. J. Postlethwaite, Electrochim. Acta, 12, 333 (1967).

30. N. D. Tomashov, O. P. Chernova and N. Markova, Corrosion, 20, 166t (1964)

31. J. R. Ambrose and J. Kruger, Proc. of The Fourth International Congress on Metallic Corrosion, (1969). In press.

32. C. L. McBee and J. Kruger, Proc. of The U. R. Evans International Conference on Localized Corrosion, NACE (1971). In press.

33. G. Bianchi, A. Cerquetti, F. Mazza and S. Torchio, Corr. Sci., 10, 19 (1970); Proc. of The U. R. Evans International Conference on Localized Corrosion, NACE (1971). In press.

34. S. C. Britton and U. R. Evans, J. Chem. Soc., 1773 (1930).

35. G. A. Bassett and C. Edeleanu, Phil. Mag., 5, 709 (1960).

36. M. J. Pryor, Proc. of The U. R. Evans International Conference on Localized Corrosion, NACE (1971). In press.

37. W. Schatt and H. Worch, Corr. Sci., 9, 869 (1969).

38. Z. Szklarska-Smialowska and M. Janik -Czachor, Corr. Sci., 7, 65 (1967).

39. A. P. Bond, G. F. Bolling and H. A. Domain, J. Electrochem. Soc., 113, 773 (1966).

40. M. A. Streicher, J. Electrochem. Soc., 103, 375 (1956).

41. B. E. Wilde and J. S. Armijo, Corrosion, 23, 208 (1967).

42. E. C. Pearson, H. J. Huff and R. H. Hay, Can. J. Tech., 30, 311 (1952).

43. U. R. Evans, 'Metallic Corrosion, Passivity and Protection', p. 278, Edward Arnold Ltd., London (1948).

44. N. D. Stolica, Corr. Sci., 9, 205 (1969).

45. W. Schwenk, Corrosion, 20, 129t (1964).

46. M. Janik-Czachor and Z. Szklarska-Smialowska, Corr. Sci., 8, 215 (1968).

47. C. Edeleanu, J. Inst. Metals, 89, 90 (1960-61).

48. I. Garz, H. Worch and W. Schatt, 9, 71 (1969).

49. T. Tokuda and M. B. Ives, J. Electrochem. Soc., 118, 1404 (1971).

50. I. L. Rosenfeld and I. S. Danilov, Zashchita Metallov., 6, Nr 1 (1970).

51. Z. Szklarska-Smialowska and M. Janik-Czachor, Brit. Corr. J., 4, 136 (1969).

52. N. D. Stolica, Corr. Sci., 9, 455 (1969).

53. R. Gressmann, Corr. Sci., 8, 325 (1968).

54. Z. Szklarska-Smialowska, Corr. Sci., 11, 209 (1971).

55. B. E. Wilde, Proc. of The U. R. Evans International Conference on Localized Corrosion, NACE (1971). In press.

56. T. Homma, N. N. Khoi, W. W. Smeltzer and J. D. Embury, J. Oxidation Metals, 3, 463 (1971).

57. G. L. Kehl, 'The Practice of Metallographic Laboratory Practice', p. 293, McGraw-Hill Book Co., Inc., New York (1949).

58. K. Ciha, Practical Metallography, 8, 26 (1971).

59. A. Akhtar and E. Teghtsoonian, J. App. Phy., 42, 4285 (1971).

60. L. Tronstad, Z. Phy. Chem., 142, 241 (1929).

61. H. Pfisterer, A. Politycki and E. Fuchs, Z. Electrochem., 63, 257 (1959).

62. K. Arnold and K. J. Vetter, Z. Electrochem., 64, 407 (1960).

63. N. Sato and G. Okamoto, J. Electrochem. Soc., 110, 605 (1963).

64. D. E. Davies and W. Barker, Corrosion, 20, 47t (1964).

65. J. Yahalom and I. Weisshauss, Proc. of The U. R. Evans International Conference on Localized Corrosion, NACE (1971). In press.

66. I. A. Ammar and S. Darwish, Electrochim. Acta, 13, 781 (1968).

67. R. C. Weast, 'Handbook of Chemistry and Physics', 49th Edition, p. B-222, The Chemical Rubber Co., Ohio (1968).

68. Z. Szklarska-Smialowska, private communication.

69. F. G. Hodge and B. E. Wilde, Corrosion, 26, 146 (1970).

70. S. F. Bubar and D. A. Vermilyea, J. Electrochem. Soc., 113, 892 (1966).

71. M. Hansen, 'Constitution of Binary Alloys', p. 1024, McGraw Hill Book Co., New York (1958).

72. J. C. Hümbert and J. F. Elliot, Trans. AIME, 218, 1076 (1960).

73. R. P. Elliot, 'Constitution of Binary Alloys', First Supplement, p. 639, McGraw Hill Book Co., New York (1965).

74. T. Busch and R. A. Dodd, Trans. AIME, 218, 488 (1960).

75. O. Kubaschewski and E. L. Evans, 'Metallurgical Thermochemistry', p. 262, The MacMillan Co., New York (1958).

76. J. W. May and L. H. Germer, Surf. Sci., 11, 443 (1968).

77. J.O'M. Bockris and A.K.N. Reddy, 'Modern Electrochemistry', Vol. 2, p. 1321, Plenum Press, New York (1970).

78. M. Zamin, D.I.I.T. Thesis, Indian Institute of Technology, Kharagpur, India (1970).

79. R. F. Stiegerwald, Corrosion, 22, 107 (1966).

80. F. C. Frank, 'Growth and Perfection in Crystals', ed. R. H. Doremus, B. W. Roberts and D. Turnbull, p. 441, John Wiley & Sons, Inc., New York (1958).

81. F. C. Frank and M. B. Ives, J. App. Phy., 31, 1996 (1960).

82. T. P. Hoar, Proc. of The U. R. Evans International Conference on Localized Corrosion, NACE (1971). In press.

83. A. J. Gould, Iron and Steel, 24, 7 (1951).

84. P. T. Gilbert, Metal. Rev., 1, 379 (1956).

85. A. H. Goodger, Proc. of International Conference on Fatigue of Metals, p. 394, Instn. Mech. Engrs. (1956).